Transmission Strategies and Performance Analysis of Resource-Constrained Wireless Relay Networks

Behrouz Maham

DISSERTATION IN PARTIAL FULFILLMENT OF THE REQUIREMENTS
FOR THE DEGREE OF PHILOSOPHIAE DOCTOR

Department of Informatics
Faculty of Mathematics and Natural Sciences
University of Oslo

Oslo 2010

Series of dissertations submitted to the
Faculty of Mathematics and Natural Sciences, University of Oslo
No. 944

ISSN 1501-7710

Cover: Inger Sandved Anfinsen.
Printed in Norway: AiT e-dit AS.

Produced in co-operation with Unipub.
The thesis is produced by Unipub merely in connection with the
thesis defence. Kindly direct all inquiries regarding the thesis to the copyright
holder or the unit which grants the doctorate.

Preface

This dissertation has been submitted to the Faculty of Mathematics and Natural Sciences at the University of Oslo in partial fulfillment of the requirements for the degree of *Philosophiae Doctor* (PhD). The studies were carried out over a period of three years, from June 2007 to May 2010. I spent the first and the third year of my PhD studies at UNIK- University Graduate Center, Kjeller, Norway, while the second year my workplace has been the Star Laboratory at Stanford University, USA. The research was funded by the Research Council of Norway through the project 176773/S10 entitled "Optimized Heterogeneous Multiuser MIMO Networks – OptiMO". My supervisors have been Prof. Are Hjørungnes, Prof. Pål Orten, and Prof. John C. Cioffi.

The symbol usage may vary from one paper to another as the papers included in this dissertation are *not* published at the same time.

Dedication

This dissertation is dedicated to my father Aliakbar and my mother Elahe.

Acknowledgments

Praise be to God, the most gracious and the most merciful. Without his blessing and guidance my accomplishment would never have been possible.

I would like to acknowledge many people who helped me during the course of this work. First, I would like to thank my PhD advisor Prof. Are Hjørungnes for giving me the opportunity to be part of his research group and for providing me the right balance of guidance and independence in my research. I am greatly indebted to his full support and constant encouragement and advice both in technical and non-technical matters.

My sincere appreciation is extended to Prof. John Cioffi at Stanford University, for his constructive suggestions and comments on my thesis work. During my 11 months visit at Stanford University I had the great fortune and honor to collaborate with his group on problems of common interests. Furthermore, I would like to thank Prof. Pål Orten for his support and encouragement.

I am thankful to my former and current group-mates: Walid Saad, Dr. Lingyang Song, Dr. Manav Bhatnagar, and Dr. Ninoslav Marina.

Last, but certainly not the least, I would like to acknowledge the commitment, sacrifice and support of my parents, who have always motivated me. In reality this thesis is partly theirs too.

Behrouz Maham
Oslo, February 14, 2010

Abstract

Demand for mobile and personal communications is growing at a rapid pace, both in terms of the number of potential users and introduction of new high-speed services. Meeting this demand is challenging since wireless communications are subject to four major constraints: A complex and harsh fading channels, a scarce usable radio spectrum, and limitations on the power and size of hand-held terminals. Space-time codes provide diversity and coding gains in multiple antenna systems over fading channels. However, in ad-hoc or distributed large scale wireless networks, nodes are often constrained in hardware complexity and size, which makes multiple antenna systems impractical for certain applications. Cooperative diversity schemes have been introduced in an effort to overcome this limitation. Cooperative techniques allow a collection of radios to relay signals amongst each other, effectively creating a virtual antenna array, which combat multipath fading in wireless channels. In resource constrained networks, such as wireless sensor networks, the advantages of cooperation can be further exploited by optimally allocating the energy and bandwidth resources among users based on the available channel state information (CSI) at each node. In this thesis, we consider the design of practical distributed space-time codes and power efficient fading mitigation techniques for wireless relay networks. We show that using the proposed techniques the system performance is significantly improved under the respective resource constraints such as the energy, bit-error rate, or outage probability. Furthermore, the performance analysis of the wireless relay networks under different protocols and fading channels are investigated. We derive formulas for the symbol error rate (SER), outage probability, and diversity order of the investigated schemes in fading channels. For sufficiently large SNR, the close-form average symbol error probabilities are derived for the number of the distributed wireless systems. The simplicity of the asymptotic results provides valuable insights into the performance

of cooperative networks and suggests means of optimizing them. Based on these SER expressions, power allocations are also proposed to further improve the performance of these systems. We next apply our proposed cooperative schemes to some practical wireless networks. For instance, we propose several amplify-and-forward cooperative schemes which consider the residual battery energy, as well as the statistical CSI, for the purpose of lifetime maximization in multi-branch, multihop wireless networks. We also propose new energy-efficient cooperative routing protocols in multihop wireless networks. In contrast to previous works, our proposed cooperating routings depend only on the statistics of the channels, and are implemented by both the centralized and distributed approaches.

List of Publications

This dissertation is based on the following seven papers, referred to in the text by letters (A-G).

A. B. Maham, A. Hjørungnes, and G. Abreu, "Distributed GABBA Space-Time Codes in Amplify-and-Forward Relay Networks," *IEEE Transactions on Wireless Communications*, volume 8, issue 2, pages 2036 - 2045, April 2009.

B. B. Maham and A. Hjørungnes, "Power Allocation Strategies for Distributed Space-Time Codes in Amplify-and-Forward Mode," *EURASIP Journal on Advances in Signal Processing*, vol. 2009, Article ID 612719, 13 pages, 2009. doi:10.1155/2009/612719.

C. B. Maham and A. Hjørungnes, "Performance Analysis of Repetition-Based Cooperative Networks with Partial Statistical CSI at Relays," *IEEE Communications Letters*, volume 12, issue 11, pages 828-830, November 2008.

D. B. Maham and A. Hjørungnes, "Asymptotic Performance Analysis of Amplify-and-Forward Cooperative Networks in a Nakagami-m Fading Environment,"*IEEE Communications Letters*, volume 13, issue 5, pages 300-302, May 2009.

E. B. Maham and A. Hjørungnes, "Performance Analysis of Amplify-and-Forward Opportunistic Relaying in Rician Fading," *IEEE Signal Processing Letters*, volume 16, issue 8, pages 643-646, August 2009.

F. B. Maham, A. Hjørungnes, and M. Debbah, "Power Allocations in Minimum-Energy SER Constrained Cooperative Networks," *Annals of Telecommunications - Annales des Télécommunications*, vol. 64, no. 7, pp. 545-555, Aug. 2009 (Published by Institut Telecom and Springer; Indexed in ISI and Scopus databases).

G. B. Maham, R. Narasimhan, and A. Hjørungnes, "Energy-Efficient Space-Time Coded Cooperative Routing in Multihop Wireless Networks," *Proc. of IEEE Global Telecommunications Conference (GLOBECOM 2009)*, Honolulu, Hawaii, USA, November - December 2009.

The list of other related publications during my PhD studies are given in Section 8 of Chapter I.

Contents

List of Figures

List of Tables

Abbreviations

A&F/AF	Amplify-and-forward
AGC	Automatic Gain Control
AP	Access point
AWGN	Additive white Gaussian noise
BER	Bit error rate
BPSK	Binary phase shift keying
BS	Base station
BW	Band-width
CDF	Cumulative distribution function
CDMA	Code division multiple access
CIOD	Coordinate interleaved orthogonal designs
CRC	Cyclic redundancy check
CSI	Channel state information
CTS	Clear-to-send
dB	Decibel
D&F/DF	Decode-and-forward
DSTBC	Distributed space-time block code
DSTC	Distributed space-time codes
FDD	Frequency division duplexing
FDMA	Frequency division multiple access
HARQ	Hybrid-automatic repeat request
Hz	Hertz
i.i.d.	Independent and identically distributed
IEEE	Institute of Electrical and Electronics Engineers
KKT	Karush-Kuhn-Tucker
LNA	Low-noise amplifiers
LOS	Line of sight
MAC	Medium access control
MGF	Moment generating function
MIMO	Multiple-input multiple-output

PW ML	Pair-wise Maximum-likelihood
MMSE	Minimum mean square error
MRC	Maximum ratio combining
MSE	Mean square error
OSTBC	Orthogonal space-time block code
PAM	Pulse amplitude modulation
PDF	Probability distribution function
PEP	Pair-wise error probability
PSK	Phase shift keying
QAM	Quadrature amplitude modulation
QoS	Quality of service
QOSTBC	Quasi-orthogonal space-time block code
QPSK	Quadrature phase shift keying
RTS	Ready-to-send
SER	Symbol error rate
SISO	Single-input single-output
SNR	Signal-to-noise ratio
SR	Selective relaying
STBC	Space-time block code
STC	Space-time coding
TDD	Time division duplexing
TDMA	Time division multiple access
ZF	Zero forcing

Part I

Introduction

Introduction

The increasing prevalence of mobile devices and need for wireless information access had led to more demands on system designers to provide higher throughput and improved battery longevity. Wireless channels differ from their wired counterparts due to a phenomenon known as *fading*. As a result, techniques and algorithms from wired systems cannot always be directly applied to wireless scenarios.

Increasing the *diversity* of the transmission is a technique used to exploit the random fading effect in wireless systems. Diversity gains are possible when an information sequence is passed through multiple, independent realizations of the channel. *Spatial* diversity gains can be achieved by using multiple antennas. Performance is improved due to the increased likelihood of one of the data streams experiencing a good channel condition. Despite the promise shown by multiple antennas in mitigating the effects of fading, increasing the number of transmit antennas on small mobile devices is often impractical as a result of size and hardware complexity constraints.

To meet the demands of increased reliability, and spectral and power efficiency without increasing the size of mobile devices, fundamentally new paradigms are needed to improve performance. User cooperation, in which nodes pool their resources together and cooperatively transmit their data, is a transmission technique that has recently emerged for the network setting. Cooperation provides a method of achieving spatial diversity without the need for multiple antennas at the mobile nodes. Furthermore, utilizing cooperation leads to a higher throughput than direct communication among nodes [1].

The cooperation paradigm is certainly useful in the communication between handsets and base stations. Cooperation can lead to improved battery life and a higher throughput, thereby, enabling high data rate of multimedia applications. Although useful in the cellular context, conceptually

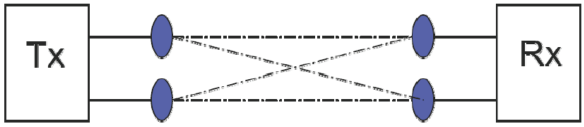

(a)

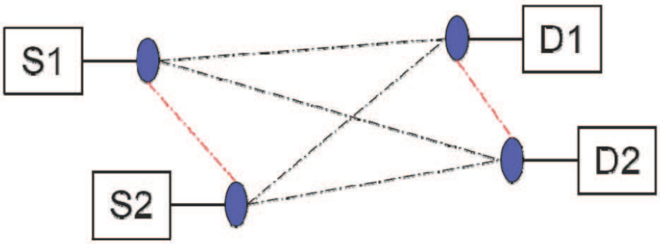

(b)

Figure 1.1: (a) Multiple input-multiple output (MIMO) technology. (b) Virtual MIMO, distributed antenna array.

cooperation can be applied in more general settings. Two immediate applications which can have improved performance from collaborating nodes are ad-hoc and sensor networks [2, 3]. For example, in sensor networks, where power conservation is of paramount importance, low complexity cooperation protocols can be used to reduce the likelihood of a decoding error. This allows the nodes to operate at a lower power and still meet target data and error rate requirements.

In the following, we first have a brief overview on the context of cooperative communications and wireless relay networks. Then, we explain the importance and literature review of the problems which are studied in this thesis. Therefore, an overview of the key concepts of power allocations methods in wireless relay network, distributed space-time code design, and performance analysis of wireless relay network is given.

In the following, we first describe the basic concepts of cooperative communications and wireless relay networks. We then address a number of challenging problems studied in this thesis. We review the related works on power allocation schemes, design of distributed space-time codes, and the performance analysis for a variety of wireless relay networks.

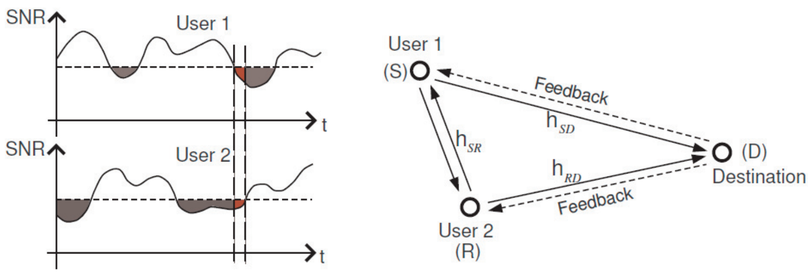

Figure 1.2: A three-node cooperative network model [8].

1 Basic Concepts of Cooperative Communications

Cooperative communications [1, 4–7] exploit the spatial diversity inherent in multiuser systems by allowing users with diverse channel qualities to cooperate and relay each other's messages to the destination. Each transmitted message is passed through multiple independent relay paths, and thus, the probability that the message fails to reach the destination is significantly reduced. Although each user may be equipped with only one antenna, their relays form a *distributed antenna array* to achieve the diversity gain of a Multiple-Input-Multiple-Output (MIMO) system. In Fig. 1.1(a), a communication link with multiple antenna technology is depicted. Fig. 1.1(b) shows a cooperative network in which nodes S1 and S2 form a distributed antenna array to transmit their data to the distributed receiving antennas D1 and D2.

Two features differentiate cooperative transmission schemes from conventional non-cooperative systems: 1) The use of multiple users' resources to transmit the data of a single source; and 2) A proper combination of signals from multiple cooperating users at the destination [8]. A canonical example is shown in Fig. 1.2, where two users are transmitting their local messages to the destination over independent fading channels. Suppose that the transmission fails when the channel enters a deep fade, i.e., when the signal-to-noise ratio (SNR) of the received signal falls below a certain threshold, as indicated with the grey region in Fig. 1.2. If the two users cooperate by relaying each others' messages and the inter-user channel is sufficiently reliable, the communication outage occurs only when both users experience poor channels simultaneously. Hence, cooperative diversity combats multipath fading by providing the receiver with redundant signal information from the relay and allowing the receiver average individual channel effects. A comparative study of various relay schemes and a discussion on the diversity gain of cooperative relay networks can be found in [9, 10].

1.1 Relay Channel

The simplest example of a cooperative network is the relay channel, which was first introduced in [11, 12]. Relaying occurs when a helper node assists the source-destination nodes in communicating. Although the concept of relaying is more than 30 years old, there are still many open problems for this channel. For example, in general the capacity of the relay channel is unknown even for the case of Gaussian channels. As a result, most of the research efforts have focused on finding efficient protocols that lead to lower bound on the capacity [5].

The basic ideas behind cooperative communication can be traced back to the ground-breaking work of Cover and El Gamal on the information theoretic properties of the relay channel [12]. This work analyzed the capacity of the three-node network consisting of a source, a destination, and a relay. It was assumed that all nodes operate in the same band, so the system can be decomposed into a broadcast channel from the viewpoint of the source and a multiple-access channel from the viewpoint of the destination. Many ideas that appeared later in the cooperation literature were first presented in [12]. However, in many respects the cooperative communication we consider is different from the relay channel in [12]. First, recent developments are motivated by the concept of diversity in a fading channel, whereas Cover and El Gamal mostly analyze capacity in an additive white Gaussian noise (AWGN) channel. Second, in [12], the relay's sole purpose is to help the main channel, whereas in cooperation the total system resources are fixed, and users act both as information sources as well as relays.

Traditionally, relays have been used to extend the range of wireless communication systems. However, in recent years, many exciting applications of relay communications have emerged. One such emerging application is to assist in the communication between the source and destination terminals via some cooperation protocol. By controlling medium access between source and relay terminals, coupled with the appropriate modulation or coding in such cooperative schemes, it has been found that the diversity of the communication system can be improved. In multi-user systems, different users can also act as cooperative partners or relays to share the resources and assist each other in information transmission, thereby creating a cooperative network.

1.2 Cooperative Protocols in Wireless Networks

We outline several cooperative protocols and demonstrate their robustness to fairly general channel conditions. We examine relaying protocols in which the relay either amplifies what it receives, or fully decodes, re-encodes, and retransmits the source message. We call these options amplify-and-forward (A&F) and decode-and-forward (D&F), respectively. Several cooperation strategies with different relaying techniques have been studied in [9]. In [13], Laneman and Wornell proposed the repetition and space-time algorithms to achieve cooperative diversity, where the mutual information and outage probability are analyzed. In repetition-based cooperation, relays retransmit the source signal in a time division multiple-access (TDMA) manner, while in space-time cooperations relays simultaneously retransmit source signal using an appropriate distributed space-time code. Distributed space-time codes (DSTC) have been proposed to improve the bandwidth efficiency of cooperative transmissions (see, e.g., [14–17]). In Section 3 of Introduction, we explain more about the DSTC.

We now review two of the main cooperative signaling methods, i.e., D&F and A&F.

1.2.1 Decode-and-Forward

This method is perhaps closest to the idea of a traditional relay. In this method a user attempts to detect and decode the partners' signal and then retransmits the decoded signal after re-encoding. The partners may be assigned mutually by the destination or via some other technique. For the purpose of partner (or relay) selection, several techniques are studied in the literature (e.g., see [18] and paper B in Chapter II of this thesis). It is possible that detection by the partner is unsuccessful, in which case cooperation can be detrimental to the eventual detection of the signal at the destination. Also, the destination needs to know the error characteristics of the inter-user channel for optimal decoding. To avoid the problem of error propagation, Laneman et al. [19] proposed a hybrid decode-and-forward method where, at times when the fading channel has high instantaneous signal-to-noise ratio (SNR), users decode-and-forward their partners' data, but when the channel has low SNR, users revert to a non-cooperative mode. In [20], the authors considered a regenerative relay in which the decision to cooperate is based on an SNR threshold and considered the effect of the possible erroneously detected and transmitted data at the relay.

1.2.2 Amplify-and-Forward

Another simple cooperative signaling is the amplify-and-forward (or non-regenerative) method. Each user in this method receives a noisy version of the signal transmitted by its partner. As the name implies, the user then amplifies and retransmits this noisy version. The destination combines the information sent by the user and partner and makes a final decision on the transmitted sinal. Although noise is amplified by cooperation, the destination receives two independently faded versions of the signal and can make better decisions on the detection of information. This method was proposed and analyzed by Laneman et al. [9, 19]. It has been shown that for the two-user case, this method achieves diversity order of two, which is the best possible outcome at high SNR. In A&F, it is assumed that the destination knows the inter-user channel coefficients to do optimal decoding, so some mechanism of exchanging or estimating this information must be incorporated into any implementation. Another potential challenge is that sampling, amplifying, and retransmitting analog values are technologically nontrivial. Nevertheless, A&F is a simple method that lends itself to analysis and thus has been very useful in furthering our understanding of cooperative communication systems.

2 Power Allocation Methods

A review of power allocation methods under different network topologies, cooperation methods, and channel state information (CSI) assumptions is given in this section. We first study the the dual-hop topology shown in Fig. 1.3, then a general multi-hop topology shown in Fig. 1.4. When the CSI is not known to the transmitter, the spatial diversity gain is achieved by allowing users to have a fair share of each others' resources. With the CSI knowledge, significant improvements in terms of bit error rate (BER),

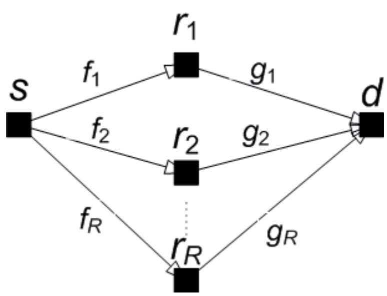

Figure 1.3: Wireless relay network consisting of a source s, a destination d, and R relays.

outage probability, or capacity can be attained by applying optimal power allocation among cooperating nodes.

2.1 Two-Hop Relay Networks

Consider the two-hop wireless relay network shown in Fig. 1.3. In the case of two-hop relay networks, power allocation becomes interesting due to the increased degree of freedom as a result of multiple transmitting nodes. As demonstrated in Fig. 1.3, let us consider R relay nodes, denoted by r_i, $i = 1, \ldots, R$, and let f_i and g_i denote the complex channel coefficients from the source s to the relay r_i and from r_i to the destination d, respectively. A two-phase cooperation is considered. That is, in the first phase, s broadcasts its message. In the second phase, the set of relays r_i, $i = 1, \ldots, R$ transmit the processed version of the received signals to the destination. The transmit powers of s and r_i are denoted by P_1 and $P_{2,i}$, respectively. The total power budget - either objective function or constraint - is imposed on the summation of relay powers, i.e., $\sum_{i=1}^{R} P_{2,i} = P_2$. The optimal power allocation scheme depends on specific quality-of service (QoS) measures such as the outage probability, capacity, SNR, and BER. The main objective is to find the optimal power allocation of P_1 and $P_{2,i}$ to maximize the QoS performance at the destination, subject to the total power constraint. The reverse optimization can be also considered, in which the total power is minimized, given some set of constraint on the QoS performance like BER or outage probability, as it is discussed in this thesis.

The system of multiple relays in Fig. 1.3 can be viewed as a virtual antenna array that transmits noisy versions of the source messages. When full CSI is known at the relays, precoding techniques can be used to compensate for both the channel gain and the phase rotation experienced by the relays to achieve better detection performance. For orthogonal relaying channels (repetition-based cooperation), d receives R copies of the source symbol from the relays with no interference among each other. With knowledge of the exact channel coefficients, the R symbols can be combined coherently at d to increase the received SNR. With the A&F scheme, the capacity of the parallel relay channel can be found as [21]

$$C_{\text{A\&F}} = \frac{1}{2} \log \left(1 + \sum_{i=1}^{R} \frac{P_1 P_{2,i} |f_i|^2 |g_i|^2}{P_1 |f_i|^2 + P_{2,i} |g_i|^2 + 1} \right), \tag{1.1}$$

and the capacity-maximizing power allocation strategy results in the following water-filling solution [21] $P_i = \frac{|f_i|^2}{\sqrt{\gamma_i}} \left(\frac{1}{\sqrt{\eta}} - \frac{1}{\sqrt{\gamma_i}} \right)^+$, where $(x)^+ = \max(x, 0)$ and $\gamma_i = \frac{|f_i|^2 |g_i|^2}{P_1 |f_i|^2 + 1}$. The Lagrange multiplier, η, is chosen to meet the total power constraint of the relay nodes. Note that relay node r_i is allowed to transmit if and only if $\gamma_i > \eta$. Power allocation for the D&F scheme with orthogonal relay channels was derived in [13] to maximize the capacity. Assume a set of relay nodes, denoted by $\mathcal{R}_d$, is able to correctly decode the messages transmitted by the source. These relays decode and forward the messages to the destination, acting as multiple antennas on a single terminal. In the low SNR regime, it is shown in [22] that optimum power allocation is to choose the relay node among $\mathcal{R}_d$ with the best channel towards the destination and allocate all the power to that node. This means that the selective relaying scheme is optimal for the D&F scheme with orthogonal relay channels.

For the case of non-orthogonal channels, in which relays simultaneously transmit toward the destination, beamforming techniques can be used. When full CSI is available at the relays, the optimal beamforming factors for A&F networks were derived in [23] to optimize the received SNR. When the phase information is not available to the relays, it is shown in [24–26] that all power should be allocated to one relay. It was shown in [25] that this selective relaying strategy is optimal in minimizing the outage probability for the D&F space-time-encoded scheme under the total power constraint. Also, in [26], we have derived a selective relaying strategy for for the A&F space-time-encoded scheme, which is optimal in the sense of minimizing the symbol error rate (SER). The power allocation strategy that maximizes the capacity or SER may not extend the network lifetime since these objective functions do not take the residual battery energy of each relay node into account. To extend the network lifetime, the selection strategies was used in [27, 28], and a power allocation scheme with considering residual battery energy at relays is proposed in this thesis (see [29]). With this strategy, the network lifetime can be extended considerably when compared to the power allocation that depends only on the channel conditions.

It is often difficult to obtain the instantaneous CSI for all links of the system in practice. To address this issue, power allocation strategies with less stringent assumptions on the CSI have been proposed. Specifically, a power allocation strategy for the D&F space-time-encoded scheme was derived in [30] by assuming that the ith relay knows only the instantaneous channel gain of the $s - r_i$ link, i.e., $|f_i|$, and the average channel gain of the $r_i - d$ link, i.e., $\mathbb{E}[|g_i|^2]$. Then, a near optimal solution that minimizes the outage probability by selecting a set of relays and allocating them with an equal share of power was developed in [30]. With the same amount of channel information, the optimal power allocation strategy for the A&F scheme was derived in [31]. Furthermore, when only statistics of channels are available at the relays, power allocation strategies for the A&F space-time-encoded scheme are proposed in [26], which is included as paper B in this thesis.

2.2 Multihop Relay Networks

The cooperative transmission system can be extended to a multihop scenario. The idea will be similar as the two-hop case. One possible hopping strategy could be that by concatenating multiples of the three-node or the two-hop networks each level of relay nodes retrieves the source information by processing the signals from the two closest previous levels of relays. Instead of restricting to the two-hop cooperation, signals from m hops away can be combined to enhance the detection at the destination.

In conventional multi-hop systems, the received signals that contain insufficient energy for reliable detection are discarded, e.g., signals from distant transmitters. On the contrary, with cooperation, the receiver may combine signals transmitted via different relays, regardless of the signal strength, to enhance the detection performance or to reduce the energy consumption. In [32], the concept of multihop diversity is introduced where the benefits of spatial diversity are achieved from the concurrent

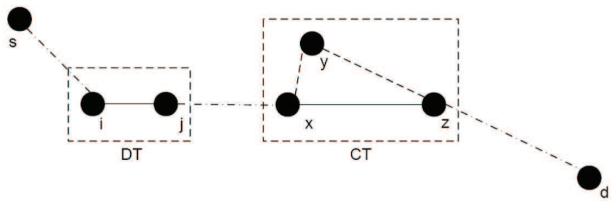

Figure 1.4: Multihop relay network: Cooperative Transmission (CT) and Direct Transmission (DT) modes as building blocks for any route [34].

reception of signals that have been transmitted by multiple previous terminals along the single primary route. This scheme exploits the broadcast nature of wireless networks where the communications channel is shared among multiple terminals.

On the other hand, the routing problem in the cooperative radio transmission model over static channels is studied in [33], where it is allowed that multiple nodes along a path coordinate together to transmit a message to the next hop as long as the combined signal at the receiver satisfies a given SNR threshold value. The gain in energy efficiency and the respective power allocation strategies have been also studied in [3, 34, 35]. In paper G, in the included papers of this thesis, a new cooperative routing protocol is introduced using the Alamouti space-time code for the purpose of energy savings, given a required outage probability at the destination. Two efficient power allocation schemes are derived, which depend only on the statistics of the channels.

It has been proven in [36] that the minimum energy cooperative path routing problem, i.e., to find the minimum-energy route using cooperative radio transmission, is *NP-complete*. This is due to the fact that the optimal path could be a combination of cooperative transmissions and point-to-point transmissions. Therefore, two types of building blocks can be considered: direct transmission (DT) and cooperative transmission (CT) building blocks. In Fig. 1.4 the DT block is represented by the link (i, j), where node i is the sender and node j is the receiver. In addition, the CT block is represented by the links (x, y), (x, z), and (y, z), where node x is the sender, node y is a relay, and node z is the receiver. The route can be considered as a cascade of any number of these two building blocks, and the total power of the route is the summation of the transmission powers along the route. Thus, the minimum energy cooperative path routing problem can be solved by applying any distributed shortest-path routing algorithm such as the distributed Bellman-Ford algorithm [34].

3 Distributed Space-Time Coding

The main problem with the repetition-based multinode D&F protocol [37] and A&F protocol [38], as it is discussed in previous section, is the loss in data rate as the number of relay nodes increases. This is due to the multi-phases nature of repetition-based cooperation. The use of orthogonal subchannels for the relay node transmissions, either through TDMA or FDMA, results in a high loss of the system spectral efficiency. This leads to the use of what is knocwn as DSTC, where relay nodes are allowed to simultaneously transmit over the same channel by emulating a space-time code.

In wireless communication systems, the spatial diversity can be achieved by multiple independent paths between multiple antennas at the transmitter and the receiver, possibly in conjunction with space-time block codes (STBCs). Recently, the idea of space time coding has been applied in wireless relay networks in the name of distributed space time coding to extract similar benefit as in point to point MIMO systems. Several works have considered the application of the existing space-time codes in a distributed fashion for the wireless relay network (e.g., see [39–41]). Most of these works have considered a two-hop relay network where a direct link between the source and destination nodes does not exist, as shown in Fig. 1.3 - In paper A of the included paper in this thesis, the direct link between the source and destination nodes is also incorporated in the DSTC. Mainly there are two types of distributed space time coding techniques discussed in the literature: (1) D&F based distributed space time coding [13], wherein a subset (chosen based on some criteria) of the relay nodes decode the symbols from the source and transmit a row/column of a STBC and (2) A&F based distributed space-time coding [42], where all the relay nodes perform linear processing on the received symbols according to a distributed space time block code (DSTBC) and transmit the resulting symbols to the destination. The A&F based distributed space time coding is of special interest because the operations at the relay nodes are greatly simplified and moreover there is no need for every relay node to inform the destination once every quasi-static duration whether it will be participating in the distributed space time coding process as is the case

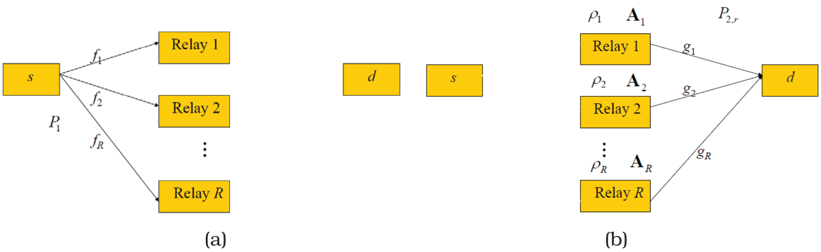

Figure 1.5: The A&F DSTC system consists of two phase: (a) In Phase 1, the source transmits T symbols with average power P_1. (b) In Phase 2, the linear combination of the amplified version of the received signals are retransmitted.

in D&F based distributed space time coding [13]. The design of practical DSTCs leading to reliable communication in wireless relay networks has been considered in [43–45].

In [46], a cooperative strategy was proposed, which achieves a diversity factor of R in a R-relay wireless network, using the so-called distributed space-time codes. In this strategy, a two-phase protocol is used. In phase one, the transmitter sends the information signal to the relays and in phase two, the relays send information to the receiver. The signal sent by every relay in the second phase is designed as a linear function of its received signals and their complex conjugate (see Fig. 1.5). It was shown that the relays can generate a linear space-time codeword at the receiver, as in a multiple antenna system, although they only cooperate distributively. The technique was also shown to achieve optimal diversity at high SNRs [46]. The design of practical DSTCs that lead to reliable communication in wireless relay networks has also been recently considered [43–45].

Consider a wireless network with $R+2$ nodes, which consists of a source s, a destination d, and R relays, $r_1, r_2, \ldots, r_R$. As shown in Fig. 1.5, there is one transmit node and one receive node. All the other R nodes work as relays. Every node has a single antenna, which can be used for both transmission and reception. Denote the channel from the transmitter to the rth relay as f_r, and the channel from the rth relay to the receiver as g_r. There is no direct link between the transmitter and receiver. We assume that f_r and g_r are i.i.d. flat fading channels, and a block-fading model is used by assuming a coherence interval T, i.e., f_r and g_r keep constant for a block of T transmissions and jump to other independent values for another block. Note that in Fig. 1.5(b), ρ_r is the scaling factor at relay r, $P_{2,r}$ is the average transmitted power from the rth relay during the second phase, and $\boldsymbol{A}_r$ of size $T \times T$ is corresponding to the rth column of the $T \times R$ dimensional space-time code matrix.

To have a simple decoding technique for DSTC like the space-time code in multi-antenna systems, the received signal at the destination can be calculated to be

$$\boldsymbol{y} = \sqrt{P_1 T}\,\boldsymbol{S}\boldsymbol{h} + \boldsymbol{w}_T, \tag{1.2}$$

where $P_1 T$ is the average total transmitted energy in T intervals, $\boldsymbol{h}$, which is $R \times 1$, is the equivalent channel matrix, and $\boldsymbol{w}_T$, which is $T \times 1$, is the equivalent noise. The vector $\boldsymbol{w}_T$ is clearly influenced by the choice of the space-time code. Hence, (1.2) shows that the $T \times R$ matrix $\boldsymbol{S}$ works like the space-time code in multi-antenna systems.

In (1.2), $\boldsymbol{S}$ is $T \times R$ dimensional DSTC code matrix. For the case of A&F, the DSTC matrix $\boldsymbol{S}$ should be appropriately designed, such as the codes proposed in [46] or [44]. For example, a QOSTBC code matrix is proposed in [46] as follows

$$\boldsymbol{S} = \begin{bmatrix} s_1 & s_2^* & s_3^* & s_4 \\ s_2 & -s_1^* & s_4^* & -s_3 \\ s_3 & s_4^* & -s_1^* & -s_2 \\ s_4 & -s_3^* & -s_2^* & s_1 \end{bmatrix}, \tag{1.3}$$

where s_1, s_2, s_3, and s_4 are transmitted symbols and $\boldsymbol{S}$ is normalized such that $\mathbb{E}[tr\{\boldsymbol{S}^H\boldsymbol{S}\}] = 1$.
For D&F scheme, $\boldsymbol{S}$ could be same as space-time codes in the context of MIMO. If the decoding at some relays fails, their corresponding columns are replaced by zero. In [45], it was shown that for real-valued i.i.d. Rayleigh channels, the DSTC design problem becomes similar to the code design problem for MIMO communication. However, in [43, 47], it is assumed that the channels have i.i.d. *complex* Gaussian distributions, which is more practical assumption. In paper A in the included papers in this thesis, the design of DSTC using generalized quasi-orthogonal STBC (QOSTBC) is proposed, in which any number of relays can be employed to increase the diversity order. In addition, suboptimal linear decoder can be used to decrease the complexity, while the full diversity order is achievable. Other DSTCs have also been proposed in [42, 48] to improve the bandwidth efficiency of cooperative.

Although A&F DSTC does not need instantaneous channel information at the relays, it requires full (transmitter-to-relays and relays-to-receiver) channel information at the receiver, implying that training symbols need to be sent from both the transmitter and relays. For example, in [42], the destination was assumed to have perfect knowledge of all the channel fading gains from the source to the relays and those from the relays to the destination. To overcome the need for channel knowledge, distributed differential space time coding was studied in [48–51], which is essentially an extension of differential unitary space time coding for point to point MIMO systems to the relay network case. In [52], a A&F DSTC involving a combination of training, channel estimation and detection in conjunction with existing coherent distributed STBCs is proposed for non-coherent communication in A&F relay networks.

Distributed space-time coding was generalized to networks with multiple-antenna nodes in [53], and the design of practical DSTCs with multiple antennas terminals has also been recently considered in [48, 54, 55]. In [54, 55], which due to the space limitation we have not included them in this thesis, the orthogonal and quasi-orthogonal space-time design is used for A&F based wireless relay networks with multiple-antenna nodes.

4 Performance Analysis of Wireless Systems

4.1 System Performance Measures

4.1.1 Average SNR

Probably the most common and well understood performance measure characteristic of a digital communication system is SNR. In simple mathematical terms, if γ denotes the instantaneous SNR (a random variable) at the receiver output that includes the effect of fading, then

$$\bar{\gamma} = \int_0^\infty \gamma p_\gamma(\gamma) d\gamma, \tag{1.4}$$

is the average SNR, where $p_\gamma(\gamma)$ denotes the probability density function (PDF) of γ.

4.1.2 Outage Probability

Another standard performance criterion characteristic of diversity systems operating over fading channels is the so-called outage probability - denoted by P_{out}. The outage probability defined as the probability that the instantaneous error probability exceeds a specified value or equivalently the probability that the output SNR, γ, falls below a certain specified threshold, γ_{th}. Mathematically speaking, we have

$$P_{\text{out}} = \int_0^{\gamma_{\text{th}}} p_\gamma(\gamma) d\gamma, \tag{1.5}$$

which is the cumulative distribution function (CDF) of γ, evaluated at $\gamma = \gamma_{\text{th}}$.

4.1.3 Average SER

The third performance criterion and undoubtedly the most difficult of the three to compute is the average SER[1]. On the other hand, it is the one that is most revealing about the nature of the system behavior and the one most often illustrated in documents containing system performance evaluations. Thus, it is of primary interest to have a method for its evaluation that reduces the degree of difficulty as much as possible. The primary reason for the difficulty in evaluating average SER lies in the fact that the conditional (on the fading) SER is, in general, a nonlinear function of the instantaneous SNR, as the nature of the nonlinearity is a function of the modulation/detection scheme employed by the system. Thus, for example, in the multichannel case, the average of the conditional SER over the fading statistics is not a simple average of the per channel performance measure as was true for average SNR. Nevertheless, the moment generating function (MGF)-based approach can be used in simplifying the analysis and in a large variety of cases allows unification under a common framework [56].

Averaging the conditional probability of error, which is the probability of error over AWGN channels, the average SER can be shown as

$$P_e = \int_0^{\infty} P(E|\gamma) p_\gamma(\gamma) d\gamma, \tag{1.6}$$

where $P(E|\gamma)$ is the conditional SER. When characterizing the performance of coherent digital communications, the generic form of the expression for the error probability involves the Gaussian Q-function with an argument proportional to the square root of the instantaneous SNR of the received

[1]The discussion that follows applies, in principle, equally well to average BER. Furthermore, the terms bit error probability (BEP) and symbol error probability (SEP) are often used in the literature as alternatives to BER and SER.

signal. In the case of communication over a slowly fading channel, the instantaneous SNR (γ) is a time-invariant random variable with a PDF, $p_\gamma(\gamma)$. To compute the average error probability, one can evaluate an integral whose integrand consists of the product of the above-mentioned Gaussian Q-function and fading PDF, that is [56, Eq. (5.1)]

$$P_e = \int_0^\infty c\, Q\left(\sqrt{g\gamma}\right) p_\gamma(\gamma) d\gamma, \tag{1.7}$$

where c and g are constants that depend on the specific modulation/detection combination. Furthermore, it can be shown that (1.7) can be rewritten as [56, Eq. (5.3)]

$$P_e = \int_0^\infty M_\gamma\left(\frac{-g}{2\,\sin^2\theta}\right) p_\gamma(\gamma) d\gamma, \tag{1.8}$$

where $M_\gamma(s)$ is the MGF of γ ,i.e., $M_\gamma(s) \triangleq \int_0^\infty e^{s\gamma} p_\gamma(\gamma) d\gamma$, which is the Laplace transform of $p_\gamma(\gamma)$ with the exponent reversed in sign. Since tables of Laplace transforms are readily available, the desired form of the Gaussian Q-function therefore allows evaluation of P_e in the simplest possible way, in most cases resulting in a single integral on θ (when the Laplace transform is available in closed form).

4.2 Multipath Fading

Multipath fading is due to the constructive and destructive combination of randomly delayed, reflected, scattered, and diffracted signal components. This type of fading is relatively fast and is therefore responsible for the short-term signal variations. Depending on the nature of the radio propagation environment, there are different models describing the statistical behavior of the multipath fading envelope. In this thesis, we consider the Rayleigh, Rician, and Nakagami-m channel models, which are mostly used for analyzing wireless systems:

4.2.1 Rayleigh

The Rayleigh distribution is frequently used to model multipath fading with no direct line-of-sight (LOS) path. In this case, the received instantaneous SNR per symbol of the channel, i.e., γ, is distributed according to

$$p_\gamma(\gamma) = \frac{1}{\overline{\gamma}} \exp\left(\frac{-\gamma}{\overline{\gamma}}\right), \tag{1.9}$$

where $\overline{\gamma} = \frac{E_s \sigma_h}{\mathcal{N}_0}$ is the average SNR per symbol, E_s is the energy per symbol, σ_h is the link path-loss or variance of the channel coefficient h, and the additive noise at all receiving terminals is modeled as zero-mean complex Gaussian random variables with variance $\mathcal{N}_0$.

Rayleigh fading is viewed as a reasonable model for tropospheric and ionospheric signal propagation as well as the effect of heavily built-up urban environments on radio signals [57].

4.2.2 Rician (Nakagami-n)

The *Rician distribution* is also known as the Nakagami-n distribution [58]. It is often used to model propagation paths consisting of one strong direct LOS component and many random weaker components. Here, the received SNR follows the distribution [56, Eq. (5.10)]

$$p_\gamma(\gamma) = \frac{(K+1)}{\overline{\gamma}} e^{-\left[K+(K+1)\frac{\gamma}{\overline{\gamma}}\right]} I_0\left(2\sqrt{\frac{K(K+1)\gamma}{\overline{\gamma}}}\right), \tag{1.10}$$

where K is the Rician factor of the source-destination link, which is defined as the ratio of the power in the LOS component to the power in the other (non-LOS) multipath components [56]. In (1.10), $I_0(\cdot)$ is the modified Bessel function of first kind and order zero, and $\overline{\gamma} = \mathbb{E}[\gamma]$. The Rician distribution spans the range from Rayleigh fading ($K = 0$) to no fading (constant amplitude) ($K = \infty$). This type of fading is typically observed in the first resolvable LOS paths of microcellular urban and suburban land-mobile [59], picocellular indoor [60], and factory [61] environments. It also applies to the dominant LOS path of satellite [62] and ship-to-ship [63] radio links.

4.2.3 Nakagami-m

The Nakagami-m PDF, which is in essence a central chi-square distribution, is given by [56, Eq. (5.14)]

$$p_\gamma(\gamma) = \frac{m^m \gamma^{m-1}}{\overline{\gamma}^m \Gamma(m)} e^{-\frac{m\gamma}{\overline{\gamma}}}, \tag{1.11}$$

where m is the Nakagami-m fading parameter, which is a real number ranging from $\frac{1}{2}$ to $+\infty$, $\Gamma(\cdot)$ is the gamma function, and $\overline{\gamma}_h = \mathbb{E}[\gamma_h]$.

The Nakagami-m distribution spans via the m parameter the wide range of the multipath distributions. For instance, it includes the one-sided

Gaussian distribution ($m = \frac{1}{2}$) and the Rayleigh distribution ($m = 1$) as special cases. In the limit as $m \to +\infty$, the Nakagami-m fading channel converges to a non-fading AWGN channel. Furthermore, when $m > 1$, there is a one-to-one mapping between the m parameter and the Rician K factor (see e.g., [56, Eq. (2.26)]), allowing the Nakagami-m distribution to closely approximate the Rician distribution.

The Nakagami-m distribution often gives the best fit to land-mobile [64] and indoor-mobile [65] multipath propagation, as well as scintillating ionospheric radio links [66].

4.3 Performance Analysis of Wireless Relay Networks

The performance analysis of multihop wireless communication systems operating in fading channels has been an important field of research in the past few years. Thus, performance analysis of cooperative networks has yielded many interesting results including average SNR, information theoretic metrics like outage probability, and average SER expressions over fading channels.

The analytical expressions for the performance of wireless relay network can also give us insight into the optimal allocation of the resources like power and bandwidth. Specially, in A&F relay networks, in which the performance metrics at the destination usually depend on channel characteristics of all hops, the performance analysis becomes more challenging, comparing to the collocated MIMO or D&F relay systems. Hence, a large portion of this thesis is dedicated to the performance analysis of A&F based relay networks.

Also in this thesis, for sufficiently large SNR, the close-form expressions for the average SER and outage probability are derived under different topologies, cooperation methods, and CSI assumptions. The simplicity of the asymptotic results provides valuable insights into the performance of cooperative networks and suggests means of optimizing them. In addition, the diversity order of the wireless systems can be found via the asymptotic behavior of the average SER or outage probability. A tractable definition of the diversity or diversity gain, which is used in this thesis is [67, Eq. (1.19)]

$$G_d = - \lim_{\mathrm{SNR} \to \infty} \frac{\log (P_e)}{\log (\mathrm{SNR})}, \tag{1.12}$$

where instead of the average SER P_e, the outage probability P_{out} can be also used.

The average symbol error rate formula allows us to clearly illustrate the advantage that the distributed diversity system has in overcoming the severe penalty in signal-to-noise ratio caused by Rayleigh fading. In [39], DSTC based on the Alamouti scheme and A&F cooperation protocol was analyzed and an expression for the average SER was derived. Authors in [68] presented an exact average symbol error rate analysis for the repetition-based cooperation, in which relays transmit in orthogonal channels via TDMA or FDMA. Using simple bounds on the probability of error, [68] shows that the cooperative network amplifying relays achieves full diversity order. Hasna and Alouini in [69] have presented a useful and semi-analytical framework for the evaluation of the end-to-end outage probability of multihop wireless systems with A&F CSI-assisted relays over Nakagami-m fading channels. Moreover, the same authors have studied the dual-hop systems with D&F and A&F (CSI-assisted or fixed gain) relays over Rayleigh [70], [71] and Nakagami-m [72] fading channels. Recently, Boyer et al. [32], have proposed and characterized four channel models for multihop wireless communication and also have introduced the concept of multihop diversity. Finally, Karagiannidis et al. [73] have studied the performance bounds for multihop wireless communications with blind (fixed gain) relays over Rice, Hoyt, and Nakagami-m fading channels, using the moments-based approach [74]. In [75], efficient performance bounds are presented for the end-to-end SNR of multihop wireless communication systems with CSI-assisted or fixed gain relays operating in non-identical Nakagami-m fading channels. Using expressions for MGF and PDF, closed-form lower bounds are presented in [75] for important end-to-end system performance metrics, such as outage probability and average SER for BPSK, while simple asymptotic expressions are also given for the bounds at high SNRs.

For sufficiently high SNR, [38] derives general average SER expressions, for A&F links with multiple cooperating branches, composed of multiple cooperating hops, as it is shown in Fig. 1.6. In [38] the authors derived asymptotic average symbol error probability for amplify-and-forward cooperative diversity networks. The resulting expressions derived in [38] (using the bounding approach) are general for any type of fading distributions provided the PDF of zero instantaneous SNR is not zero, which is not applicable for the Nakagami-m fading distribution. In [76], the error rate and the outage probability of cooperative diversity wireless networks with A&F relaying are determined over independent, non-identical, Nakagami-m fading channels.

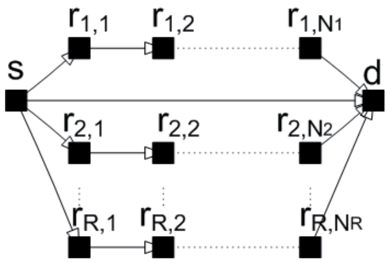

Figure 1.6: Wireless relay network with multihop, multi-branch transmission.

In [40], a performance analysis of the gain of using D&F based cooperation among nodes was considered, assuming that the number of relays that are available for cooperation is a Poisson random variable. The authors compared the performance of different distributed space-time codes designed for the MIMO channels under this assumption. In [77], authors considered a D&F cooperation protocol, and derived closed-form SER for the D&F cooperation systems with M-PSK and M-QAM signals. Since the closed-form SER formulation is complicated, [77] established two SER upper bounds to show the asymptotic performance of the cooperation system, in which one of them is tight at high SNR. Based on the SER performance analysis, the optimum power allocation for the cooperation systems is determined.

5 Summary of the Included Papers

This dissertation consists of seven papers numbered with letters (A-G). In this section, we present a brief summary of these papers.

5.1 Paper A

B. Maham, A. Hjørungnes, and G. Abreu, "Distributed GABBA Space-Time Codes in Amplify-and-Forward Relay Networks," *IEEE Transactions on Wireless Communications*, volume 8, issue 2, pages 2036 - 2045, April 2008.

In Paper A, we give a more comprehensive presentation of the results we presented in [44]. We consider the design of practical distributed space-time codes for wireless relay networks using the A&F scheme, where each relay transmits a scaled version of the linear combinations of the received symbols and their complex conjugate.

Our focus is on the space-time cooperation using generalized ABBA (GABBA) codes [78, 79], which are systematically constructed, orthogonally decodable, full-rate, full-diversity space-time block codes. Our scheme is valid for any number of relays with linear orthogonal decoding in the destination, which make it feasible to employ large numbers of potential relays to improve the diversity order. We generalize the distributed space-time codes in A&F mode when the source-destination link contributes in both phases of the transmission.

Another contribution is that we derive the approximate average SER for A&F DSTC with M-PSK and M-QAM modulations over Rayleigh-fading channels, which is valid for *any* full-diversity, full-rate space-time block codes, such as distributed GABBA codes and the codes given in [43]. The analytical results are confirmed by simulations, indicating both the accuracy of the analysis, and the fact that low-complexity, flexible, and high-performing distributed space-time block codes can be designed based on GABBA codes.

5.2 Paper B

B. Maham and A. Hjørungnes, "Power Allocation Strategies for Distributed Space-Time Codes in Amplify-and-Forward Mode," *EURASIP Journal on Advances in Signal Processing*, volume 2009, Article ID 612719, 13 pages, 2009. doi:10.1155/2009/612719.

In this paper, we show that the DSTC based on [46], in which relays transmit the linear combinations of the scaled version of their received signals leads to a new opportunistic relaying, when maximum instantaneous SNR based power allocation is used. Furthermore, assuming M-PSK and M-QAM modulations, we analyze the performance of cooperative diversity wireless networks using A&F opportunistic relaying. We also derive an approximate formula for the SER of A&F DSTC. First, the probability density function is derived and then MGF of the received SNR at the destination. Then, the MGF is used to determine the SER in Rayleigh fading channels. Assuming the use of full-diversity space-time codes, we derive two power allocation strategies minimizing the approximate SER expressions, for constrained transmit power. We analyze the diversity order of AF opportunistic relaying based on the asymptotic behavior of average SER. Based on the proposed approximated SER expression, it is shown that the proposed scheme achieves the diversity order of R.

5.3 Paper C

B. Maham and A. Hjørungnes, "Performance Analysis of Repetition-Based Cooperative Networks with Partial Statistical CSI at Relays," *IEEE Communications Letters*, volume 12, issue 11, pages 828-830, November 2008.

In Paper C, we apply AF relaying with partial statistical CSI to the case of repetition-based cooperation, in which R amplifying relays retransmit the source's signal in a TDMA manner. The network channels are modeled as independent, non-identical, Rayleigh distributed coefficients. The exact symbol error rate is derived using the MGF. We derive the probability density function and MGF of the total SNR. Then, the MGF is used to determine the SER. The diversity order of the amplify-and-forward cooperation with partial statistical channel state information is also found via the asymptotic behavior of the average SER, and it is shown that the cooperative network achieves full diversity.

5.4 Paper D

B. Maham and A. Hjørungnes, "Asymptotic Performance Analysis of Amplify-and-Forward Cooperative Networks in a Nakagami-m Fading Environment," *IEEE Communications Letters*, volume 13, issue 5, pages 300-302, May 2009.

In Paper D, we derive tight approximations for the average SER of repetition-based cooperative networks over independent non-identical Nakagami-m fading channels in AF mode. The network consists of a source, R parallel relays. The approximated average SER is investigated. For sufficiently large SNR, this letter derives a closed-form average SER when m is an integer. The simplicity of the asymptotic results provides valuable insights into the performance of cooperative networks and suggests means of optimizing them.

5.5 Paper E

B. Maham and A. Hjørungnes, "Performance Analysis of Amplify-and-Forward Opportunistic Relaying in Rician Fading," *IEEE Signal Processing Letters*, volume 16, issue 8, pages 643-646, August 2009.

In Paper E, we derive tight approximations for the average SER of opportunistic relaying networks over independent non-identical Rician fading channels in AF mode. We first derive the PDF of the approximate value of the total SNR. Then, assuming M-PSK or M-QAM modulations, the PDF is used to determine the SER. For sufficiently large SNR, this letter derives the closed-form average SER. The simplicity of the asymptotic results provides valuable insights into the performance of cooperative networks and suggests means of optimizing them.

5.6 Paper F

B. Maham, A. Hjørungnes, and M. Debbah "Power Allocations in Minimum-Energy SER Constrained Cooperative Networks," *Annals of Telecommunications - Annales des Télécommunications, special issue on Cognitive Radio*, volume 64, issue 7, pages 545-555, August 2009.

In this paper, we propose power allocation strategies that take both the statistical CSI and the residual energy information into account to prolong the network lifetime while meeting the SER QoS requirement of the destination. In particular, we focus on the repetition-based AF cooperation scheme in an environment with one source transmitting to the destination through multiple relays that form a distributed antenna array employing the repetition-based cooperation [38]. In [27] and [28], the received instantaneous SNR at the destination is assumed as a required QoS. However, SER is a more meaningful metric to be considered as QoS. Moreover, our proposed power allocation scheme is independent of the knowledge of instantaneous CSI at the relay nodes. Thus, the proposed scheme can easily be employed in practical low-complex wireless relay networks, like sensor networks. In [38] and [80], uniform power allocation among the source and relays is assumed for a given SER constraint, which is not efficient in term of network lifetime maximization. Here, we propose algorithms that maximize the network lifetime with SER constraint in AF based cooperative networks given in [38].

5.7 Paper G

B. Maham, R. Narasimhan, and A. Hjørungnes, "Energy-Efficient Space-Time Coded Cooperative Routing in Multihop Wireless Networks," in *Proc. of IEEE Global Telecommunications Conference (GLOBECOM 2009)*, Honolulu, Hawaii, USA, November - December 2009.

In this paper, a cooperative multihop routing scheme is proposed for Rayleigh fading channels. The investigated system can achieve considerable energy savings compared to non-cooperative multihop transmission, when there is an outage probability QoS requirement at the destination node. Two power control schemes, i.e., *distributed* and *centralized* power allocations are derived to minimize the total transmission power given the outage probability constraint. Using some tight approximations, simple closed-form power allocations are presented without requiring the knowledge of CSI; hence, the proposed schemes can be implemented in real wireless systems. Numerical results show that the proposed power allocation strategies provide considerable gains compared to non-cooperative multihop transmission.

6 Main Contributions of the Dissertation

The main contributions of this dissertation can be summarized as follows:

- Design of distributed GABBA codes which are applicable in A&F DSTC system.
- Found approximate SER expressions for A&F DSTC with M-PSK and M-QAM modulations over Rayleigh-fading channels.
- Analyzed the diversity order of A&F DSTCs based on the asymptotic behavior of average SER.
- Derived the optimum power allocations among relays for A&F DSTC system by maximizing the SNR at the destination.
- Derived the average SER of A&F opportunistic relaying system with M-PSK or M-QAM modulations over Rayleigh-fading channels.
- Analyzed the diversity order of AF opportunistic relaying based on the asymptotic behavior of average SER.

- Proposed two power allocation schemes for A&F DSTC based on minimizing the target SER, given the knowledge of statistical CSI of source-relay links at the relays.

- Found the exact average SER and the diversity order of A&F relaying with repetition-based cooperation and partial statistical CSI over Rayleigh-fading channels.

- Derived tight approximations for the average SER of repetition-based cooperative networks over independent non-identical Nakagami-m fading channels in A&F mode.

- Assuming sufficiently high SNR, found a simple closed-form average SER expression for repetition-based cooperative networks over independent non-identical Nakagami-m fading.

- Derived tight approximations for the average SER of opportunistic relaying networks over independent non-identical Rician fading channels in A&F mode.

- Assuming sufficiently high SNR, derived a simple closed-form average SER expression, for A&F opportunistic relaying links over independent non-identical Rician fading.

- Derived the optimal power allocation strategy in A&F cooperative network that minimizes the total relay power subject to the SER requirement at the destination.

- Obtained power allocation strategies that maximize the network lifetime given a required SER constraint for energy-limited nodes in the cooperative network.

- Proposed a new energy-efficient cooperative multihop routing scheme for Rayleigh fading channels when there is an outage probability quality-of-service (QoS) requirement at the destination node.

- Implemented two *distributed* and *centralized* power control schemes to minimize the total transmission power given the outage probability constraint.

7 Suggestions for Future Research and Extensions

In this section, we will discuss some issues that can be interesting to investigate in the future.

A large part of this thesis is about design and performance analysis of orthogonal and quasi-orthogonal space-time block codes. On the other hand, STBCs from coordinate interleaved orthogonal designs (CIOD) have been attracting wider attention due to their amenability for fast (single-symbol) maximum-likelihood decoding, and full-rate with full-rank over quasi-static fading channels [81]. Hence, a natural extension of our work is to apply CIOD space-time codes to a distributed network and study the performance analysis and optimum rotation angles in such systems.

In this thesis, simple network models are considered and strict synchronization among distributed users are always assumed, which are difficult to achieve in practice. A major challenge lies in the design of asynchronous cooperation strategies. Furthermore, since cooperation involves the interaction between multiple users, the system inevitably requires a cross-layered study between the physical layer and the medium access control (MAC) or higher layers. In the future, we focus on the advantages of cooperative communications in resource constrained networks and show how the resource utilization can be made more efficient with power allocation and by exploiting data dependencies.

As an extension of our work over cooperative routing in resource-constrained wireless multihop networks, the effect of delay constraint can be studied. It can be shown that our proposed distributed power allocation can be employed in a broadcast network with cooperating destinations for the purpose of minimizing the total transmit power of the network. In this scenario, there is one source and multiple cooperating destinations with a given outage probability for each node. An important extension might be to study the ways to increase the achievable rate of the system, which is affected due to the multi-phases nature of the multihop transmission. For example, the incremental relaying method can be embedded in the cooperative routing. Other possible approach could be multihop communication with spatial reuse, in which source start transmitting new symbols before the previously transmitted ones reach the destination. In addition, as an extension of work in paper G, one can take into account decoding errors at relay nodes as proposed in [82], and find more efficient power allocation factors.

In this thesis, we proposed some opportunistic relaying techniques.

In the future, one can apply relay selection techniques into HARQ multi-relay protocols which leads to full spatial diversity. Then, the delay-limited throughput [83] is going to be maximized given a target outage probability, defined as the probability of packet failure after L HARQ rounds, and maximum number of HARQ rounds L, which represents the delay constraint.

8 Journal and Conference Contributions during Ph.D. Studies

During the Ph.D. studies, the author has contributed to the following journals and conference publications:

List of journal publications during Ph.D. studies:

- B. Maham and A. Hjørungnes, *"Opportunistic Relaying for Space-Time Coded Cooperation with Multiple Antenna Terminals,"* Submitted August 9, 2009 to IEEE Transactions on Vehicular Technology.
- B. Maham and A. Hjørungnes, *"Power Allocation Strategies for Distributed Space-Time Codes in Amplify-and-Forward Mode,"* EURASIP Journal on Advances in Signal Processing, volume 2009, Article ID 612719, 13 pages, 2009. doi:10.1155/2009/612719.
- B. Maham, M. Debbah, and A. Hjørungnes, *"Energy-Efficient Cooperative Routing in BER Constrained Multihop Networks,"* Springer Journal of Frontiers of Computer Science in China, vol. 3, no. 2, pp. 263-271, Jun. 2009 (Published by Higher Education Press and Springer-Verlag).
- B. Maham and A. Hjørungnes *"Performance Analysis of Amplify-and-Forward Opportunistic Relaying in Rician Fading,"* IEEE Signal Processing Letters, vol. 16, no. 8, pp. 643 - 646, Aug. 2009.
- B. Maham, A. Hjørungnes, and M. Debbah, *"Power Allocations in Minimum-Energy SER Constrained Cooperative Networks,"* Annals of Telecommunications - Annales des Télécommunications, special issue on Cognitive Radio, vol. 64, no. 7, pp. 545-555, Aug. 2009.
- B. Maham and A. Hjørungnes, *"Asymptotic Performance Analysis of Amplify-and-Forward Cooperative Networks in a Nakagami-m Fading Environment,"* IEEE Communications Letters, vol. 13, no. 5, pp. 300-302, May 2009.

- B. Maham and A. Hjørungnes, *"Symbol Error Rate of Amplify-and-Forward Distributed Space-Time Codes over Nakagami-m Fading Channel,"* IET Electronics Letters (former IEE), vol. 45, no. 3, pp. 174-175, Jan. 2009.

- B. Maham, A. Hjørungnes, and G. Abreu, *"Distributed GABBA Space-Time Codes in Amplify-and-Forward Relay Networks,"* IEEE Transactions on Wireless Communications, vol. 8, no. 2, pp. 2036 - 2045, Apr. 2009.

- B. Maham and A. Hjørungnes, *"Performance Analysis of Repetition-Based Cooperative Networks with Partial Statistical CSI at Relays"* IEEE Communications Letters, vol. 8, no. 4, pp. 828-830, Nov. 2008.

List of conference publications during Ph.D. studies:

- B. Maham and A. Hjørungnes, *"Near-Optimum Power Allocation for BER Restricted Multihop Cooperative Networks,"* in Proc. IEEE International Conference on Communications (ICC'10), Cape Town, South Africa, May 2010.

- B. Maham, A. Hjørungnes, and B. Sundar Rajan, *"Quasi-Orthogonal Design and Performance Analysis of Amplify-and-Forward Relay Networks with Multiple-Antennas,"* in Proc. IEEE Wireless Communications and Networking Conference (WCNC'10), Sydney, Australia, April 2010.

- B. Maham, B. Sundar Rajan, and A. Hjørungnes, *"Performance Analysis of Single-Symbol Maximum Likelihood Decodable Linear STBCs,"* invited paper, in Proc. International Symposium on Communications, Control, and Signal Processing (ISCCSP'10), Limassol, Cyprus, March 2010.

- B. Maham and A. Hjørungnes, *"Orthogonal Code Design for MIMO Amplify-and-Forward Cooperative Networks,"* in Proc. IEEE Information Theory Workshop (ITW'10), Cairo, Egypt, January 2010.

- B. Maham, R. Narasimhan, and A. Hjørungnes, *"Energy-Efficient Space-Time Coded Cooperative Routing in Multihop Wireless Networks,"* in Proc. of IEEE Global Telecommunications Conference, GLOBECOM 2009, Honolulu, Hawaii, USA, November - December 2009.

- B. Maham and A. Hjørungnes, *"Opportunistic Relaying for Space-Time Coded Cooperation with Multiple Antennas Terminals,"* in the 20th IEEE Personal, Indoor and Mobile Radio Communications Symposium (PIMRC 2009), Tokyo, Japan, September 2009.
- B. Maham and A. Hjørungnes,*"Minimum Power Allocation for Cooperative Routing in Multihop Wireless Networks,"* in Proc. 32th IEEE Sarnoff Symposium, (SARNOFF 2009), Princeton, NJ, USA, March 2009.
- B. Maham and A. Hjørungnes, *"Opportunistic Relaying through Amplify-And-Forward Distributed Space-Time Codes with Partial Statistical CSI at Relays,"* in Proc. the Forty-Sixth Annual Allerton Conference on Communication, Control, and Computing (Allerton 2008), IEEE index, pp. 1004-1009, Urbana-Champaign, IL, USA, Sep. 2008.
- B. Maham, M. Debbah, and A. Hjørungnes, *"Energy-Efficient Cooperative Routing in BER Constrained Multihop Networks,"* invited Paper, in Proc. International Conference on Communications and Networking in China (CHINACOM 2008), Hangzhou, China, pp. 168- 172, Aug. 2008.
- B. Maham and A. Hjørungnes, *"Power Allocation Strategies for Distributed Space-Time Codes in Amplify-and-Forward Mode,"* in Proc. IEEE International Wireless Communications and Mobile Computing Conference (IWCMC 2008), Crete Island, Greece, pp. 905-909, Aug. 2008.
- B. Maham and A. Hjørungnes, G. Abreu, *"Distributed GABBA Space-Time Codes with Complex Signal Constellations,"* in 5th IEEE Sensor Array and Multi-Channel Signal Processing Workshop (SAM'08), pp. 118-121, Darmstadt, Germany, July 2008.
- B. Maham and A. Hjørungnes, *"Minimum Power Allocation in SER Constrained Amplify-and- Forward Cooperation,"* in Proc. IEEE Vehicular Technology Conference (VTC 2008-Spring), pp. 2431-2435, Singapore, May 2008.
- B. Maham and A. Hjørungnes, *"Amplify-and-Forward Space-Time Coded Cooperation via Incremental Relaying,"* in Proc. IEEE International Symposium on Wireless Communication Systems 2007 (ISWCS '07), pp. 407-411, Trondheim, Norway, Oct. 2007.

- B. Maham and A. Hjørungnes, *"Distributed GABBA Space-Time Codes in Amplify-and- Forward Cooperation,"* in Proc. IEEE Information Theory Workshop (ITW'07), pp. 189-193, Bergen, Norway, July 2007.
- B. Maham and A. Hjørungnes, *"Power Allocation in Cooperative Networks Using Differential Space-Time Codes,"* in Proc. IEEE Int. Symp. Information Theory (ISIT'07), pp. 1916-1920, Nice, France, June 2007.

References

[1] A. Sendonaris, E. Erkip, and B. Aazhang, "User cooperation diversity. Part I. System description," *IEEE Trans. Commun.*, vol. 51, no. 11, pp. 1927–1938, Nov. 2003.

[2] A. Nosratinia, T. Hunter, and A. Hedayat, "Cooperative communication in wireless networks," *IEEE Commun. Mag.*, vol. 42, no. 10, pp. 74–80, Oct. 2004.

[3] Y. W. Hong and A. Scaglione, "Energy-efficient broadcasting with cooperative transmissions in wireless sensor networks," *IEEE Trans. Wireless Commun.*, vol. 5, no. 10, pp. 2844–2855, Oct. 2006.

[4] A. Sendonaris, E. Erkip, and B. Aazhang, "User cooperation diversity. Part II. Implementation aspects and performance analysis," *IEEE Trans. Commun.*, vol. 51, no. 11, pp. 1939–1948, Nov. 2003.

[5] J. N. Laneman and G. Wornell, "Distributed space-time coded protocols for exploiting cooperative diversity in wireless networks," in *IEEE GLOBECOM 2002*, vol. 1, no. 11, Taipei, Taiwan, R.O.C., Nov. 2002, pp. 77–81.

[6] A. Scaglione and Y.-W. Hong, "Opportunistic large arrays: Cooperative transmission in wireless multi-hop ad hoc networks for the reach back channel," *IEEE Trans. Signal Process.*, vol. 51, no. 8, no. 1, pp. 341–355, Aug. 2003.

[7] M. Janani, A. Hedayat, T. E. Hunter, and A. Nosratinia, "Coded cooperation in wireless communications: Space-time transmission and iterative decoding," *IEEE Trans. Signal Process.*, vol. 52, no. 2, pp. 362–371, Feb. 2004.

[8] Y.-W. Hong, W.-J. Huang, F.-H. Chiu, and C.-C. J. Kuo, "Cooperative communications in resource-constrained wireless networks," *IEEE Signal Processing Magazine*, vol. 24, pp. 47–57, May 2007.

[9] J. N. Laneman, D. Tse, and G. Wornell, "Cooperative diversity in wireless networks: Efficient protocols and outage behavior," *IEEE Trans. Inform. Theory*, vol. 50, no. 12, pp. 3062–3080, Dec. 2004.

[10] P. Herhold, E. Zimmermann, and G. Fettweis, "On the performance of cooperative amplify-and-forward relay networks," in *in Proc. Conf. Source and Channel Coding*, 2004, pp. 451–458.

[11] E. van der Meulen, "Three-terminal communication channel," *Adv. Appl. Prob.*, vol. 3, pp. 120–154, May 1971.

[12] T. Cover and A. Gamal, "Capacity theorems for the relay channel," *IEEE Trans. Info. Theory*, vol. 25, pp. 572–584, Sep. 1979.

[13] J. Laneman and G. Wornell, "Distributed space-time coded protocols for exploiting cooperative diversity in wireless networks," *IEEE Trans. Info. Theory*, vol. 49, no. 10, pp. 2415–2425, Oct. 2003.

[14] R. U. Nabar, H. Bölcskei, and F. W. Kneubuhler, "Fading relay channels: Performance limits and space-time signal design," *IEEE J. Sel. Areas Commun.*, vol. 22, no. 6, pp. 1099–1109, Aug. 2004.

[15] M. Uysal and O. Canpolat, "On the distributed space-time signal design for a large number of relay terminals," in *Proc. IEEE Wireless Communications and Networking Conference (WCNC)*, vol. 2, New Orleans, USA, Mar. 13–17 2005, pp. 990–994.

[16] K. Seddik, A. Sadek, A. Ibrahim, and K. Liu, "Design criteria and performance analysis for distributed space-time coding," *IEEE Trans. on Vehicular Technology*, vol. 57, no. 4, pp. 2280–2292, Jul. 2008.

[17] T. Wang, Y. Yao, and G. B. Giannakis, "Non-coherent distributed space-time processing for multiuser cooperative transmissions," *IEEE Trans. Wireless Commun.*, vol. 5, no. 12, pp. 3339–3343, Dec. 2006.

[18] A. Bletsas, A. Khisti, D. P. Reed, and A. Lippman, "A simple cooperative method based on network path selection," *IEEE Journal on Selected Areas in Communications*, vol. 24, no. 3, pp. 659–672, Mar. 2006.

[19] J.N.Laneman, G.W.Wornell, and D.N.C.Tse, "An efficient protocol for realizing cooperative diversity in wireless networks," in *Proceedings of IEEE International Symposium on Information Theory*, Washington DC, USA, Jun. 2001.

[20] K. Tourki, M.-S. Alouini, and L. Deneire, "Blind cooperative diversity using distributed space-time coding in block fading channels," in *Proceedings of IEEE International Conference on Communications*, Beijing, China, May 2008.

[21] I. Maric and R. D. Yates, "Bandwidth and power allocation for cooperative strategies in gaussian relay networks," in *Proc. Asilomar Conf. Signals, Systems, and Computers*, Monterey, CA, Nov. 2004.

[22] ——, "Forwarding strategies for gaussian parallel-relay networks," in *Proceedings of the Conference on Infocrmation Sciences and Systems (CISS)*, Monterey, CA, Mar. 2004.

[23] I. Hammerstroem, M. Kuhn, and A. Wittneben, "Impact of relay gain allocation on the performance of cooperative diversity networks," in *Proc. of IEEE Vehicular Technology Conference (VTC)*, 2004.

[24] Y. Zhao, R. Adve, and T. Lim, "Improving amplify-and-forward relay networks: optimal power allocation versus selection," in *Proceedings on the IEEE International Symposium on Information Theory (ISIT)*, Monterey, CA, 2006.

[25] A. Bletsas, H. Shin, and M. Win, "Outage-optimal cooperative communications with regenerative relays," in *Proceedings of the Conference on Information Science and Systems (CISS)*, 2006.

[26] B. Maham and A. Hjørungnes, "Power allocation strategies for distributed space-time codes in amplify-and-forward mode," *EURASIP Journal on Advances in Signal Processing*, vol. 2009, Article ID 310247, 13 pages, 2009.

[27] Y. Chen and Q. Zhao, "Maximizing the lifetime of sensor network using local information on channel state and residual energy," in *Proceedings of the Conference on Information Science and Systems (CISS)*, Mar. 2005.

[28] W. Huang, Y. Hong, and C. J. Kuo, "Lifetime maximization for amplify-and-forward cooperative networks," in *Proc. IEEE Wireless Communications and Networking Conference (WCNC)*, Hong Kong, China, 2007.

[29] B. Maham and A. Hjørungnes, "Minimum power allocation in SER constrained amplify-and-forward cooperation," in *Proc. IEEE Vehicular Technology Conference (VTC 2008-Spring)*, Singapore, May 2008, pp. 2431–2435.

[30] J. Luo, R. Blum, L. Cimini, L. Greenstein, and A. Haimovich, "Decode-and-forward cooperative diversity with power allocation in wireless networks," in *Proceedings of IEEE Global Telecommunications Conference*, Nov. 2005, pp. 3048–3052.

[31] Z. Yi and I. Kim, "Joint optimization of relay-precoders and decoders with partial channel side information in cooperative networks," *IEEE Journal on Selected Areas in Communications (JSAC)*, vol. 25, pp. 447–458, Feb. 2007.

[32] J. Boyer, D. D. Falconer, and H. Yanikomeroglu, "Multihop diversity in wireless relaying channels," *IEEE Trans. Commun.*, vol. 52, no. 10, pp. 1820–1830, Oct. 2004.

[33] A. E. Khandani, J. Abounadi, E. Modiano, and L. Zheng, "Cooperative routing in static wireless networks," *IEEE Trans. Commun.*, vol. 55, no. 11, pp. 2185–2192, Nov. 2007.

[34] A. S. Ibrahim, Z. Han, and K. J. R. Liu, "Distributed energy-efficient cooperative routing in wireless networks," *IEEE Trans. Wireless Commun.*, vol. 7, no. 11, pp. 757–759, Oct. 2008.

[35] B. Maham, R. Narasimhan, and A. Hjørungnes, "Energy-efficient space-time coded cooperative routing in multihop wireless networks," in *IEEE GLOBECOM*, Honolulu, Hawaii, USA, Nov.- Dec. 2009.

[36] F. Li, K. Wu, and A. Lippman, "Energy-efficient cooperative routing in multi-hop wireless ad hoc networks," in *IEEE International Performance, Computing, and Communications Conference*, Apr. 2006, pp. 215–222.

[37] A. K. Sadek, W. Su, and K. J. R. Liu, "Multinode cooperative communications in wireless networks," *IEEE Trans. Signal Process.*, vol. 55, no. 1, pp. 341–355, Jan. 2007.

[38] A. Ribeiro, A. Cai, and G. B. Giannakis, "Symbol error probablity for general cooperative links," *IEEE Trans. Wireless Commun.*, vol. 4, no. 3, pp. 1264–1273, May 2005.

[39] P. A. Anghel, G. Leus, and M. Kaveh, "Multi-user space-time coding in cooperative networks," in *Proc. ICASSP*, Apr. 2003, pp. IV–73–IV–76.

[40] S. Barbarossa, L. Pescosolido, D. Ludovici, L. Barbetta, and G. Scutari, "Cooperative wireless networks based on distributed space-time coding," in *IEEE International Workshop on Wireless Ad-hoc Networks (IWWAN)*, Oulu, Finland, May 31–June 3 2004.

[41] B. Sirkeci-Mergen and A. Scaglione, "Randomized space-time coding for distributed cooperative communication," in *IEEE International Conference on Communications (ICC 2006)*, Istanbul, Turkey, 2006.

[42] Y. Jing and H. Jafarkhani, "Using orthogonal and quasi-orthogonal designs in wireless relay networks," in *IEEE GLOBECOM*, San Fransisco, USA, Nov. 2006.

[43] ——, "Using orthogonal and quasi-orthogonal designs in wireless relay networks," *IEEE Trans. Info. Theory*, vol. 53, no. 11, pp. 4106–4118, Nov. 2007.

[44] B. Maham and A. Hjørungnes, "Distributed GABBA space-time codes in amplify-and-forward cooperation," in *Proc. IEEE Information Theory Workshop (ITW'07)*, Bergen, Norway, Jul. 2007, pp. 189–193.

[45] G. S. Rajan and B. S. Rajan, "Distributed space-time codes for cooperative networks with partial CSI," in *Proc. IEEE Wireless Communications and Networking Conference (WCNC)*, Hong Kong, China, March 2007, pp. 902–906.

[46] Y. Jing and B. Hassibi, "Distributed space-time coding in wireless relay networks," *IEEE Trans. Wireless Commun.*, vol. 5, no. 12, pp. 3524–3536, Dec. 2006.

[47] B. Maham, A. Hjørungnes, and G. Abreu, "Distributed GABBA space-time codes in amplify-and-forward relay networks," *IEEE Trans. Wireless Commun.*, vol. 8, no. 4, pp. 2036–2045, Apr. 2009.

[48] F. Oggier and B. Hassibi, "An algebraic coding scheme for wireless relay networks with multiple-antenna nodes," *IEEE Trans. Signal Process.*, vol. 56, no. 7, pp. 2957–2966, Jul. 2008.

[49] K. T. and B. S. Rajan, "Partially-coherent distributed space-time codes with differential encoder and decoder," *IEEE J. Sel. Areas Commun.*, vol. 25, no. 2, pp. 426–433, Feb. 2007.

[50] Y. Jing and H. Jafarkhani, “Distributed differential space-time coding for wireless relay networks,” *IEEE Trans. Commun.*, vol. 56, no. 7, pp. 1092–1100, Jul. 2008.

[51] G. S. Rajan and B. S. Rajan, “Algebraic distributed differential space-time codes with low decoding complexity,” *IEEE Trans. Inform. Theory*, 2009, to appear in IEEE Trans. Wireless Commun.. Available in arXiv: 0708.4407.

[52] G. Rajan and B. Rajan, “Leveraging coherent distributed space-time codes for noncoherent communication in relay networks via training,” *IEEE Trans. Wireless Commun.*, vol. 8, no. 2, pp. 683–688, Feb. 2009.

[53] Y. Jing and B. Hassibi, “Cooperative diversity in wireless relay networks with multiple-antenna nodes,” in *IEEE Int. Symp. Inform. Theory*, Adelaide, Australia, 2005.

[54] B. Maham and A. Hjørungnes, “Orthogonal code design for MIMO amplify-and-forward cooperative networks,” in *Proc. IEEE Information Theory Workshop (ITW’07)*, Cairo, Egypt, Jan. 2010.

[55] B. Maham, A. Hjørungnes, and B. S. Rajan, “Quasi-orthogonal design and performance analysis of amplify-and-forward relay networks with multiple-antennas,” in *Proc. IEEE Wireless Communications and Networking Conference (WCNC)*, Sydney, Australia, April 2010.

[56] M. K. Simon and M.-S. Alouini, *Digital Communication over Fading Channels: A Unified Approach to Performance Analysis.* New York, USA: Wiley, 2005.

[57] J. G. Proakis, *Digital Communications, 4th ed.* New York, USA: McGraw-Hill, 2001.

[58] S. O. Rice, “Statistical properties of a sine wave plus random noise,” *Bell Syst. Tech. J.*, vol. 27, pp. 109–157, Jan. 1948.

[59] K. A. Stewart, G. P. Labedz, and K. Sohrabi, “Wideband channel measurements at 900 MHz,” in *Proc. IEEE Veh. Technol. Conf. (VTC’95)*, Chicago, IL, pp. 236–240.

[60] R. J. C. Bultitude, S. A. Mahmoud, , and W. A. Sullivan, “A comparison of indoor radio propagation characteristics at 910 MHz and 1.75 GHz,” *IEEE J. Select. Areas Commun.*, vol. SAC-7, pp. 20–30, Jan. 1989.

[61] T. S. Rappaport and C. D. McGillem, “Uhf fading in factories,” *IEEE J. Select. Areas Commun.*, vol. SAC-7, pp. 40–48, Jan 1989.

[62] P. D. Shaft, “On the relationship between scintillation index and rician fading,” *IEEE Trans. Commun.*, vol. COM-22, pp. 731–732, May 1974.

[63] T. L. Staley, R. C. North, W. H. Ku, and J. R. Zeidler, “Performance of coherent MPSK on frequency selective slowly fading channels,” in *Proc. IEEE Veh. Technol. Conf. (VTC'96)*, Atlanta, GA, pp. 784–788.

[64] W. R. Braun and U. Dersch, “A physical mobile radio channel model,” *IEEE Trans. Veh. Technol.*, vol. VT-40, pp. 472–482, May 1991.

[65] A. U. Sheikh, M. Handforth, and M. Abdi, “Indoor mobile radio channel at 946 mhz: Measurements and modeling,” in *Proc. IEEE Veh. Technol. Conf. (VTC'93)*, Secaucus, NJ, pp. 73–76.

[66] R. C. L. E. J. Fremouw and D. A. Miller, “On the statistics of scintillating signals,” *J. Atmos. Terr. Phys.*, vol. 42, pp. 717–731, Aug. 1980.

[67] H. Jafarkhani, *Space-Time Coding Theory and Practice.* Cambridge, UK: Cambridge Academic Press, 2005.

[68] P. A. Anghel and M. Kaveh, “Exact symbol error rate probability of a cooperative network in a Rayleigh-fading environment,” *IEEE Trans. Wireless Commun.*, vol. 3, no. 5, pp. 1416–1421, Sep. 2004.

[69] M. O. Hansa and M. S. Alouini, “Outage probability of multihop transmissions over Nakagami fading channels,” *IEEE Commun. Letters*, vol. 7, no. 1, pp. 216–218, May 2003.

[70] M. O. Hansa and M.-S. Alouini, “Optimal power allocation for relayed transmissions over Rayleigh-fading channels,” *IEEE Trans. Wireless Commun.*, vol. 3, no. 6, pp. 1999–2004, Nov. 2004.

[71] ——, “End-to-end performance of transmission systems with relays over Rayleigh fading channels,” *IEEE Trans. Wireless Commun.*, vol. 2, no. 6, pp. 1126–1131, Nov. 2003.

[72] ——, “Harmonic mean and end-to-end performance of transmission systems with relays,” *IEEE Trans. Commun.*, vol. 52, no. 1, pp. 130–135, Jan. 2004.

[73] G. K. Karagiannidis, “Performance bounds of multihop wireless communications with blind relays over generalized fading channels,” *IEEE Trans. Wireless Commun.*, vol. 5, no. 3, pp. 498–503, Mar. 2006.

[74] ——, “Moments-based approach to the performance analysis of equal-gain diversity in Nakagami-*m* fading,” *IEEE Trans. Commun.*, vol. 52, no. 5, pp. 685–69, May 2004.

[75] G. K. Karagiannidis, T. A. Tsiftsis, and R. K. Mallik, “Bounds for multihop relayed communications in Nakagami-*m* fading,” *IEEE Trans. Commun.*, vol. 54, no. 1, pp. 18–22, Jan. 2006.

[76] S. Ikki and M. H. Ahmed, “Performance analysis of cooperative diversity wireless networks over Nakagami-*m* fading channel,” *IEEE Comm. Letters*, vol. 11, no. 4, pp. 334–336, Apr. 2007.

[77] W. Su, A. K. Sadek, and K. J. R. Liu, “SER performance analysis and optimum power allocation for decode-and-forward cooperation protocol in wireless networks,” in *Proc. of the IEEE Wireless Communications and Networking Conference*, 2005, pp. 984–989.

[78] G. Abreu, “GABBA codes: Generalized full-rate orthogonally decodable space-time block codes,” in *Thirty-Ninth Asilomar Conference on Signals, Systems and Computers*, Monterey, CA, Nov. 2005.

[79] ——, “Generalized ABBA space-time block codes,” Internet draft, [Online]. Available: http://arxiv.org/abs/cs/0510003v1.

[80] J. Vazifehdan and H. Shafiee, “Optimal configuration of wireless co-operative networks,” in *Conference on Wireless and Optical Communications Networks/IFIP*, Dubai, United Arab Emirates, Mar. 2005.

[81] M. Z. A. Khan and B. S. Rajan, “Single-symbol maximum likelihood decodable linear STBCs,” *IEEE Trans. Info. Theory*, vol. 52, no. 5, pp. 2062–2091, May 2006.

[82] M. Abdallah and H. C. Papadopoulos, “Beamforming algorithms for decode-and-forward relaying in wireless networks,” in *Proceedings of the Conference on Information Sciences and Systems (CISS)*, Monterey, CA, Mar. 2005.

[83] R. Narasimhan, “Throughput-delay performance of half-duplex hybrid-arq relay channels,” in *Proc. IEEE Int. Conf. Commun. (ICC)*, Beijing, China, May 2008.

Part II

Included Papers

Paper A

Distributed GABBA Space-Time Codes in Amplify-and-Forward Relay Networks

B. Maham, A. Hjørungnes, and G. Abreu

IEEE Transactions on Wireless Communications, volume 8, issue 2, pages 2036 - 2045, April 2009.

Abstract

Cooperative communications via distributed space-time codes has been recently proposed as a way to form virtual multiple-antennas that provide dramatic gains in slow fading wireless environments. In this paper, we consider the design of practical distributed space-time codes for wireless relay networks using the amplify-and-forward (AF) scheme, where each relay transmits a scaled version of the linear combinations of the received symbols and their complex conjugate. We employ GABBA codes, which are systematically constructed, orthogonally decodable, full-rate, full-diversity space-time block codes, in a distributed fashion. Our scheme is valid for any number of relays with linear orthogonal decoding in the destination, which make it feasible to employ large numbers of potential relays to improve the diversity order. We generalize the distributed space-time codes in AF mode when the source-destination link contributes in both phases of the transmission. Assuming M-PSK or M-QAM constellations and maximum likelihood (ML) detection, we derive an approximate formula for the symbol error probability of the investigated scheme in Rayleigh fading channels. The analytical results are confirmed by simulations, indicating both the accuracy of the analysis, and the fact that low-complexity, flexible, and high-performing distributed space-time block codes can be designed based on GABBA codes.

1 Introduction

Space-time codes provide diversity and coding gains in multiple antenna systems over fading channels. In ad-hoc or distributed large scale wireless networks, nodes are often constrained in hardware complexity and size, which makes multiple antenna systems impractical for certain applications. Cooperative diversity schemes [1, 2] have been introduced in an effort to overcome this limitation. Cooperative techniques allow a collection of radios to relay signals amongst each other, effectively creating a virtual antenna array, which combat multipath fading in wireless channels. This makes cooperative techniques attractive for deployment in cellular mobile devices as well as in ad-hoc mobile networks.

Several cooperation strategies with different relaying techniques, including amplify-and-forward (AF), decode-and-forward (DF), and selective relaying (SR), have been studied in Laneman et al.'s seminal paper [3]. Distributed space-time codes (DSTC) have also been proposed to improve the bandwidth efficiency of cooperative transmissions (see, e.g., [4–7]).

In [8], a cooperative strategy was proposed, which achieves a diversity factor of R in a R-relay wireless network, using the so-called distributed space-time codes. In this strategy, a two-phase protocol is used. In phase one, the transmitter sends the information signal to the relays and in phase two, the relays send information to the receiver. The signal sent by every relay in the second phase is designed as a linear function of its received signals and their complex conjugate. It was shown that the relays can generate a linear space-time codeword at the receiver, as in a multiple antenna system, although they only cooperate distributively. The technique was also shown to achieve optimal diversity at high SNRs [8]. Although distributed space-time coding does not need instantaneous channel information at the relays, it requires full (transmitter-to-relays and relays-to-receiver) channel information at the receiver, implying that training symbols need to be sent from both the transmitter and relays.

Distributed space-time coding was generalized to networks with multiple-antenna nodes in [9], and the design of practical DSTCs that lead to reliable communication in wireless relay networks, has also been recently considered [10–12]. In [12], it was shown that for real-valued i.i.d. Rayleigh channels, the DSTC design problem becomes similar to the code design problem for MIMO communication. In this article, however, we follow [10] and [11] and assume the channels have i.i.d. *complex* Gaussian distributions, which is more realistic. Our focus is on the space-time cooperation using generalized ABBA (GABBA) codes [13, 14], which are systematically constructed, orthogonally decodable, full-rate, full-diversity space-time block codes. Note that generalized quasi-orthogonal space-time block codes (QOSTBC) [15] have the similar performance to GABBA codes, but their code structure and code construction process are different. In [16], the performance analysis of QOSTBC in a MIMO link is studied, when linear receivers (ZF and MMSE) are employed, instead of ML receiver, which do not lead to the full-diversity. In our scheme, the maximum number of employed relays is chosen based on the coherence time of the network channels. In [11], it was shown that using *real* constellations, GABBA codes can be directly used as DSTC for any number of relays in the network. In this paper, we propose a GABBA-based DSTC design in which any *complex* signal constellations can be used. Using GABBA codes with linear orthogonal decoding, we can employ large number of potential relays to improve the diversity order. The previous work on the use of full-rate, full-diversity codes in wireless relay networks has limited structures (e.g., 2×2 code matrix in [17], and 2×2 or 4×4 code matrices in [10]). On the other hand, complex decoding techniques, like maximum-likelihood (ML) and pairwise ML [18], prevent applicability of the code matrices with large dimensions. We also study the contribution of the source-destination link in two phases of AF DSTC. In [4], the contribution of the source-destination link in both phases was studied for the space-time coded cooperation under AF mode, when *one* relay is employed. Furthermore, we compare DSTC systems with different scaling (amplification) factors, with or without knowledge of local source-relay instantaneous channel state information (CSI) at the relays.

Our main contributions can be summarized as follows:

1. We show that the transpose of GABBA codes are applicable in AF DSTC, in which relays transmit the linear combinations of the scaled version of the received signals and their complex conjugate. Our proposed scheme is valid for *any* number of relays.

2. We derive the approximate average symbol error rate (SER) for AF DSTC with M-PSK and M-QAM modulations over Rayleigh-fading channels, which is valid for *any* full-diversity, full-rate space-time block codes, such as distributed GABBA codes and the codes given in [10].

3. We extend and analyze the DSTC in AF mode, when the source-destination link is contributing in the both phases of transmission.

4. We analyze the diversity order of AF DSTCs based on the asymptotic behavior of average SER. The proposed MGF-based approach can be used for diversity analyzing of other wireless systems where the MGF is available.

The remainder of this paper is organized as follows: In Section II, the system model is given. The direct formulation of DSTC in the AF mode is considered in Section III. The distributed version of GABBA codes for complex signal constellations in DSTC is presented in Section IV. In Section V, the average SER of DSTC under M-PSK and M-QAM modulations is derived, and a diversity analysis is carried out. In Section VI, the overall system performance is presented for different numbers of relays, and the correctness of the analytical formula is confirmed by simulation results. Conclusions are presented in Section VII. The article contains three appendices which present various proofs.

Notations: The superscripts ^{t}, ^{H}, and * stand for transposition, conjugate transposition, and element-wise conjugation, respectively. The expectation operation is denoted by $\mathbb{E}\{\cdot\}$. The covariance of the $T \times 1$ zero-mean vector $\boldsymbol{x}_T$ consisting of T random variables is $\text{Cov}(\boldsymbol{x}_T) = \mathbb{E}\{\boldsymbol{x}_T\boldsymbol{x}_T^H\}$. The symbols $\mathbf{0}_T$ and $\boldsymbol{I}_T$ stand for the $T \times T$ zero matrix and identity matrix, respectively. $|x|$ is the absolute value of the scalar x, while $\|\boldsymbol{A}\|_F$ denotes the Frobenius norm of the matrix $\boldsymbol{A}$. The trace of the matrix $\boldsymbol{A}$ is denoted by $\text{Tr}\{\boldsymbol{A}\}$. The floor and ceil of x are denoted by $\lfloor x \rfloor$ and $\lceil x \rceil$, respectively. All logarithms are the natural logarithm.

2 System Model

Consider a network consisting of a source node denoted *s*, one or more relays denoted $r = 1, 2, \ldots, R$, and one destination node *d* (see Fig. A.1). It is assumed that each node is equipped with a single antenna. We denote the source-to-destination, source-to-rth relay, and rth relay-to-destination links by f_0, f_r, and g_r, respectively. Under the assumption that each link undergoes independent Rayleigh process, f_0, f_r, and g_r are independent complex Gaussian random variables with zero-mean and variances σ_0^2, $\sigma_{f_r}^2$, and $\sigma_{g_r}^2$, respectively.

Similar to [8], our scheme requires two phases of transmission. During the first phase, the source should transmit a vector $\boldsymbol{s} = [s_1, \ldots, s_T]^t$, con-

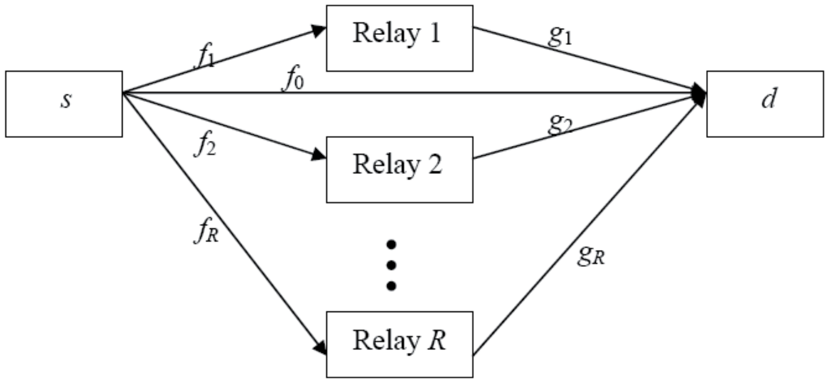

Fig. A.1: Wireless relay network including one source, R relays, and one destination.

sisting of T symbols to *all* relays. We assume the following normalization $\mathbb{E}\{\boldsymbol{s}^H \boldsymbol{s}\} = 1$. Thus, from time 1 to T, signals $\sqrt{P_1 T} s_1, \ldots, \sqrt{P_1 T} s_T$ are sent to all relays by the source, where $P_1 T$ is the average total transmitted energy in T intervals. Assuming that f_r does not vary during T successive intervals, the $T \times 1$ receive signal vector at the rth relay is

$$\boldsymbol{y}_r = \sqrt{P_1 T} f_r \boldsymbol{s} + \boldsymbol{v}_r, \tag{A.1}$$

where $\boldsymbol{v}_r$ is a $T \times 1$ complex zero-mean white Gaussian noise vector with variance N_1.

In the second phase of the transmission, all relays simultaneously transmit linear functions of their received signals $\boldsymbol{y}_r$ and $\boldsymbol{y}_r^*$. In order to construct a distributed space-time codes, the received signal at the destination is collected inside the $T \times 1$ vector $\boldsymbol{y}$ [10] as

$$\boldsymbol{y} = \sum_{r=1}^{R} g_r \left(\rho_r^* \boldsymbol{A}_r \boldsymbol{y}_r + \rho_r \boldsymbol{B}_r \boldsymbol{y}_r^* \right) + \boldsymbol{w}, \tag{A.2}$$

where $\boldsymbol{w}$ is a $T \times 1$ complex zero-mean white Gaussian noise vector with the variance of N_2, ρ_r is the scaling factor at relay r, and $\boldsymbol{A}_r$ and $\boldsymbol{B}_r$, of size $T \times T$, are obtained by representing the rth column of the $T \times R$ dimensional space-time code matrix $\boldsymbol{S}$ as $\boldsymbol{c}_r = \boldsymbol{A}_r \boldsymbol{s} + \boldsymbol{B}_r \boldsymbol{s}^*$. Thus, after receiving the vector $\boldsymbol{y}_r$ at the rth relay, $\boldsymbol{y}_r$ and $\boldsymbol{y}_r^*$ are multiplied by $\rho_r^* \boldsymbol{A}_r$ and $\rho_r \boldsymbol{B}_r$, respectively. In general, $\boldsymbol{A}_r$ and $\boldsymbol{B}_r$ can be arbitrary matrices satisfying $\|\boldsymbol{A}_r\|_F^2 + \|\boldsymbol{B}_r\|_F^2 \leq 1$. However, in this paper, we study a subclass of full-rate, full-diversity distributed space-time codes, like GABBA codes and the codes proposed in [10], in which either $\boldsymbol{A}_r$ is unitary and $\boldsymbol{B}_r = \boldsymbol{0}_T$, or vice versa.

Notice that the extension of the scheme explained above to the case where a source-destination link is contributing in both phases is possible. In this case, the received signal at the destination through the first phase and the second phase become

$$\boldsymbol{y}_0 = \sqrt{P_1 T} f_0 \boldsymbol{s} + \boldsymbol{w}, \tag{A.3}$$

$$\boldsymbol{y} = \sqrt{P_{2,r} T} f_0 \left(\boldsymbol{A}_0 \boldsymbol{s} + \boldsymbol{B}_0 \boldsymbol{s}^* \right) + \sum_{r=1}^{R} g_r \left(\rho_r^* \boldsymbol{A}_r \boldsymbol{y}_r + \rho_r \boldsymbol{B}_r \boldsymbol{y}_r^* \right) + \boldsymbol{w}, \tag{A.4}$$

respectively, where $P_{2,r}$ is the average transmitted power from each transmitter during the second phase, and $\boldsymbol{A}_i$ and $\boldsymbol{B}_i$, $i = 0, 1, \ldots, R$, are $T \times T$ matrices, corresponding to the ith column of $T \times (R+1)$ dimensional space-time code. Here, it is assumed that the source acts as a virtual relay in the second phase of transmission with the matrices $\boldsymbol{A}_0$ and $\boldsymbol{B}_0$.

For the clarity of presentation, we call the protocol based on (A.1) and (A.2) as Protocol I. When the source-destination link contributes in the second phase, but not in the first phase, i.e., (A.4), we call it Protocol II, and, finally, the protocol in which the destination is receiving the source data in two phases is named Protocol III. In the rest of the paper all equations, unless specified, are based on Protocol I.

3 Distributed Space-Time Codes in Amplify-and-Forward Mode

From (A.1)-(A.2), the received signal at the destination can be calculated to be

$$\boldsymbol{y} = \sqrt{P_1 T}\, \boldsymbol{S} \boldsymbol{h} + \boldsymbol{w}_T, \tag{A.5}$$

where the DSTC matrix $\boldsymbol{S}$ should be appropriately designed, such as the codes proposed in [8] or [11]. Combining (A.1)-(A.2), the total noise vector

$\boldsymbol{w}_T$ in (A.5) is given by

$$\boldsymbol{w}_T = \sum_{r=1}^{R} g_r \left(\rho_r^* \boldsymbol{A}_r \boldsymbol{v}_r + \rho_r \boldsymbol{B}_r \boldsymbol{v}_r^*\right) + \boldsymbol{w}. \tag{A.6}$$

The $R \times 1$ vector $\boldsymbol{h}$ in (A.5) is the equivalent relay channel, whfose rth component is

$$h_r = \begin{cases} \rho_r^* f_r g_r, & \text{if } \boldsymbol{c}_r \in \Omega, \\ \rho_r f_r^* g_r, & \text{if } \boldsymbol{c}_r \in \Omega^*, \end{cases} \tag{A.7}$$

where $\boldsymbol{c}_r$ is the rth column of the code matrix $\boldsymbol{S}$. The set Ω consists of the columns of the DSTC matrix that contain the linear combinations of symbols without conjugation, i.e., $s_1, s_2, \ldots, s_T$, while Ω^* consists of the columns containing the linear combinations of conjugate of symbols, i.e., $s_1^*, s_2^*, \ldots, s_T^*$.

In order to write the received signal in the form of (A.5), it is necessary that each rth column of the code matrix is taken from either Ω or Ω^*. In other words, the combining matrix at the rth relay, $\boldsymbol{D}_r$, which is corresponding to the rth column of the code matrix $\boldsymbol{S}$, satisfy the following condition

$$\boldsymbol{D}_r = \begin{cases} \boldsymbol{A}_r, & \text{if } \boldsymbol{c}_r \in \Omega, \\ \boldsymbol{B}_r, & \text{if } \boldsymbol{c}_r \in \Omega^*. \end{cases} \tag{A.8}$$

Now, we derive the covariance of $\boldsymbol{w}_T$ which will be used for calculating the received SNR at the destination. Let $\mathcal{F} \triangleq \{f_1, f_2, \ldots, f_R\}$ and $\mathcal{G} \triangleq \{g_1, g_2, \ldots, g_R\}$. Since g_r, $\boldsymbol{v}_r$, and $\boldsymbol{w}$ are complex Gaussian random variables and mutually independent, the covariance matrix of $\boldsymbol{w}_T$ can be shown to be

$$\begin{aligned}\mathrm{Cov}(\boldsymbol{w}_T|\mathcal{F},\mathcal{G}) &= \sum_{r=1}^{R} |g_r|^2 \mathbb{E}_{\boldsymbol{v}} \left\{ (\rho_r^* \boldsymbol{A}_r \boldsymbol{v}_r + \rho_r \boldsymbol{B}_r \boldsymbol{v}_r^*)(\rho_r \boldsymbol{v}_r^H \boldsymbol{A}_r^H + \rho_r^* \boldsymbol{v}_r^t \boldsymbol{B}_r^H) \right\} + N_2 \boldsymbol{I}_T \\ &= \left(\sum_{r=1}^{R} |g_r|^2 |\rho_r|^2 N_1 + N_2 \right) \boldsymbol{I}_T + \mathbb{E}_{\boldsymbol{v}} \left\{ (\rho_r^*)^2 \boldsymbol{A}_r \boldsymbol{v}_r \boldsymbol{v}_r^t \boldsymbol{B}_r^H + (\rho_r)^2 \boldsymbol{B}_r \boldsymbol{v}_r^* \boldsymbol{v}_r^H \boldsymbol{A}_r^H \right\}, \end{aligned} \tag{A.9}$$

The second equality in (A.9) follows from the fact that for each relay, one of the matrices $\boldsymbol{A}_r$ and $\boldsymbol{B}_r$ is unitary and the other one is zero, or equivalently, $\boldsymbol{D}_r$ in (A.8) is a unitary matrix. It is well-known that the expectation of the square of a circular symmetric complex Gaussian random variable is zero, i.e., $\mathbb{E}\{\boldsymbol{v}_r \boldsymbol{v}_r^t\} = \mathbb{E}\{\boldsymbol{v}_r^* \boldsymbol{v}_r^H\} = \boldsymbol{0}_T$ [17, Chap. 3]. Hence, using (A.9), the conditional covariance of $\boldsymbol{w}_T$ is

$$\operatorname{Cov}\left(\boldsymbol{w}_T|\mathcal{F},\mathcal{G}\right)=\left(\sum_{r=1}^{R}|g_r|^2|\rho_r|^2N_1+N_2\right)\boldsymbol{I}_T, \tag{A.10}$$

and thus, the noise vector $\boldsymbol{w}_T$ is white.

If maximal-ratio combining (MRC) is applied at the destination, the instantaneous SNR at the receiver can be obtained from (A.5), yielding

$$\mathrm{SNR}_{\mathrm{ins}}=\frac{\sum_{r=1}^{R}P_1\,|g_r|^2\operatorname{Tr}\left\{\operatorname{Cov}\left(\rho_r^*\boldsymbol{A}_rf_r\boldsymbol{s}+\rho_r\boldsymbol{B}_rf_r\boldsymbol{s}^*|\mathcal{F},\mathcal{G}\right)\right\}}{\sum_{r=1}^{R}|g_r|^2|\rho_r|^2N_1+N_2}, \tag{A.11}$$

with

$$\begin{aligned}&\operatorname{Tr}\left\{\operatorname{Cov}\left(\rho_r^*\boldsymbol{A}_rf_r\boldsymbol{s}+\rho_r\boldsymbol{B}_rf_r\boldsymbol{s}^*|\mathcal{F},\mathcal{G}\right)\right\}=\\&\quad=\mathbb{E}_{\boldsymbol{s}}\left\{\left(\rho_rf_r^*\boldsymbol{s}^H\boldsymbol{A}_r^H+\rho_r^*f_r\boldsymbol{s}^t\boldsymbol{B}_r^H\right)\left(\rho_r^*f_r\boldsymbol{A}_r\boldsymbol{s}+\rho_rf_r^*\boldsymbol{B}_r\boldsymbol{s}^*\right)\right\}=|f_r|^2|\rho_r|^2,\end{aligned} \tag{A.12}$$

where the second equality in (A.12) results from the facts that $\boldsymbol{A}_r^H\boldsymbol{B}_r=\boldsymbol{0}_T$ and $\boldsymbol{D}_r^H\boldsymbol{D}_r=\boldsymbol{I}_T$. The conditional variance of the received noise in the denominator of (A.11) attained from (A.10). Combining (A.11) and (A.12), $\mathrm{SNR}_{\mathrm{ins}}$ can be written as

$$\mathrm{SNR}_{\mathrm{ins}}=\frac{\sum_{r=1}^{R}P_1|f_r|^2|g_r|^2|\rho_r|^2}{\sum_{r=1}^{R}|g_r|^2|\rho_r|^2N_1+N_2}. \tag{A.13}$$

For the choice of the scaling factor ρ_r several constraints can be imposed at the relay to satisfy an average output energy constraint per symbol. Such choices also imply, or result from, different assumptions on channel state information knowledge at the relays and, therefore, amount to different strategies for AF schemes, which we discuss below.

3.1 Scheme 1: Statistical CSI at Relays

When there is no instantaneous CSI at the relays, but statistical CSI is available, a useful constraint is

$$\rho_r = \sqrt{\frac{P_{2,r}}{\sigma_{f_r}^2 P_1 + N_1}}. \tag{A.14}$$

The AF strategy based on (A.14) will be referred to as Scheme 1. This constraint, which was utilized in the DSTCs designs proposed in [8] and [11], ensures that an average output energy per symbol is maintained, but allows for the instantaneous output power to be much larger than the average. It was shown in [8] that if f_k and g_k are i.i.d., the optimal value of $P_{2,r}$ in (A.14), in the sense of minimizing pairwise error probability (PEP), is equal to $\frac{P}{2R}$, where $P = P_1 + \sum_{r=1}^{R} P_{2,r}$ is the total power consumed for the transmission of a single symbol. In Section V, we will show that using this scaling factor the full diversity is obtainable. Since the equivalent relay channel $\boldsymbol{h}$ in this case must be in the form described in (A.7), Scheme 1 requires dedicated space-time code designs.

3.2 Scheme 2: Known Backward Channel Coefficients in Relays

Discovering f_r and g_r by the destination can be accomplished through a training symbol sequence transmitted by the source. The relay can similarly use this sequence to discover the backward channel gain f_r. Thus, it is reasonable to assume that f_r is known at the rth relay. In this case, the following scaling factor can be used [10]

$$\rho_r = \sqrt{\frac{P_{2,r}}{\sigma_{f_r}^2 P_1 + N_1}} \frac{f_r}{|f_r|}. \tag{A.15}$$

The AF strategy based on (A.15) will be called Scheme 2. Although with Scheme 2 the instantaneous output power may be larger than the average, the rth component of the equivalent relay channel reduces to

$$h_r = \sqrt{\frac{P_{2,r}}{\sigma_{f_r}^2 P_1 + N_1}} |f_r| g_r. \tag{A.16}$$

Therefore, unlike Scheme 1, all existing space-time block codes can be used with Scheme 2. In Section V, we will show that the schemes with ρ_r in (A.14) and (A.15) have the same performance.

3.3 Scheme 3: Automatic Gain Control (AGC) at the Relays

A third scheme results by considering that some applications require AGC at the relays in order to comply with certain standards (see e.g., [19]) and prevent saturating the relay amplifier. Besides adjusting the input power to the amplifier, the AGC facilitates controlling the instantaneous output power of each relay so that it remains constant. An appropriate scaling factor for this case and its corresponding h_r would be

$$\rho_r = \sqrt{\tfrac{P_{2,r}}{|f_r|^2 P_1 + N_1}}\tfrac{f_r}{|f_r|}, \tag{A.17a}$$

$$h_r = \sqrt{\tfrac{P_{2,r}}{|f_r|^2 P_1 + N_1}}|f_r| g_r. \tag{A.17b}$$

In Section VI, we will show that unlike Schemes 1 and 2, Scheme 3, obtained with the use of ρ_r in (A.17a), *cannot* achieve full diversity.

4 Complex DSTC Design with Distributed GABBA Codes

As stated in Section III, Scheme 1 based on the scaling factor given in (A.14), requires dedicated space-time code designs. In complex DSTC design, we are going to apply the designs which have full-rate, i.e., $1/2$ (due to the two-phase transmission nature of the relaying mechanism under consideration) and whose columns are composed exclusively by either the information symbols $s_1, \ldots, s_T$, or their conjugate $s_1^*, \ldots, s_T^*$.

We employ transposed GABBA codes in a way similar to the Alamouti-based and [20] the QOSTBC-based designs [21] investigated in [10]. This is because the fact that the transpose of the $T \times T$ GABBA mother code has the structure $\boldsymbol{S} = [\boldsymbol{G}_1 \, \boldsymbol{G}_2^*]$, where $\boldsymbol{G}_1$ and $\boldsymbol{G}_2^*$ are $T \times T/2$ matrices whose columns belong to the sets Ω and Ω^*, respectively. In this case, the sets Ω and Ω^* can be written as

$$\Omega = \left\{ \boldsymbol{c}_k |\, k = 1, \ldots, \frac{T}{2} \right\}, \quad \Omega^* = \left\{ \boldsymbol{c}_k |\, k = \frac{T}{2} + 1, \ldots, T \right\}. \tag{A.18}$$

4.1 Code Construction

In this subsection, we propose *complex* distributed GABBA designs to construct DSTC that achieve full-diversity and full-rate. We define a complex distributed GABBA design of size $T \times R$, where T is power of two, and R is the number of relays which can be $R \leq T$, as a submatrix of the transpose of GABBA codes. Distributed GABBA codes can be constructed by simply removing arbitrary $T - R$ columns of the transpose of $T \times T$ GABBA codes.

As an example, we explain the application of the 2×2, 4×4, and 8×8 GABBA codes. Since all symbol appears once and only once in each column, which is true for all GABBA codes, $\boldsymbol{A}_i$ and $\boldsymbol{B}_i$ has the structure of a matrix whose entries can be 1, 0, or -1.

The 2×2 distributed GABBA code matrix is the transpose of Alamouti code itself,

$$\boldsymbol{S} = \begin{bmatrix} s_1 & -s_2^* \\ s_2 & s_1^* \end{bmatrix}. \tag{A.19}$$

In this case, the matrices used at the relays are

$$\boldsymbol{A}_1 = \begin{bmatrix} 1 & 0 \\ 0 & -1 \end{bmatrix}, \boldsymbol{B}_1 = \boldsymbol{A}_2 = \boldsymbol{0}_2 \text{, and } \boldsymbol{B}_2 = \begin{bmatrix} 0 & 1 \\ 1 & 0 \end{bmatrix}. \tag{A.20}$$

The 4×4 distributed GABBA code matrix can be shown as

$$\boldsymbol{S} = \begin{bmatrix} s_1 & -s_2 & -s_3^* & -s_4^* \\ s_2 & s_1 & s_4^* & -s_3^* \\ s_3 & -s_4 & s_1^* & s_2^* \\ s_4 & s_3 & -s_2^* & s_1^* \end{bmatrix}. \tag{A.21}$$

The matrices used at the relays are $\boldsymbol{B}_1 = \boldsymbol{B}_2 = \boldsymbol{A}_3 = \boldsymbol{A}_4 = \boldsymbol{0}_4$, and

$$\boldsymbol{A}_1 = \boldsymbol{I}_4,\ \boldsymbol{A}_2 = \begin{bmatrix} 0 & -1 & 0 & 0 \\ 1 & 0 & 0 & 0 \\ 0 & 0 & 0 & -1 \\ 0 & 0 & 1 & 0 \end{bmatrix}, \boldsymbol{B}_3 = \begin{bmatrix} 0 & 0 & -1 & 0 \\ 0 & 0 & 0 & 1 \\ 1 & 0 & 0 & 0 \\ 0 & -1 & 0 & 0 \end{bmatrix}, \boldsymbol{B}_4 = \begin{bmatrix} 0 & 0 & 0 & -1 \\ 0 & 0 & -1 & 0 \\ 0 & 1 & 0 & 0 \\ 1 & 0 & 0 & 0 \end{bmatrix}. \tag{A.22}$$

It is easy to see that $\boldsymbol{A}_i$ and $\boldsymbol{B}_i$ in (A.20) and (A.22) are either zero or unitary.

Finally, the 8×8 distributed GABBA code matrix is

$$\boldsymbol{S}=\begin{bmatrix} s_1 & -s_2 & -s_3 & s_4 & -s_5^* & -s_6^* & -s_7^* & -s_8^* \\ s_2 & s_1 & -s_4 & -s_3 & s_6^* & -s_5^* & s_8^* & -s_7^* \\ s_3 & -s_4 & s_1 & -s_2 & s_7^* & s_8^* & -s_5^* & -s_6^* \\ s_4 & s_3 & s_2 & s_1 & -s_8^* & s_7^* & s_6^* & -s_5^* \\ s_5 & -s_6 & -s_7 & s_8 & s_1^* & s_2^* & s_3^* & s_4^* \\ s_6 & s_5 & -s_8 & -s_7 & -s_2^* & s_1^* & -s_4^* & s_3^* \\ s_7 & -s_8 & s_5 & -s_6 & -s_3^* & -s_4^* & s_1^* & s_2^* \\ s_8 & s_7 & s_6 & s_5 & s_4^* & -s_3^* & -s_2^* & s_1^* \end{bmatrix}. \tag{A.23}$$

Since $\boldsymbol{A}_i$ corresponds to the ith column of the code matrix $\boldsymbol{S}$, one can easily construct the matrices $\{\boldsymbol{A}_1, \boldsymbol{A}_2, \boldsymbol{A}_3, \boldsymbol{A}_4\}$ and $\{\boldsymbol{B}_5, \boldsymbol{B}_6, \boldsymbol{B}_7, \boldsymbol{B}_8\}$ to be used at the relays. For higher dimension GABBA mother codes, like 16×16 and 32×32 GABBA codes, the same characteristic holds, because of the structure $\boldsymbol{S} = [\boldsymbol{G}_1\, \boldsymbol{G}_2^*]$. Due to lack of space, however, we omit to write the corresponding matrices $\boldsymbol{S}$, $\boldsymbol{A}_i$, and $\boldsymbol{B}_i$ here.

4.2 The Decoding Algorithm

For the case of 2×2 distributed GABBA code, which reduces to the transpose of Alamouti code, the orthogonal decoder is equivalent to the ML decoder. For $R > 2$, maximum-likelihood decoding formula similar to that in [18, Eq. (4.79)] can be applied for the decoding of distributed GABBA codes. Moreover, since the log-likelihood ratio cost function in the $T \times R$ distributed GABBA code can be decomposed into two separate functions (see e.g., [13, Eq. (8)]), pairwise maximum-likelihood (PW ML) decoding [18] is equivalent to ML decoding, similar to quasi-orthogonal (QO) DSTC.

For Protocol III, in which the source-destination link contributed in both phases of the cooperative transmission scheme, the ML decoder has the form

$$\arg\min_{\boldsymbol{s}} \left(\|\boldsymbol{y} - \boldsymbol{S}\boldsymbol{h}\|^2 + \delta \|\boldsymbol{y_0} - f_0 \boldsymbol{s}\|^2 \right), \tag{A.24}$$

where δ is a parameter that normalized the received noise in two phases, i.e., $\boldsymbol{w}$ and $\boldsymbol{w}_T$.

The complex decoding techniques, like maximum likelihood (ML) and pairwise ML [18], prevent applicability of the code matrices with large dimensions. Using distributed GABBA codes with linear orthogonal decoding, we can employ a large number of potential relays to improve the diversity order. Therefore, instead of complex ML decoding for general full-rate, full-diversity space-time codes or pairwise ML decoding, we can use GABBA linear orthogonal decoding for full-rate, full-diversity $T \times R$ GABBA codes.

In the case of distributed GABBA codes, the same orthogonal decoder presented in [13] can be used, except that the output of the decoder should be passed again to the GABBA encoder, since the first column of the output of GABBA encoder corresponds to the recovered signal.

4.3 Enhanced Distributed GABBA Codes

The GABBA orthogonal decoder suboptimally separates non-orthogonal columns of the matrix $\boldsymbol{G}_1$, i.e., $\boldsymbol{c}_r \in \Omega$, and $\boldsymbol{G}_2$, i.e., $\boldsymbol{c}_r \in \Omega^*$. However, due to the orthogonality of the columns in $\boldsymbol{G}_1$ and $\boldsymbol{G}_2^*$, the performance of the $T \times R$ distributed GABBA codes can be improved when $R \in \{2, 3, \ldots, T-2\}$. To this end, the relays are divided into two categories. We should allocate almost half of the relays with $\boldsymbol{c}_i \in \Omega$, and the remaining relays should be corresponding to $\boldsymbol{c}_i \in \Omega^*$. In this scheme, we put the ith column of code matrix $\boldsymbol{S}$, i.e., $\boldsymbol{c}_i$, which is corresponding to $\boldsymbol{A}_i$ and $\boldsymbol{B}_i$ in the rth relay. One possible choice of the index i which satisfies the condition stated above is

$$i(r) = \begin{cases} r, & \text{if } r \leq \lceil R/2 \rceil, \\ T - R + r, & \text{if } r > \lceil R/2 \rceil. \end{cases} \tag{A.25}$$

Thus, with $r = 1, \ldots, R$, (A.8) will be changed to

$$\boldsymbol{D}_r = \begin{cases} \boldsymbol{A}_{i(r)}, & \text{if } r \leq \lceil R/2 \rceil, \\ \boldsymbol{B}_{i(r)}, & \text{if } r > \lceil R/2 \rceil. \end{cases} \tag{A.26}$$

Therefore, the main idea behind this DSTC transmission is that we increase the orthogonality among the distributed code columns by simply allocating the selected relays with equal number of columns from sets Ω and Ω^*.

In the case of fixed relay scenarios, in which all R deployed relays are used for relaying the transmitter's data, we simply assign the index of the appropriate column to the rth relay. In dynamic scenarios, in which the number of active relays varies depending on channel conditions, some control bits should be exchanged between the relays and the destination to inform them of the appropriate index i at the rth relay.

5 Performance Analysis

In [22], the asymptotic behavior of AF relay networks with Alamouti code is studied under frequency division duplexing (FDD) scheme, i.e., two different frequency bands are allocated for transmitting and receiving signals at the relays. In this section, we will derive the SER formulas of any full-rate, full-diversity DSTC, e.g., space-time GABBA codes, under time division duplexing (TDD) setup. The employed signals could have arbitrary complex constellations.

5.1 SER Expression

The conditional SER of the protocol described in Section II, with R relays, can be approximated as [23, Eq. (9.17)]

$$P_e\left(R|\mathcal{F},\mathcal{G}\right) = c\,Q\left(\sqrt{\kappa\sum_{r=1}^{R}\mu_r|f_r\,g_r|^2}\right), \tag{A.27}$$

where $Q(x) = 1/\sqrt{2\pi}\int_x^\infty e^{-u^2/2}\,du$, and the parameters c and κ are represented as

$$c_{\text{QAM}} = 4\frac{\sqrt{M}-1}{\sqrt{M}},\; c_{\text{PSK}} = 2,\; \kappa_{\text{QAM}} = \frac{3}{M-1},\; \kappa_{\text{PSK}} = 2\sin^2\left(\frac{\pi}{M}\right).$$

Using (A.13), and replacing the ρ_r from (A.14) or (A.15), μ_r can be written as

$$\mu_r = \frac{\frac{P_1P_{2,r}}{\sigma_{f_r}^2P_1+N_1}}{\sum_{k=1}^{R}\frac{P_{2,k}}{\sigma_{f_k}^2P_1+N_1}\sigma_{g_k}^2N_1+N_2}. \tag{A.28}$$

It is important to note that in (A.28), we approximated the conditional variance of the noise vector $\boldsymbol{w}_T$ in (A.6), which is obtained in (A.10), with its expected value. At high SNRs, the average variance of the noise at the destination becomes $\frac{(1-\alpha)\sigma_g^2}{\alpha\,\sigma_f^2}N_1+N_2$, where we have replaced $P_1=\alpha P$ and $P_{2,r}=(1-\alpha)\frac{P}{R}$, in which $0<\alpha<1$. This approximation is particularly accurate if low-noise amplifiers (LNAs) are used at the relay terminals, such that $N_1<N_2$, if source-relays distances are longer than relays-destination distances, such that $\sigma_f^2>\sigma_g^2$, or if we allocate more power in the first phase of the cooperation, i.e., if value of α is large.

In the following, we will derive the probability density function (PDF) and MGF of

$$\gamma_r = \mu_r |f_r\, g_r|^2, \tag{A.29}$$

that appears in (A.27) and is needed for calculating the average SER.

Theorem 1 *For the* γ_r *in* (A.29)*, the PDF* $p(\gamma_r)$ *can be written as*

$$p(\gamma_r) = \frac{2}{\mu_r \sigma_{f_r}^2 \sigma_{g_r}^2} K_0 \left(2 \sqrt{\frac{\gamma_r}{\mu_r \sigma_{f_r}^2 \sigma_{g_r}^2}} \right), \tag{A.30}$$

where $K_i(x)$ *is the modified Bessel function of the second kind of order* i *[24].*

Proof: *The proof is given in Appendix I.* □

Theorem 2 *Let* X *and* Y *be two independent exponential random variables with mean* $\sigma_{f_r}^2$ *and* $\sigma_{g_r}^2$*, respectively. Then, the MGF of* $Z = \mu_r XY$*, i.e.,* $\mathbb{E}_\gamma\{e^{sZ}\}$*, is given by*

$$M_r(-s) = -\frac{1}{s\,\mu_r \sigma_{f_r}^2 \sigma_{g_r}^2} e^{\frac{1}{s\mu_r \sigma_{f_r}^2 \sigma_{g_r}^2}} E_i \left(\frac{-1}{s\,\mu_r \sigma_{f_r}^2 \sigma_{g_r}^2} \right), \tag{A.31}$$

where $E_i\,(x)$ *is the exponential integral function [24]*

Proof: *Considering* (A.30)*, we can express* $M_r(-s)$ *as*

$$M_r(-s) = \int_0^\infty e^{-s\gamma} \frac{2}{\mu_r \sigma_{f_r}^2 \sigma_{g_r}^2} K_0 \left(2 \sqrt{\frac{\gamma}{\mu_r \sigma_{f_r}^2 \sigma_{g_r}^2}} \right) d\gamma. \tag{A.32}$$

Using [25, Eq. (6.643)], we obtain after some manipulations

$$M_r(-s) = \sqrt{\frac{1}{s\,\mu_r \sigma_{f_r}^2 \sigma_{g_r}^2}} e^{\frac{1}{2s\mu_r \sigma_{f_r}^2 \sigma_{g_r}^2}} W_{-\frac{1}{2},0} \left(\frac{1}{s\,\mu_r \sigma_{f_r}^2 \sigma_{g_r}^2} \right), \tag{A.33}$$

where $W_{a,b}(x)$ *is Whittaker's function of orders* a *and* b *(see e.g., [25, Eq. (9.224)] and [24]). Using [25, Eq. (9.224)], we can represent* $W_{-\frac{1}{2},0}(\cdot)$ *in terms of the exponential integral function, that is*

$$W_{-\frac{1}{2},0}(x) = -x^{\frac{1}{2}} e^{\frac{x}{2}} E_i(-x). \tag{A.34}$$

Equation (A.31) *results from the combination of* (A.33) *and* (A.34)*.* □

Now, we can use the MGF to derive the approximate SER expression for the relay network discussed in Section II. Using (A.29), (A.27) can be written as

$$P_e\left(R|\{\gamma_r\}_{r=1}^R\right) = c\,Q\left(\sqrt{\kappa\sum_{r=1}^{R}\gamma_r}\right). \tag{A.35}$$

Since the γ_rs are independent, the average SER would be

$$P_e(R) = \int_{0;R-\text{fold}}^{\infty} P_b\left(R|\{\gamma_r\}_{r=1}^R\right)\prod_{r=1}^{R}(p(\gamma_r)\,d\gamma_r) = \int_{0;R-\text{fold}}^{\infty} c\,Q\left(\sqrt{\kappa\sum_{r=1}^{R}\gamma_r}\right)\prod_{r=1}^{R}(p(\gamma_r)\,d\gamma_r). \tag{A.36}$$

Using the moment generating function approach, we get

$$P_e(R) = \int_{0;\,R-\text{fold}}^{\infty}\frac{c}{\pi}\int_0^{\frac{\pi}{2}}\prod_{r=1}^{R} e^{-\frac{\kappa\,\gamma_r}{2\sin^2\phi}}\,d\phi\prod_{r=1}^{R}(p(\gamma_r)\,d\gamma_r) = \frac{c}{\pi}\int_0^{\frac{\pi}{2}}\prod_{r=1}^{R} M_r\left(-\frac{\kappa}{2\sin^2\phi}\right)d\phi, \tag{A.37}$$

where $M_r(s)$ is the MGF of γ_r in (A.31).

In the sequel, we consider a space-time coded relay network based on Protocol III, in which the source-destination link contributes to both phases based on (A.3) and (A.4). The total transmit power, however, is assumed to be the same as in Protocol I. In this case, assuming equal power transmission the power distribution would be $P_1 = \frac{P}{2}$ and $P_{2,r} = \frac{P}{2\,(R+1)}$.

Now, we derive the SER formula of full-diversity and full-rate space-time codes in AF mode under Protocol III. The conditional SER of Protocol III, with R relays, can be written as

$$P_e\left(R|f_0,\mathcal{F},\mathcal{G}\right) = c\,Q\left(\sqrt{\kappa\,\text{SNR}^{\text{out}}}\right), \tag{A.38}$$

where

$$\text{SNR}^{\text{out}} = \gamma_{1,0} + \gamma_{2,0} + \sum_{r=1}^{R}\gamma_r, \tag{A.39}$$

where $\gamma_{1,0} = \mu_{1,0}|f_0^{(1)}|^2$ and $\gamma_{2,0} = \mu_{2,0}|f_0^{(2)}|^2$, in which $f_0^{(1)}$ and $f_0^{(2)}$ are the channel coefficients of the source-destination path during Phases I and II, respectively. We can write the coefficients $\mu_{1,0}$ and $\mu_{2,0}$ as

$$\mu_{1,0} = \frac{P_1}{N_0},\ \ \mu_{2,0} = \frac{P_{2,r}}{\sum_{k=1}^{R} \frac{P_{2,k}}{\sigma_{f_k}^2 P_1 + N_1} \sigma_{g_k}^2 N_1 + N_2}. \tag{A.40}$$

The random variables $\gamma_{1,0}$ and $\gamma_{2,0}$ have an exponential distribution, and γ_r has a distribution as (A.30).

Since the γ_r's are independent, and assuming that the coherence time of the direct channel is such that $\gamma_{1,0}$ and $\gamma_{2,0}$ are independent, the MGF approach yields

$$\begin{aligned} P_e(R) &= \int_{0;\,(R+2)-\text{fold}}^{\infty} P_e\left(R|f_0, \mathcal{F}, \mathcal{G}\right) p_0(\gamma_{1,0}) d\gamma_{1,0}\, p_0(\gamma_{2,0}) d\gamma_{2,0} \prod_{r=1}^{R} \left(p(\gamma_r)\, d\gamma_r\right) \\ &= \frac{c}{\pi} \int_0^{\frac{\pi}{2}} M_{1,0}\left(-\frac{\kappa}{2\sin^2\phi}\right) M_{2,0}\left(-\frac{\kappa}{2\sin^2\phi}\right) \prod_{r=1}^{R} M_r\left(-\frac{\kappa}{2\sin^2\phi}\right) d\phi, \end{aligned} \tag{A.41}$$

where $M_r(\cdot)$ is the MGF of the RV γ_r, as obtained given in Theorem 2, while $M_{i,0}(s) = \frac{1}{1-\mu_{i,0}\sigma_{f_0}^2 s}$, $i = 1, 2$, is the MGF of the random variables $\gamma_{i,0}$.

The SER formula in (A.37) is a special case of (A.41). If the source node does not contribute in both phases, we can set $\mu_{1,0} = \mu_{2,0} = 0$, and since $M_i(0) = 1$, the SER expression in (A.37) is found form (A.41). When the network channels have spatial or temporal correlations, the corresponding SER is lower-bounded by (A.41).

For the case of Scheme 3, in which the scaling factor is as (**??**), the received SNR at the destination in (A.13) becomes

$$\text{SNR}_{\text{ins}} = \frac{\sum_{r=1}^{R} P_1 |f_r|^2 |g_r|^2 \frac{P_{2,r}}{P_1|f_r|^2 + N_1}}{\sum_{k=1}^{R} \frac{P_{2,k}}{P_1|f_k|^2 + N_1} |g_k|^2 N_1 + N_2}. \tag{A.42}$$

We can rewrite (A.42) as $\text{SNR}_{\text{ins}} = \sum_{r=1}^{R} \epsilon_r\, \xi_r$, where

$$\xi_r = \frac{R\, P_1 P_{2,r} |f_r|^2 |g_r|^2}{N_1 N_2 + P_1 N_2 |f_r|^2 + P_{2,r} N_1 |g_r|^2}, \tag{A.43}$$

$$\epsilon_r = \frac{1}{R} \frac{\frac{N_1 N_2 + P_1 N_2 |f_r|^2 + P_{2,r} N_1 |g_r|^2}{P_1 |f_r|^2 + N_1}}{\sum_{k=1}^{R} \frac{P_{2,k}}{P_1|f_k|^2 + N_1} |g_k|^2 N_1 + N_2}. \tag{A.44}$$

The weights in (A.44) are such that $\sum_{r=1}^{R} \epsilon_r = 1$. Because of the summation terms in the denominator of (A.42), which is consisting of another rational function, obtaining the corresponding PDF is not possible. Therefore, we analyze an upper-bound on SNR$_{\text{ins}}$ in (A.42), i.e.,

$$\text{SNR}_{\text{ins}}^{u} = \max\left\{\xi_1^u, \xi_2^u, \ldots, \xi_R^u\right\},$$

since $\epsilon_r \in [0, 1]$, where

$$\xi_r^u = \frac{R\,P_1 P_{2,r}|f_r|^2|g_r|^2}{P_1 N_2|f_r|^2 + P_{2,r}N_1|g_r|^2}.$$

For calculating the average SER, we need to find the PDF of SNR$_{\text{ins}}^{u}$, which it is found in [26, Eq. (16)].

Now, we are deriving the SER expression for AF DSTC with Scheme 3. Averaging over conditional SER, i.e., $P_e\left(R|\mathcal{F},\mathcal{G}\right) = c\,Q\left(\sqrt{\kappa\,\text{SNR}_{\text{ins}}^{u}}\right)$, we have a lower-bound SER expression as

$$P_e(R) \geq \int_0^\infty P_e\left(R|\mathcal{F},\mathcal{G}\right)\,p_{\max}(\gamma)\,d\gamma = \int_0^\infty c\,Q\left(\sqrt{\kappa\,\gamma}\right)\,p_{\max}(\gamma)\,d\gamma.$$

where $p_{\max}(\gamma)$ is the PDF of SNR$_{\text{ins}}^{u}$.
A tighter bound on SNR$_{\text{ins}}$ can be obtained when we use ξ_r itself, instead of ξ_r^u, i.e., SNR$_{\text{ins}}^{u}$ $= \max\left\{\xi_1, \xi_2, \ldots, \xi_R\right\}$. In this case, PDF and cumulative distribution function (CDF) of ξ_r can be achieved similar to the approach used in the proof of Theorem 1. Then, using order statistics, the PDF of $\gamma_{\max}$ can be written as

$$p_{\max}(\gamma) = \frac{d}{d\gamma}\Pr\{\gamma_{\max} < \gamma\} = \sum_{i=1}^{R} p(\gamma) \prod_{\substack{j=1 \\ j\neq i}}^{R} \Pr\{\xi_j \leq \gamma\}.$$

where $p(\gamma)$ and $\Pr\{\xi_j \leq \gamma\}$ are the PDF and CDF of ξ_j, respectively.

5.2 Diversity Analysis

In this subsection, we will study the achievable diversity gains in a AF DSTC network containing R relays. In particular, we consider relay networks with no CSI at the relay terminal and also relays with partial CSI of f_r with the scaling factor presented in (A.15). As discussed in Subsection IV-A, Scheme 1 and Scheme 2 achieve the same performance. However, Scheme 2 – with the scaling factor in (A.15) – can be used with any space-time block code structure.

It is difficult to analytically derive the diversity order of the system employing Scheme 3, where the scaling factor in (A.17) is used. However, since the conditional variance of the noise from the rth relay path is proportional to $\frac{1}{|f_r|^2}$ at high SNR (see (44)), the total noise is amplified when a source-to-rth relay channel experiences a bad condition. Hence, intuitively it is obvious that this scheme cannot provide the diversity order of more than one.

Before studying the diversity order of the AF DSTC network, we present the following lemma, which can be used in several other applications for evaluating the diversity order.

Lemma 1 *The diversity order of a wireless fading system with MGF $M_\gamma(s)$, where γ is the RV representing the equivalent received SNR, is lower-bounded as*

$$G_d \geq -\lim_{\mu\to\infty} \frac{\log\left(M_\gamma\left(\frac{-\kappa}{2}\right)\right)}{\log(\mu)}. \qquad \text{(A.45)}$$

Proof: *The proof is given in Appendix II.* □

Theorem 3 *The AF DSTC with scaling factor presented in* (A.14)*, in which relays have no CSI, i.e., Scheme 1, provides full diversity R.*

Proof: *The proof is given in Appendix III.* □

Corollary 1 *The AF DSTC with partial CSI of their backward channels with the scaling factor presented in* (A.15)*, i.e., Scheme 2, provides full diversity R.*

Proof: *Since both scaling factors in* (A.14) *and* (A.15) *have equal magnitude, i.e., $|\rho_r|$, and the procedure for deriving Theorem 2 is depending on statistics of $|\rho_r|^2$ and is independent of the phase of ρ_r, the desired result in Corollary 1 is achieved.* □

6 Simulation Results

In this section, the performance of distributed GABBA space-time codes are studied through simulations. The error event is bit error rate (BER) and we use the block fading model. Equal power allocation is used in

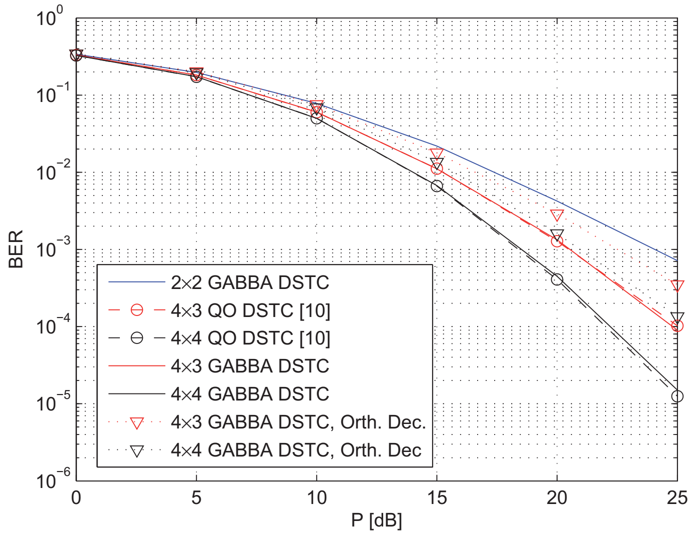

Fig. A.2: The average BER curves of relay networks employing distributed space-time codes with BPSK signals, using Protocol I and Scheme 1.

two phases and also among the relays. Assume that the relays and the destination have the same value of noise power, i.e., $N_1 = N_2$, and all the links have unit-variance Rayleigh flat fading, i.e., $\sigma^2_{f_r} = \sigma^2_{g_r} = 1$. To be in consistency with the result presented in [10], in all figures we consider the total transmission power consumed per symbol in two phases, i.e., P is plotted along with horizontal axis.

In Fig. A.2, the BERs of the system with different DSTCs and decoding techniques are considered, when BPSK signal is employed. Since the log-likelihood ratio cost function in the 4×4 GABBA code can be decomposed into two separate function, pairwise maximum-likelihood (PW ML) decoding is equivalent to ML decoding, similar to QO-DSTC [10]. Fig. A.2 demonstrates that $T \times R$ GABBA DSTC and QO-DSTC with PW ML decoding [10] have a similar performance. Note that for QO-DSTC codes to be fully-diverse, some of the information signals need rotation. Moreover, it can be seen that GABBA DSTCs with linear orthogonal decoding have some performance loss, in expense of simple decoding, although they

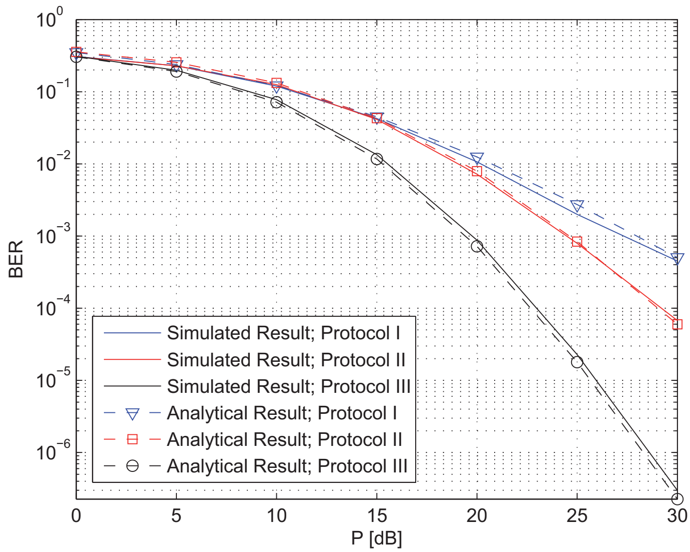

Fig. A.3: Performance comparison of analytical and simulated results of a relay network with $R = 2$ and employing different protocols with QPSK signals, and under Scheme 1.

achieve the same diversity order as GABBA DSTCs with PW ML decoding.

Fig. A.3 and A.4 confirm that the analytical SER expressions in Subsection V-A for finding SER have similar performance as practical full-diversity distributed space-time codes. In Fig. A.3, we consider a network with $R = 2$ and QPSK signals. The analytical results are based on (A.41), where by assuming that Gray coding is used, BER becomes SER divided by $\log_2(M)$. Since Protocol III uses all degrees of freedom in the network, full space-time diversity is obtained. In Fig. A.4, we consider a network with $R = 1, 2, 3, 4$ and QPSK signals under Protocol II. Fig. A.4 confirms that, even when more than two relays are employed, the analytical results approximate the simulated results with a good precision, especially in high SNR values.

Fig. A.5 compares the performance of distributed GABBA space-time codes with the indexing format in (A.8) and Enhanced Distributed GABBA codes presented in Subsection IV-C, when GABBA orthogonal decoding is

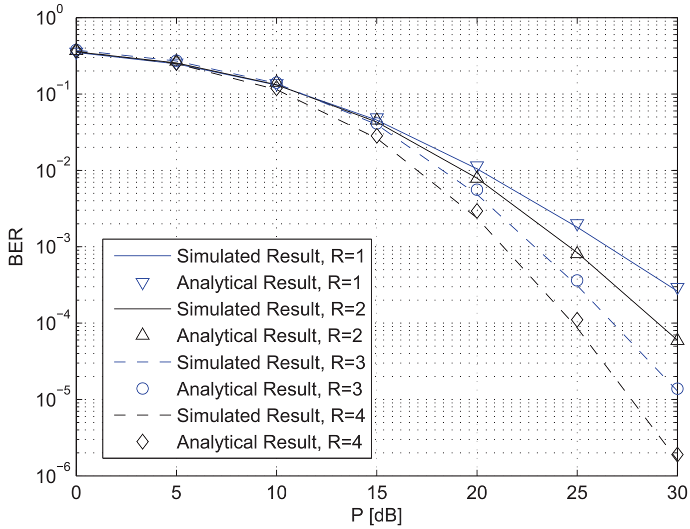

Fig. A.4: Performance comparison of analytical and simulated results of a relay network employing Protocol II with QPSK signals.

used. The coherence time of network channels is such that $T = 8$, and the number of relays is assumed to be $R = 2, 3, \ldots, 6$. In this case, the best choice of GABBA codes is the 8×8 GABBA mother code, shown in (A.23). Note that $T \times R$ DSTC codes can be constructed by simply removing $T - R$ columns of $T \times T$ general DSTC code. Since distributed GABBA codes and Enhanced Distributed GABBA codes have the same performance when $R = 1, 7, 8$, we do not show the corresponding curves in Fig. A.5. One can observe that at BER $= 10^{-2}$, a gain of 7 dB is obtained using Enhanced Distributed GABBA codes comparing to distributed GABBA codes, when $R = 4$. On the other hand, the linear decodability of such codes allow us to increase the scale (R) of the cooperative network in feasible wireless systems, such as wireless sensor networks.

In Fig. A.6, the BERs of the system with different DSTCs and decoding techniques are considered. For $R \leq 2$, 2×2 GABBA mother code, or the transpose of Alamouti code, can be employed. Note that the linear orthogonal decoder is equivalent to ML decoder, in this case. When $2 < R \leq 4$,

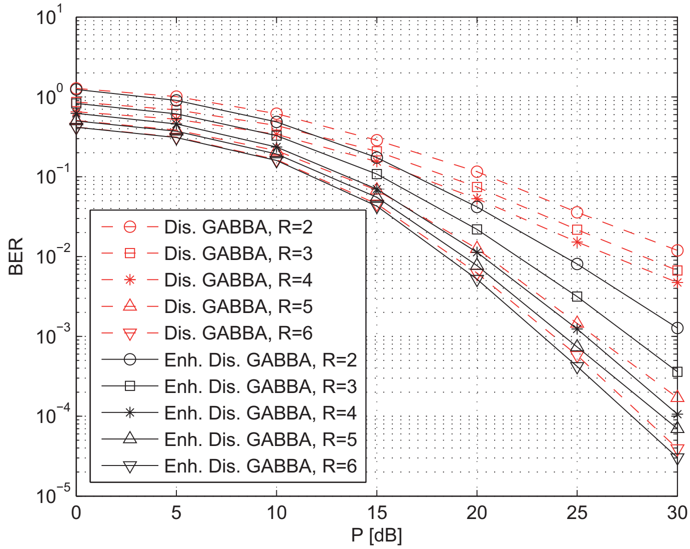

Fig. A.5: The average BER curves of linear orthogonal decoded $8 \times R$ distributed GABBA codes and their enhanced version with QPSK signals, under Protocol I and Scheme 1.

the 4×4 GABBA mother code, stated in (A.21), is an appropriate choice. For this case, we applied both GABBA linear decoder and PW ML. It can be seen that the 4×4 code with PW ML outperforms the same code using linear decoder by about 3 dB at BER $= 10^{-3}$. Finally, for $R > 4$, a suitable choice for DSTC is the 8×8 GABBA mother code. Fig. A.6 demonstrates that the 8×8 code with PW ML outperforms from the same code using linear decoder by about 3 dB at BER $= 10^{-4}$. Thus, GABBA DSTCs with linear orthogonal decoding have simple decoding, in expense of some performance loss, although they achieve the same diversity order as GABBA DSTCs with PW ML decoding.

In Fig. A.7, we compare the performance of systems with different scaling factors using $R = 2$ and QPSK signals. The figure shows that using a single relay, a network with our proposed scaling factor in (A.17), i.e., Scheme 3, outperforms the system with the scaling factor in (A.14) and (A.15), which introduced in [10], around 5 dB, when one relay is used.

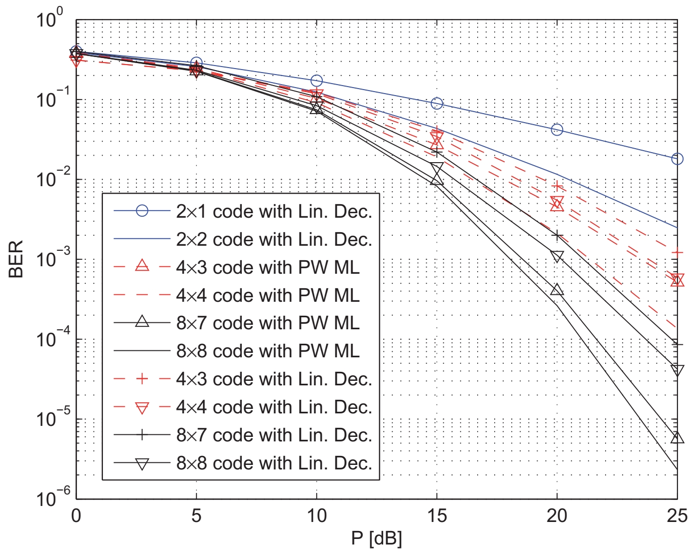

Fig. A.6: The average BER curves of relay networks employing distributed space-time codes using different decoding techniques, with QPSK signals, $T = 8$, under Protocol I and Scheme 1.

Due to the reason explained in Subsection V-A, Scheme 1 and Scheme 2 have the same performance. Thus, we omitted the curves corresponding to Scheme 2. Furthermore, comparing the curves related to 2×2 DSTC, it can be seen that by using Scheme 3 we loose the diversity gain. However, using Scheme 3 and $R = 2$ a considerable coding gain will be obtained comparing to $R = 1$ relay network, and the instantaneous transmit power from each relay is constant.

7 Conclusion

In this paper, we proposed using distributed GABBA space-time codes for a general R-relay cooperative system. Relays simply transmit the scaled version of the linear combinations of the received signals. The applicability of linear orthogonal decoding is also investigated. We analyzed the performance of the system with M-PSK and M-QAM signals, when ML de-

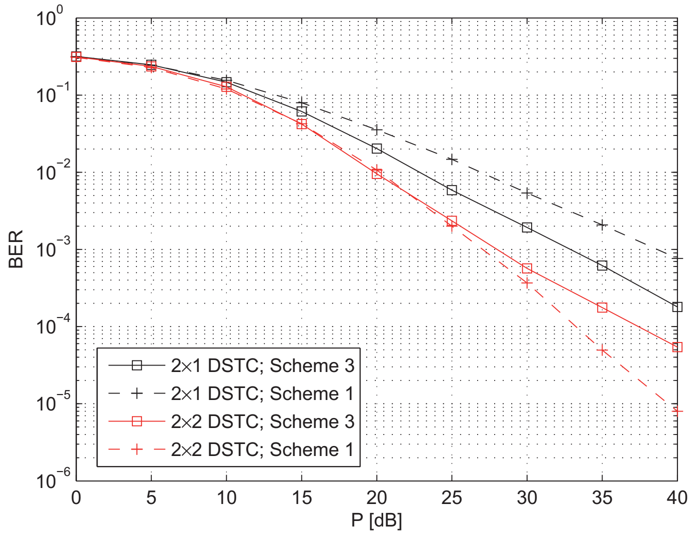

Fig. A.7: The average BER curves of relay networks employing different scaling factors at relays with QPSK signals, $T = 2$, and under Protocol I.

coding is utilized. Based on the proposed approximated SER expression, it is shown that using DSTC, full-diversity can be obtained. We also generalized the DSTC in AF mode, when source-destination link is contributing in both phases, where full space-time diversity is also obtainable. Simulations are in accordance with the proposed analytic results and show that using linear GABBA decoder, we can extend the network size with acceptable performance. Finally, simulations show that a network with our proposed scaling factor outperforms the system with the existing scaling factors by about 5 dB, when one relay is used.

Appendix I: Proof of Theorem 1

Suppose $Z = \gamma_r$, $X = |f_r|^2$, and $Y = |g_r|^2$, where X and Y are exponentially distributed with means $\overline{X} = \sigma_f^2$ and $\overline{Y} = \sigma_g^2$, respectively. The cumulative density function of the RV $Z = \mu_r XY$ is

$$\Pr\{Z < z\} = \Pr\{XY < z/\mu_r\} = \int_0^\infty \Pr\{Xy < z/\mu_r\} p_Y(y) dy = \frac{1}{\overline{Y}} \int_0^\infty \left(1 - e^{-\frac{z}{y\mu_r \overline{X}}}\right) e^{-\frac{y}{\overline{Y}}} dy$$
$$= \frac{1}{\overline{Y}} \int_0^\infty e^{-\frac{y}{\overline{Y}}} - e^{-\left(\frac{y}{\overline{Y}} + \frac{z}{y\mu_r \overline{X}}\right)} dy = 1 - 2\sqrt{\frac{z}{\mu_r \overline{X}\,\overline{Y}}} K_1\left(2\sqrt{\frac{z}{\mu_r \overline{X}\,\overline{Y}}}\right),$$

where we used [25, Eq. (3.324)] for the last equality. The pdf of Z can be written as (A.21)

$$p_Z(z) = \frac{d}{dz}\Pr\{Z < z\} = \frac{2}{\mu_r \overline{X}\,\overline{Y}} K_0\left(2\sqrt{\frac{z}{\mu_r \overline{X}\,\overline{Y}}}\right), \tag{A.46}$$

where for the derivative of $\frac{d}{dz}\Pr\{Z < z\}$ we have used the following equality (see, e.g., [24])

$$x\frac{d}{dx}K_i(x) = -xK_{i-1}(x) - iK_i(x). \tag{A.47}$$

Finally, from (A.46) and (A.47), we obtain the result in (A.30).

Appendix II: Proof of Lemma 1

From the definition of MGF, i.e., $M_\gamma(\sigma) = \int_0^\infty \exp(\sigma\gamma)p(\gamma)d\gamma$, where σ is a real-valued number, it is clear that the MGF is maximized when $\exp(\sigma\gamma)$ is maximized. Consider the relationship between the MGF and the SER expressions, i.e., $P_e(R) = \frac{c}{\pi}\int_0^{\pi/2} M_\gamma(\frac{-\kappa}{2\sin^2\phi})d\phi$. Since $\exp(\frac{-\kappa}{2\sin^2\phi})$ has a single maximum that occurs at $\phi = \pi/2$, $M_\gamma(\frac{-\kappa}{2})$ is the maximum value for MGF. Hence, an upper bound for SER is of the form

$$P_e(R) \leq \frac{c}{2} M_\gamma\left(\frac{-\kappa}{2}\right). \tag{A.48}$$

Note that in the case of M-PSK modulation, we can have the tighter upper bound of $P_e(R) \leq (1 - \frac{1}{M})M_\gamma\left(\frac{-\kappa}{2}\right)$ [23, Eq. (9.27)].

A tractable definition of the diversity, or diversity gain, is [18, Eq. (1.19)]

$$G_d = -\lim_{\mu\to\infty} \frac{\log\left(P_e(R)\right)}{\log\left(\mu\right)}. \tag{A.49}$$

Now, we replace the upper bound of $\frac{c}{2}M_\gamma\left(\frac{-\kappa}{2}\right)$ in (A.49), and (A.45) can be achieved.

Appendix III: Proof of Theorem 3

Using the fact that the MGF of the sum of independent RVs is the product of the MGFs of the individual RVs, the integrand in (A.37) is the MGF of the summation of RVs γ_r, i.e., $\gamma_{\text{eq}} = \sum_{r=1}^{R} \gamma_r$. Therefore, using Lemma 1, we can find the diversity order of AF DSTC system in which relays have no CSI. Hence, we have

$$\begin{aligned} G_d &\geq - \lim_{\mu\to\infty} \frac{\log\left(M_{eq}(\frac{-\kappa}{2})\right)}{\log(\mu)} = - \lim_{\mu\to\infty} \frac{\sum_{r=1}^{R} \log\left(M_r(\frac{-\kappa}{2})\right)}{\log(\mu)} \\ &= - \sum_{r=1}^{R} \lim_{\mu_r\to\infty} \frac{\log\left(-\frac{2}{\kappa\mu_r\sigma_{f_r}^2\sigma_{g_r}^2} e^{\frac{2}{\kappa\mu_r\sigma{f_r}^2\sigma_{g_r}^2}} E_i\left(\frac{-2}{\kappa\mu_r\sigma_{f_r}^2\sigma_{g_r}^2}\right)\right)}{\log(\mu_r)}, \end{aligned} \tag{A.50}$$

where $M_{\text{eq}}(\cdot)$ is the MGF of γ_{eq}. The second equality is obtained by replacing the integrand of (A.37), and also by assuming that all relays are located in a fixed area. Furthermore, for $x < 0$, the series representation of $E_i(x)$ can be expressed as [25, Eq. (8.213)]

$$E_i(x) = \tau + \log(-x) + \sum_{k=1}^{\infty} \frac{x^k}{k\,k!}, \tag{A.51}$$

where $\tau \approx 0.5772156$ is Euler's constant. Then, using (A.51), we can rewrite (A.50) as

$$\begin{aligned} G_d &\geq - \sum_{r=1}^{R} \lim_{\mu_r\to\infty} \frac{\log\left[-\frac{1}{\chi_r} e^{\frac{1}{\chi_r}} \left(\tau - \log(\chi_r) + \sum_{k=1}^{\infty} \frac{(-\chi_r)^{-k}}{k\,k!}\right)\right]}{\log\left(\mu_r\right)} \\ &= - \sum_{r=1}^{R} \lim_{\mu_r\to\infty} \frac{\left(-\log\left(\chi_r\right) + \frac{1}{\chi_r} + \log\left[\log(\chi_r)\right]\right)}{\log\left(\mu_r\right)} = \sum_{r=1}^{R} \lim_{\mu_r\to\infty} \frac{\log(\chi_r)}{\log\left(\mu_r\right)} = R, \end{aligned} \tag{A.52}$$

where $\chi_r = \kappa\mu_r\sigma_{f_r}^2\sigma_{g_r}^2/2$. Hence, it is proven that AF DSTC with the scaling factor presented in (A.14), in which relays have no CSI, provides full diversity, i.e., diversity R.

References

[1] A. Sendonaris, E. Erkip, and B. Aazhang, “User cooperation diversity. Part 1: System description; Part 2: Implementation aspects and performance analysis,” *IEEE Trans. Commun.*, vol. 51, no. 11, pp. 1927–1938, Nov. 2003.

[2] J. N. Laneman and G. Wornell, “Distributed space-time coded protocols for exploiting cooperative diversity in wireless networks,” in *IEEE GLOBECOM 2002*, vol. 1, no. 11, Taipei, Taiwan, R.O.C., Nov. 2002, pp. 77–81.

[3] J. N. Laneman, D. Tse, and G. Wornell, “Cooperative diversity in wireless networks: Efficient protocols and outage behavior,” *IEEE Trans. Inform. Theory*, vol. 50, no. 12, pp. 3062–3080, Dec. 2004.

[4] R. U. Nabar, H. Bölcskei, and F. W. Kneubuhler, “Fading relay channels: Performance limits and space-time signal design,” *IEEE J. Sel. Areas Commun.*, vol. 22, no. 6, pp. 1099–1109, Aug. 2004.

[5] M. Uysal and O. Canpolat, “On the distributed space-time signal design for a large number of relay terminals,” in *Proc. IEEE Wireless Communications and Networking Conference (WCNC)*, vol. 2, New Orleans, USA, Mar. 13–17 2005, pp. 990–994.

[6] K. Seddik, A. Sadek, A. Ibrahim, and K. Liu, “Design criteria and performance analysis for distributed space-time coding,” *IEEE Trans. on Vehicular Technology*, vol. 57, no. 4, pp. 2280–2292, Jul. 2008.

[7] T. Wang, Y. Yao, and G. B. Giannakis, “Non-coherent distributed space-time processing for multiuser cooperative transmissions,” *IEEE Trans. Wireless Commun.*, vol. 5, no. 12, pp. 3339–3343, Dec. 2006.

[8] Y. Jing and B. Hassibi, "Distributed space-time coding in wireless relay networks," *IEEE Trans. Wireless Commun.*, vol. 5, no. 12, pp. 3524–3536, Dec. 2006.

[9] ——, "Cooperative diversity in wireless relay networks with multiple-antenna nodes," in *IEEE Int. Symp. Inform. Theory*, Adelaide, Australia, 2005.

[10] Y. Jing and H. Jafarkhani, "Using orthogonal and quasi-orthogonal designs in wireless relay networks," *IEEE Trans. Info. Theory*, vol. 53, no. 11, pp. 4106–4118, Nov. 2007.

[11] B. Maham and A. Hjørungnes, "Distributed GABBA space-time codes in amplify-and-forward cooperation," in *Proc. IEEE Information Theory Workshop (ITW'07)*, Bergen, Norway, Jul. 2007, pp. 189–193.

[12] G. S. Rajan and B. S. Rajan, "Distributed space-time codes for cooperative networks with partial CSI," in *Proc. IEEE Wireless Communications and Networking Conference (WCNC)*, Hong Kong, China, March 2007, pp. 902–906.

[13] G. Abreu, "GABBA codes: Generalized full-rate orthogonally decodable space-time block codes," in *Thirty-Ninth Asilomar Conference on Signals, Systems and Computers*, Monterey, CA, Nov. 2005.

[14] ——, "Generalized ABBA space-time block codes," Internet draft, [Online]. Available: http://arxiv.org/abs/cs/0510003v1.

[15] L. Xian and H. Liu, "Rate-one space-time block codes with full-diversity," *IEEE Trans. Commun.*, vol. 5, no. 3, pp. 1986–1990, Dec. 2005.

[16] C. Mecklenbräuker and M. Rupp, "Generalized Alamouti codes for trading quality of service against data rate in MIMO UMTS," *EURASIP Journal on Applied Signal Processing*, pp. 662–675, May 2004.

[17] J. R. Barry, E. A. Lee, and D. G. Messerschmitt, *Digital Communication.* Norwell, USA: Kluwer Academic Publishers, 3rd ed., 2004.

[18] H. Jafarkhani, *Space-Time Coding Theory and Practice.* Cambridge, UK: Cambridge Academic Press, 2005.

[19] *CDMA 2000 Standard.* Telecommunications Industry Association/Electronic Industries Alliance, 2000.

[20] S. M. Alamouti, "A simple transmitter diversity scheme for wireless communications," *IEEE Journal on Selected Areas in Communications*, vol. 16, pp. 1451–1458, Oct. 1998.

[21] H. Jafarkhani, "A quasi-orthogonal space-time block code," *IEEE Trans. Commun.*, vol. 49, pp. 1–4, Jan. 2001.

[22] P. A. Anghel and M. Kaveh, "On the performance of distributed space-time coding systems with one and two non-regenerative relays," *IEEE Trans. Wireless Commun.*, vol. 5, no. 12, pp. 682–692, Mar. 2006.

[23] M. K. Simon and M.-S. Alouini, *Digital Communication over Fading Channels: A Unified Approach to Performance Analysis.* New York, NY: Wiley, 2000.

[24] M. Abramowitz and I. A. Stegun, *Handbook of Mathematical Functions.* New York, USA: Dover Publications, 1972.

[25] I. S. Gradshteyn and I. M. Ryzhik, *Table of Integrals, Series, and Products.* San Diego, USA: Academic, 1996.

[26] A. S. Ibrahim, A. K. Sadek, W. Su, and K. R. Liu, "Cooperative communications with relay-selection: When to cooperate and whom to cooperate with?" *IEEE Trans. Wireless Commun.*, vol. 7, no. 7, pp. 2814–2827, Jul. 2008.

Paper B

Power Allocation Strategies for Distributed Space-Time Codes in Amplify-and-Forward Mode

B. Maham and A. Hjørungnes

EURASIP Journal on Advances in Signal Processing, vol. 2009, Article ID 612719, 13 pages, 2009. doi:10.1155/2009/612719.

Abstract

We consider a wireless relay network with Rayleigh fading channels, and apply distributed space-time coding (DSTC) in *amplify-and-forward* (AF) mode. It is assumed that the relays have statistical channel state information (CSI) of the local source-relay channels, while the destination has full instantaneous CSI of the channels. It turns out that, combined with the minimum SNR-based power allocation in the relays, AF DSTC results in a new opportunistic relaying scheme, in which the *best* relay is selected to retransmit the source's signal. Furthermore, we have derived the optimum power allocation between two cooperative transmission phases by maximizing the average received SNR at the destination. Next, assuming M-PSK and M-QAM modulations, we analyze the performance of cooperative diversity wireless networks using AF opportunistic relaying. We also derive an approximate formula for the symbol error rate (SER) of AF DSTC. We first derive the probability density function and the moment generating function (MGF) of the received SNR at the destination. Then, the MGF is used to determine the SER in Rayleigh fading channels. Assuming the use of full-diversity space-time codes, we derive two power allocation strategies minimizing the approximate SER expressions, for constrained transmit power. Our analytical results have been confirmed by simulation results, using full-rate, full-diversity distributed space-time codes.

1 Introduction

Space-time coding (STC) has received a lot of attention in the last years as a way to increase the data rate and/or reduce the transmitted power necessary to achieve a target bit error rate (BER) using multiple antenna transceivers. In ad-hoc network applications or in distributed large scale wireless networks, the nodes are often constrained in the complexity and size. This makes multiple-antenna systems impractical for certain network applications [1]. In an effort to overcome this limitation, cooperative diversity schemes have been introduced [1–4]. Cooperative diversity allows a collection of radios to relay signals for each other and effectively create a virtual antenna array for combating multipath fading in wireless channels. The attractive feature of these techniques is that each node is equipped with only *one* antenna, creating a virtual antenna array. This property makes them outstanding for deployment in cellular mobile devices as well as in ad-hoc mobile networks, which have problem with exploiting multiple-antenna due to the size limitation of the mobile terminals.

Among the most widely used cooperative strategies are amplify-and-forward (AF) [4], [5] and decode-and-forward (DF) [1, 2, 4]. The authors in [6] applied Hurwitz-Radon space-time codes in wireless relay networks and conjecture a diversity factor around $R/2$ for large R from their simulations, where R is the number of relays.

In [7], a cooperative strategy was proposed, which achieves a diversity factor of R in a R-relay wireless network, using the so-called distributed space-time codes (DSTC). In this strategy, a two-phase protocol is used. In phase one, the transmitter sends the information signal to the relays and in phase two, the relays send information to the receiver. The signal sent by every relay in the second phase is designed as a linear function of its received signal. It was shown in [7] that the relays can generate a linear space-time codeword at the receiver, as in a multiple antenna system, although they only cooperate distributively. This method does not require decoding at the relays and for high SNR it achieves the optimal diversity factor [7]. Although distributed space-time coding does not need instantaneous channel information at the relays, it requires full channel information at the receiver of both the channel from the transmitter to relays and the channel from relays to the receiver. Therefore, training symbols have to be sent from both the transmitter and relays. Distributed space-time coding was generalized to networks with multiple-antenna nodes in [8], and the design of practical DSTCs that lead to reliable communication in wireless relay networks, has also been recently considered [9–11].

Power efficiency is a critical design consideration for wireless networks such as ad-hoc and sensor networks, due to the limited transmission power of the nodes. To that end, choosing the appropriate relays to forward the source data, as well as the transmit power levels of all the nodes become important design issues. Several power allocation strategies for relay networks were studied based on different cooperation strategies and network topologies in [12]. In [13], we proposed power allocation strategies for repetition-based cooperation that take both the statistical CSI and the residual energy information into account to prolong the network lifetime while meeting the BER QoS requirement of the destination. Distributed power allocation strategies for decode-and-forward cooperative systems are investigated in [14]. Power allocation in three-node models are discussed in [15] and [16], while multi-hop relay networks are studied in [17–19]. Recent works also discuss relay selection algorithms for networks with multiple relays, which result in power efficient transmission strategies. Recently proposed practical relay selection strategies include pre-select one relay [20], best-select relay [20], blind-selection-algorithm [21], informed-selection-algorithm [21], and cooperative relay selection [22]. In [23], an opportunistic relaying scheme is introduced. According to opportunistic relaying, a single relay among a set of R relay nodes is selected, depending on which relay provides the *best* end-to-end path between source and destination. Bletsas et al. [23] proposed two heuristic methods for selecting the best relay based on the end-to-end instantaneous wireless channel conditions. Performance and outage analysis of these heuristic relay selection schemes are studied in [24] and [25]. In this paper, we propose a decision metric for opportunistic relaying based on maximizing the received instantaneous SNR at the destination in amplify-and-forward (AF) mode, when statistical CSI of the source-relay channel is available at the relay. Furthermore, similar to [7], knowledge of whole CSI is required for decoding at the destination. In this paper, we use a simple feedback from the destination toward the relays to select the best relay.

In [9] and [10], a network with symmetric channels is assumed, in which all source-to-relay and relay-to-destination links have i.i.d. distributions. In [7], using the pair-wise error probability (PEP) analysis in high SNR scenario, it is shown that uniform power allocation along relays is optimum. However, this assumption is hardly met in practice and the path lengths among nodes could vary. Therefore, power control among the relays is required for such a cooperation. In [10], a closed-form expression for the moment generating function (MGF) of AF space-time cooperation is derived as a function of Whittaker function. However, this function is not well-behaved and cannot be used for finding an analytical solution for power allocation.

Our main contributions can be summarized as follows:

- We show that the DSTC based on [7], in which relays transmit the linear combinations of the scaled version of their received signals leads to a new opportunistic relaying, when maximum instantaneous SNR based power allocation is used.
- The optimum power allocation between two phases is derived by maximizing the average SNR at the destination.
- We derive the average symbol error rate (SER) of AF opportunistic relaying system with M-PSK or M-QAM modulations over Rayleigh-fading channels. Furthermore, the probability density function (PDF) and moment generating function (MGF) of the received SNR at the destination are obtained.
- We analyze the diversity order of AF opportunistic relaying based on the asymptotic behavior of average SER. Based on the proposed approximated SER expression, it is shown that the proposed scheme achieves the diversity order of R.
- The average SER of AF DSTC system for Rayleigh fading channels is derived, using two new methods based on MGF.
- We propose two power allocation schemes for AF DSTC based on minimizing the target SER, given the knowledge of statistical CSI of source-relay links at the relays. An outstanding feature of the proposed schemes is that they are independent of the instantaneous channel variations, and thus, power control coefficients are varying slowly with time.

The rest of this paper is organized as follows. In Section II, the system model is given. Power allocation schemes for AF DSTC based on minimizing the received SNR at the destination are presented in Section III. In Section IV, the average SER of AF opportunistic relaying and AF DSTC with

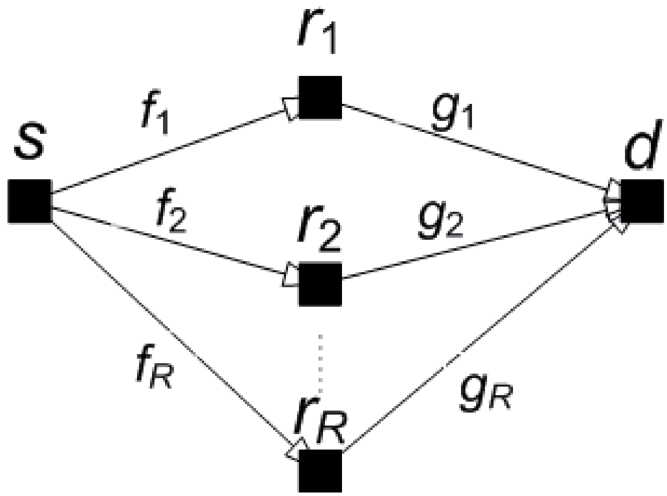

Fig. B.1: Wireless relay network consisting of a source *s*, a destination *d*, and *R* relays.

relays with partial statistical CSI is derived. Two power allocation schemes minimizing the SER are proposed in Section V. In Section VI, the overall performance of the system are presented for different number of relays through simulations. Finally, Section VI summarized the conclusions.

Throughout the article, the following notation is applied: The superscripts ^{t} and ^{H} stand for transposition and conjugate transpose, respectively. $\mathbb{E}\{\cdot\}$ denotes the expectation operation. $\mathrm{Cov}(\boldsymbol{x}_T)$ is the covariance of the $T \times 1$ vector $\boldsymbol{x}_T$. All logarithms are the natural logarithm.

2 System Model

Consider the network in Fig. B.1 consisting of a source denoted *s*, one or more relays denoted Relay $r = 1, 2, \ldots, R$, and one destination denoted *d*. It is assumed that each node is equipped with a single antenna. We denote the source-to-*r*th relay and *r*th relay-to-destination links by f_r and g_r, respectively. Suppose each link has a flat Rayleigh fading, and channels are independent of each others. Therefore, f_r and g_r are i.i.d. complex Gaussian random variables with zero-mean and variances $\sigma^2_{f_r}$ and $\sigma^2_{g_r}$, respectively. Similar to [7], our scheme requires two phases of transmission. During the first phase, the source node transmits a scaled version of the signal $\boldsymbol{s} = [s_1, \ldots, s_T]^t$, consisting of T symbols to *all* relays, where it is assumed that $\mathbb{E}\{\boldsymbol{s}\boldsymbol{s}^H\} = \frac{1}{T}\boldsymbol{I}_T$. Thus, from time 1 to T, the signals $\sqrt{P_1 T}s_1, \ldots, \sqrt{P_1 T}s_T$ are sent to all relays by the source. The average total transmitted energy in *T* intervals will be $P_1 T$. Assuming f_r is not varying during *T* successive intervals, the received $T \times 1$ signal at the *r*th relay can be written as

$$\boldsymbol{r}_r = \sqrt{P_1 T} f_r \boldsymbol{s} + \boldsymbol{v}_r, \tag{B.1}$$

where $\boldsymbol{v}_r$ is a $T \times 1$ complex zero-mean white Gaussian noise vector with variance N_1. Using amplify-and-forward, each relay scales its received signal, i.e.,

$$\boldsymbol{y}_r = \rho_r \boldsymbol{r}_r, \tag{B.2}$$

where ρ_r is the scaling factor at Relay *r*. When there is no instantaneous CSI available at the relays, but statistical CSI is known, a useful constraint is to ensure that a given average transmitted power is maintained. That is,

$$\rho_r^2 = \frac{P_{2,r}}{\sigma^2_{f_r} P_1 + N_1}, \tag{B.3}$$

where $P_{2,r}$ is the average transmitted power at Relay *r*. The total power used in the whole network for one symbol transmission is therefore $P = P_1 + \sum_{r=1}^{R} P_{2,r}$.

DSTC, proposed in [7], uses the idea of linear dispersion space-time codes of multiple-antenna systems. In this system, the $T \times 1$ received signal at the destination can be written as

$$\boldsymbol{y} = \sum_{r=1}^{R} g_r \boldsymbol{A}_r \boldsymbol{y}_r + \boldsymbol{w}, \tag{B.4}$$

where $\boldsymbol{y}_r$ is given by (B.2), $\boldsymbol{w}$ is a $T \times 1$ complex zero-mean white Gaussian noise vector with the component-wise variance of N_2, and the $T \times T$ dimensional matrix $\boldsymbol{A}_r$ is corresponding to the rth column of a proper $T \times T$ space-time code. The DSTCs designed in [9] and [10] are such that $\boldsymbol{A}_r$,

$r = 1, \ldots, R$, are unitary. Combining (B.1)-(B.4), the *total* noise vector $\boldsymbol{w}_T$ is given by

$$\boldsymbol{w}_T = \sum_{r=1}^{R} \boldsymbol{A}_r \sqrt{\frac{P_{2,r}}{\sigma_{f_r}^2 P_1 + N_1}} g_r \boldsymbol{v}_r + \boldsymbol{w}. \tag{B.5}$$

Since, g_i, $\boldsymbol{v}_i$, and $\boldsymbol{w}$ are independent complex Gaussian random variables, which are jointly independent, the conditional auto-covariance matrix of $\boldsymbol{w}_T$ can be shown to be

$$\text{Cov}\left(\boldsymbol{w}_T | \{f_r\}_{r=1}^R, \{g_r\}_{r=1}^R\right) = \left(\sum_{r=1}^{R} \frac{P_{2,r}|g_r|^2 N_1}{\sigma_{f_r}^2 P_1 + N_1} + N_2\right) \boldsymbol{I}_T, \tag{B.6}$$

where $\boldsymbol{I}_T$ is the $T \times T$ identity matrix. Thus, $\boldsymbol{w}_T$ is white.

3 Opportunistic Relaying through AF DSTC

In this section, we propose power allocation schemes for the AF distributed space-time codes introduced in [7], based on maximizing the received SNR at the destination *d*. First, the optimum power transmitted in the two phases, i.e., P_1 and $P_2 = \sum_{r=1}^{R} P_{2,r}$, will be obtained by maximizing the average received SNR at the destination. Then, we will find the optimum distribution of transmitted powers among relays, i.e., $P_{2,r}$, based on instantaneous SNR.

3.1 Power Control between Two Phases

In the following proposition, we derive the optimal value for the transmitted power in the two phases when backward and forward channels have different variances by maximizing the average SNR at the destination.

Proposition 1 *Assume α portion of the total power is transmitted in the first phase and the remaining power is transmitted by relays at the second phase, where $0 < \alpha < 1$, that is $P_1 = \alpha P$ and $P_2 = (1-\alpha)P$, where P is the total transmitted power during two phases. Assuming $\sigma_{f_r}^2 = \sigma_f^2$ and $\sigma_{g_r}^2 = \sigma_g^2$, the optimum value of α by maximizing the average SNR at the destination is*

$$\alpha = \frac{N_1 \sigma_g^2 P + N_1 N_2}{\left(N_2 \sigma_f^2 - N_1 \sigma_g^2\right) P} \left(\sqrt{1 + \frac{\left(N_2 \sigma_f^2 - N_1 \sigma_g^2\right) P}{N_1 \sigma_g^2 P + N_1 N_2}} - 1\right). \tag{B.7}$$

Proof: *The average SNR at the destination can be obtained by dividing the average received signal power by the variance of the noise at the destination (approximation of* $\mathbb{E}\{SNR\}$ *using Jensen's inequality). Using* (B.1)-(B.6)*, the average SNR can be written as*

$$SNR = \frac{\alpha(1-\alpha)P^2\sigma_f^2\sigma_g^2}{\alpha(N_2\sigma_f^2 - N_1\sigma_g^2)P + N_1\sigma_g^2 P + N_1N_2}, \tag{B.8}$$

where we have assumed $\sigma_{f_r}^2 = \sigma_f^2$ *and* $\sigma_{g_r}^2 = \sigma_g^2$*, for* $r = 1, \ldots, R$*, and thus,* $P_{2,r} = \frac{P_2}{R}$*. First, we consider the case in which* $N_2\sigma_f^2 > N_1\sigma_g^2$*. In this case, the optimum value of* α *which maximizes* (B.8)*, subject to the constraint* $0 < \alpha < 1$*, is obtained as*

$$\alpha = \frac{\sqrt{1+\beta} - 1}{\beta}, \tag{B.9}$$

where

$$\beta = \frac{(N_2\sigma_f^2 - N_1\sigma_g^2)\,P}{N_1\sigma_g^2 P + N_1N_2}. \tag{B.10}$$

Similarly, when $N_2\sigma_f^2 < N_1\sigma_g^2$*, the optimum value of* α*, which maximizes SNR in* (B.8)*, subject to constraint* $0 < \alpha < 1$*, is also* (B.9) *and* (B.10)*. Therefore, observing* (B.9) *and* (B.10)*, the desired result in* (B.7) *is achieved.* □

For the special case of $N_2\sigma_f^2 = N_1\sigma_g^2$, the optimum α is equal to $\frac{1}{2}$, which is in compliance with the result obtained in [7], where assumed $N_1 = N_2$ and $\sigma_f^2 = \sigma_g^2$. In this case, we have $\alpha = \lim_{\beta\to 0^+} \frac{1}{\beta}(\sqrt{1+\beta} - 1) = \lim_{\beta\to 0^+} \frac{1}{\beta}\left(\frac{\beta}{2} + o(1)\right) = \frac{1}{2}$.

3.2 Power Control among Relays with Source-Relay link CSI at Relay

Now, we are going to find the optimum distribution of the transmitted powers among relays during the second phase, in a sense of maximizing the instantaneous SNR at the destination.

The conditional variance of the equivalent received noise is obtained in (B.6). Thus, using (B.1), (B.2), and (B.4), the instantaneous received SNR at the destination can be written as

$$\mathrm{SNR_{ins}} = \frac{\sum_{r=1}^{R} P_1|f_r|^2|g_r|^2 \frac{P_{2,r}}{\sigma_{f_r}^2 P_1 + N_1}}{\sum_{r=1}^{R} |g_r|^2 \frac{P_{2,r}}{\sigma_{f_r}^2 P_1 + N_1} N_1 + N_2}. \tag{B.11}$$

For notational simplicity, we represent $\mathrm{SNR_{ins}}$ in (B.11) in a matrix format as

$$\mathrm{SNR_{ins}} = \frac{\boldsymbol{p}^t \boldsymbol{U} \boldsymbol{p}}{\boldsymbol{p}^t \boldsymbol{V} \boldsymbol{p} + N_2}, \tag{B.12}$$

where $\boldsymbol{p} = [\sqrt{P_{2,1}}, \sqrt{P_{2,2}}, \ldots, \sqrt{P_{2,R}}]^t$ and the positive definite diagonal matrices $\boldsymbol{U}$ and $\boldsymbol{V}$ are defined as

$$\begin{aligned} \boldsymbol{U} &= \mathrm{diag}\left[\frac{P_1|f_1|^2|g_1|^2}{\sigma_{f_1}^2 P_1 + N_1}, \frac{P_1|f_2|^2|g_2|^2}{\sigma_{f_2}^2 P_1 + N_1}, \ldots, \frac{P_1|f_R|^2|g_R|^2}{\sigma_{f_R}^2 P_1 + N_1}\right], \\ \boldsymbol{V} &= \mathrm{diag}\left[\frac{|g_1|^2 N_1}{\sigma_{f_1}^2 P_1 + N_1}, \frac{|g_2|^2 N_1}{\sigma_{f_2}^2 P_1 + N_1}, \ldots, \frac{|g_R|^2 N_1}{\sigma_{f_R}^2 P_1 + N_1}\right]. \end{aligned} \tag{B.13}$$

Then, the optimization problem is formulated as

$$\boldsymbol{p}^* = \arg\max_{\boldsymbol{p}} \mathrm{SNR_{ins}}, \quad \text{subject to} \quad \boldsymbol{p}^t \boldsymbol{p} = P_2. \tag{B.14}$$

where the $R \times 1$ vector $\boldsymbol{p}^*$ denotes the optimum values of power control coefficients. Moreover, since $\boldsymbol{p}^t\boldsymbol{p} = P_2 = (1-\alpha)P$, we can rewrite (B.12) as

$$\mathrm{SNR_{ins}} = \frac{\boldsymbol{p}^t \boldsymbol{U} \boldsymbol{p}}{\boldsymbol{p}^t \boldsymbol{W} \boldsymbol{p}}, \tag{B.15}$$

where diagonal matrix $\boldsymbol{W}$ is defined as $\boldsymbol{W} = \boldsymbol{V} + \frac{N_2}{P_2}\boldsymbol{I}_R$. Since $\boldsymbol{W}$ is a positive semi-definite matrix, we define $\boldsymbol{q} \triangleq \boldsymbol{W}^{\frac{1}{2}}\boldsymbol{p}$, where $\boldsymbol{W} = (\boldsymbol{W}^{\frac{1}{2}})^t\boldsymbol{W}^{\frac{1}{2}}$. Then, (B.15) can be rewritten as

$$\mathrm{SNR_{ins}} = \frac{\boldsymbol{q}^t \boldsymbol{Z} \boldsymbol{q}}{\boldsymbol{q}^t \boldsymbol{q}}, \tag{B.16}$$

where diagonal matrix $\boldsymbol{Z}$ is $\boldsymbol{Z} = \boldsymbol{U}\boldsymbol{W}^{-1}$. Now, using Rayleigh-Ritz theorem [26], we have

$$\frac{\boldsymbol{q}^t \boldsymbol{Z} \boldsymbol{q}}{\boldsymbol{q}^t \boldsymbol{q}} \leq \lambda_{\max}, \tag{B.17}$$

where $\lambda_{\max}$ is the largest eigenvalue of $\boldsymbol{Z}$, which is corresponding to the largest diagonal element of $\boldsymbol{Z}$, i.e.,

$$\lambda_{\max} = \max_{r\in\{1,\ldots,R\}} \lambda_r = \max_{r\in\{1,\ldots,R\}} \frac{P_1P_2|f_r|^2|g_r|^2}{P_2|g_r|^2N_1 + N_2(\sigma_{f_r}^2 P_1 + N_1)}. \tag{B.18}$$

The equality in (B.17) holds if $\boldsymbol{q}$ is proportional to the eigenvector of $\boldsymbol{Z}$ corresponding to $\lambda_{\max}$. Since $\boldsymbol{Z}$ is a diagonal matrix with real elements, the eigenvectors of $\boldsymbol{Z}$ are given by the orthonormal bases $\boldsymbol{e}_r$, defined $e_{r,l} = \delta_{r,l}$, $l = 1, \ldots, R$. Hence, the optimum $\boldsymbol{q}_{\max}$ can be chosen to be proportional to $\boldsymbol{e}_{r_{\max}}$. On the other hand, since $\boldsymbol{p} = \boldsymbol{W}^{-\frac{1}{2}}\boldsymbol{q}$, and $\boldsymbol{W}$ is a diagonal matrix, the optimum $\boldsymbol{p}^*$ is also proportional to $\boldsymbol{e}_{r_{\max}}$. Using the power constraint of the transmitted power in the second phase, i.e., $\boldsymbol{p}^t\boldsymbol{p} = P_2$, we have $\boldsymbol{p}^* = \sqrt{P_2}\boldsymbol{e}_{r_{\max}}$. This means that for each realization of the network channels, the best relay should transmit all the available power P_2 and all other relays should stay silent. Hence, the optimum power allocation based on maximizing the instantaneous received SNR at the destination is to select the relay with the highest instantaneous value of $\frac{P_1P_2|f_r|^2|g_r|^2}{P_2|g_r|^2N_1+N_2(\sigma_{f_r}^2 P_1+N_1)}$.

3.3 Relay Selection Strategy

In the previous subsection, it is shown that the optimum power allocation of AF DSTC based on maximizing the instantaneous received SNR at the destination is to select the relay with the highest instantaneous value of $\frac{P_1P_2|f_r|^2|g_r|^2}{P_2|g_r|^2N_1+N_2(\sigma_{f_r}^2 P_1+N_1)}$. We assume the knowledge of magnitude of source-to-rth relay link to be available for the process of relay selection. The process of selecting the best relay could be done by the destination. This is feasible since the destination node should be aware of all channels for coherent decoding. Thus, the same channel information could be exploited for the purpose of relay selection. However, if we assume a distributed relay selection algorithm, in which relays independently decide to select the best relay among them, such as work done in [23], the knowledge of local channels f_r and g_r is required for the rth relay. The estimation of f_r and g_r can be done by transmitting a ready-to-send (RTS) packet and a clear-to-send (CTS) packet in MAC protocols.

4 Performance Analysis

4.1 Performance Analysis of the Selected Relaying Scheme

4.1.1 SER Expression

In the previous section, we have shown that the optimum transmitted power of AF DSTC system based on maximizing the instantaneous received SNR at the destination led to opportunistic relaying. In this section, we will derive the SER formulas of best relay selection strategy under the amplify-and-forward mode. For this reason, we should first derive the received SNR at the destination due to the rth relay, when other relays are silent, that is

$$\gamma_r = \frac{P_1 P_2 |f_r|^2 |g_r|^2}{P_2 |g_r|^2 N_1 + N_2(\sigma_{f_r}^2 P_1 + N_1)}. \tag{B.19}$$

In the following, we will derive the PDF of γ_r in (B.19), which is required for calculating the average SER.

Proposition 2 *For the γ_r in* (B.19)*, the probability density function $p_r(\gamma_r)$ can be written as*

$$p_r(\gamma_r) = 2A_r e^{-B_r\gamma_r} K_0\left(2\sqrt{A_r\gamma_r}\right) + 2B_r\sqrt{A_r\gamma_r}e^{-B_r\gamma_r} K_1\left(2\sqrt{A_r\gamma_r}\right), \tag{B.20}$$

where A_r and B_r are defined as

$$A_r = \frac{N_2(\sigma_{f_r}^2 P_1 + N_1)}{P_1 P_2 \sigma_{f_r}^2 \sigma_{g_r}^2}, \; B_r = \frac{N_1}{P_1 \sigma_{f_r}^2}, \tag{B.21}$$

and $K_\nu(x)$ is the modified Bessel function of the second kind of order ν [27].

Proof: *The proof is given in Appendix I.* □

Define $\gamma_{\max} \triangleq \max\{\gamma_1, \gamma_2, \ldots, \gamma_R\}$. The conditional SER of the best relay selection system under AF mode with R relays can be written as

$$P_e\left(R|\{f_r\}_{r=1}^R, \{g_r\}_{r=1}^R\right) = c\,Q\left(\sqrt{g\,\gamma_{\max}}\right), \tag{B.22}$$

where $Q(x) = 1/\sqrt{2\pi}\int_x^\infty e^{-u^2/2}\,du$, and the parameters c and g are represented as

$$c_{\text{QAM}} = 4\frac{\sqrt{M}-1}{\sqrt{M}}, \; c_{\text{PSK}} = 2, \; g_{\text{QAM}} = \frac{3}{M-1}, \; g_{\text{PSK}} = 2\sin^2\left(\frac{\pi}{M}\right).$$

For calculating the average SER, we need to find the PDF of $\gamma_{\max}$. Thus, in the following proposition, we derive the PDF of the maximum of R random variables expressed in (B.19).

Proposition 3 *For the γ_r in* (B.19)*, the probability density function of the maximum of the R random variables, γ_r, can be written as*

$$p_{\max}(\gamma) = \sum_{r=1}^{R} p_r(\gamma) \prod_{\substack{i=1 \\ i\neq r}}^{R} \left[1 - 2e^{-B_i\gamma}\sqrt{A_i\gamma}K_1\left(2\sqrt{A_i\gamma}\right)\right], \tag{B.23}$$

where $p_r(\gamma)$ is derived in (B.20)*.*

Proof: *The proof is given in Appendix II.* □

Now, we are deriving the SER expression for the selection relaying scheme discussed in Section III. Averaging over conditional SER in (B.22), we have the exact SER expression as

$$P_e(R) = \int_0^\infty P_e\left(R|\{f_r\}_{r=1}^R, \{g_r\}_{r=1}^R\right) p_{\max}(\gamma)\, d\gamma = \int_0^\infty c\, Q\left(\sqrt{g\,\gamma}\right) p_{\max}(\gamma)\, d\gamma. \tag{B.24}$$

Using the moment generating function approach, we can express $P_e(R)$ given in (B.24) as

$$P_e(R) = \int_0^\infty \frac{c}{\pi}\int_0^{\frac{\pi}{2}} e^{-\frac{g\,\gamma}{2\sin^2\phi}} p_{\max}(\gamma)\, d\phi d\gamma = \frac{c}{\pi}\int_0^{\frac{\pi}{2}} M_{\max}\left(-\frac{g}{2\sin^2\phi}\right) d\phi, \tag{B.25}$$

where $M_{\max}(-s) = \mathbb{E}_\gamma(e^{-s\gamma})$ is the moment generating function of $\gamma_{\max}$. In the following theorem, we state a closed-form expression for $M_{\max}(-s)$ in (B.25).

Theorem 1 *For the R independent random variables γ_r, which is stated in* (B.19)*, the MGF of $\gamma_{\max} = \max\{\gamma_1, \gamma_2, \ldots, \gamma_R\}$ is given by*

$$M_{\max}(-s) \approx \left(\prod_{r=1}^{R} B_r\right) \sum_{r=1}^{R} \frac{(R-1)!}{(s+B_r)^R} e^{\frac{A_r}{2(s+B_r)}} \left\{ \frac{\sqrt{A_r(s+B_r)}}{B_r}(R-1)! \cdot W_{-R+\frac{1}{2},0}\left(\frac{A_r}{s+B_r}\right) + R!\, W_{-R,\frac{1}{2}}\left(\frac{A_r}{s+B_r}\right)\right\}, \tag{B.26}$$

where $W_{a,b}(x)$ is Whittaker function of orders a *and* b *(see e.g., [27] and [28, Eq. 9.224]).*

Proof: *The proof is given in Appendix III.* □

4.1.2 Diversity Analysis

From [27, Eq. (9.6.8)] and [27, Eq. (9.6.9)], the following properties can be obtained

$$K_0(x) \approx -\log(x), \quad K_1(x) \approx \frac{1}{x}. \tag{B.27}$$

Specially, for small values of x, which corresponds to the small value of A and B in (B.21), or equivalently, high SNR scenario, the approximations in (B.27) are more accurate. In Fig. B.2, we have shown that $K_0(x)$ and $\log\left(\frac{1}{x}\right)$, and also $K_1(x)$ and $\frac{1}{x}$ have the same asymptotic behavior when $x \to 0^+$. Therefore, we can approximate $p_r(\gamma)$ in (B.20) as

$$p_r(\gamma) \approx (B_r - A_r \log(4A_r))\, e^{-B_r\gamma} - A_r e^{-B_r\gamma} \log(\gamma), \tag{B.28}$$

and hence, $p_{\max}(\gamma)$ in (B.23) is approximated as

$$p_{\max}(\gamma) \approx \sum_{r=1}^{R} \left[(B_r - A_r \log(4A_r))\, e^{-B_r\gamma} - A_r e^{-B_r\gamma} \log(\gamma)\right] \prod_{\substack{i=1\\ i\neq r}}^{R} \left(1 - e^{-B_r\gamma}\right). \tag{B.29}$$

Using (B.29), we can approximate the moment generating function of $\gamma_{\max}$, i.e., $M_{\max}(-s) = \mathbb{E}_\gamma(e^{-s\gamma})$, in high SNRs as

$$\begin{aligned} M_{\max}(-s) &= \int_0^\infty e^{-s\,\gamma} p_{\max}(\gamma)\, d\gamma \\ &\approx \sum_{r=1}^{R} (\prod_{\substack{i=1\\ i\neq r}}^{R} B_i) \int_0^\infty e^{-(s+B_r)\,\gamma} \left[B_r - A_r \log(4A_r) - A_r \log(\gamma)\right] \gamma^{R-1} d\gamma, \end{aligned} \tag{B.30}$$

where we have approximated $\left(1 - e^{-B_r\gamma}\right)$ with $B_r\gamma$, due to the high SNR assumption we made. Simplifying (B.30), we have

$$\begin{aligned} M_{\max}(-s) \approx & \sum_{r=1}^{R} (\prod_{\substack{i=1\\ i\neq r}}^{R} B_i) \left[B_r - A_r \log(4A_r)\right] \int_0^\infty e^{-(s+B_r)\gamma} \gamma^{R-1} d\gamma \\ & - \sum_{r=1}^{R} A_r (\prod_{\substack{i=1\\ i\neq r}}^{R} B_i) \int_0^\infty e^{-(s+B_r)\gamma} \log(\gamma) \gamma^{R-1} d\gamma, \end{aligned} \tag{B.31}$$

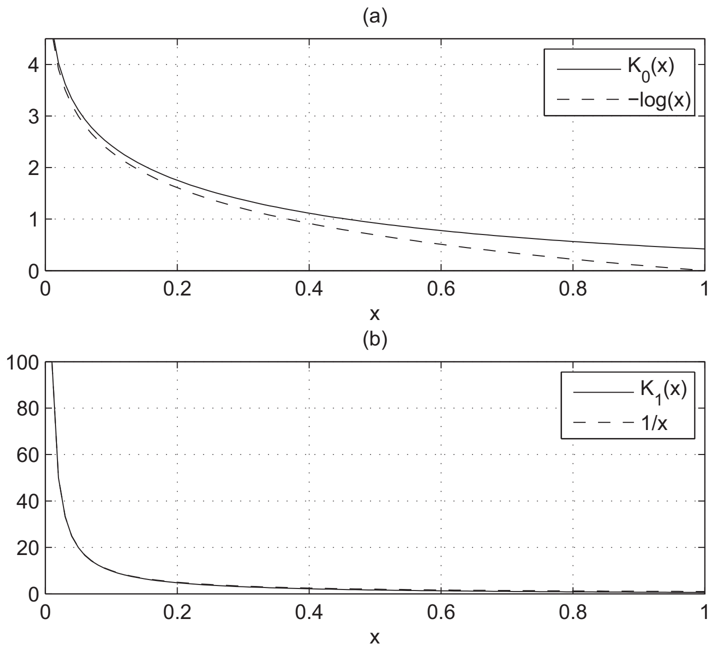

Fig. B.2: Diagrams of $K_0(x)$ and $\log(\frac{1}{x})$ in (a) and $K_1(x)$ and $\frac{1}{x}$ in (b), which have the same asymptotic behavior when $x \to 0$.

where the first integral can be calculated as $\int_0^\infty e^{-(s+B_r)\gamma}\gamma^{R-1}d\gamma = (R-1)!(s+B_r)^{-R}$. With the help of [28, Eq. (4.352)], the second integral in (B.31) can be computed as

$$\int_0^\infty e^{-(s+B_r)\gamma}\log(\gamma)\gamma^{R-1}d\gamma = (R-1)!\,(s+B_r)^{-R}\left(\xi(R)-\log(s)\right),$$

where $\xi(R) = 1+\frac{1}{2}+\frac{1}{3}+\cdots+\frac{1}{R-1}-\kappa$, and κ is the Euler's constant, that is $\kappa \approx 0.5772156$. Therefore, the closed-form approximation for the MGF function of $\gamma_{\max}$ is given by

$$M_{\max}(-s) \approx (R-1)! \sum_{r=1}^{R} (\prod_{\substack{i=1 \\ i \neq r}}^{R} B_i)(s+B_r)^{-R} \left[B_r - A_r \log(4A_r) + A_r (\log(s) - \xi(R))\right]. \tag{B.32}$$

To have more insight into the MGF derived in (B.32), we represent A_r and B_r as functions of the transmit SNR, i.e., $\mu = \frac{P}{N_1}$, assuming the destination and relays have the same value of noise, i.e., $N_1 = N_2$. Thus, A_r and B_r in (B.21) can be represented in high SNRs as

$$A_r = \frac{1}{(1-\alpha)\mu\sigma_{g_r}^2}, \; B_r = \frac{1}{\alpha\mu\sigma_{f_r}^2}, \tag{B.33}$$

and then, $M_{\max}(-s)$ in (B.32) can be rewritten as

$$M_{\max}(-s) \approx \left(\prod_{i=1}^{R} \frac{1}{\sigma_{f_i}^2}\right) \sum_{r=1}^{R} \frac{(R-1)!}{[(s+B_r)\mu\alpha]^R} \left[1 + \alpha\sigma_{f_r}^2 \frac{\log\left(\frac{s\mu(1-\alpha)\sigma_{g_r}^2}{4}\right) - \xi(R)}{(1-\alpha)\sigma_{g_r}^2}\right]. \tag{B.34}$$

Now, we are using the moment generating function method to derive an approximate SER expression for the opportunistic relaying scheme discussed in Section III. Using the moment generating function approach, we can express $P_e(R)$ given in (B.24) as

$$\begin{aligned} P_e(R) &= \int_0^{\infty} \frac{c}{\pi} \int_0^{\frac{\pi}{2}} e^{-\frac{g\gamma}{2\sin^2\phi}} p_{\max}(\gamma)\, d\phi d\gamma = \frac{c}{\pi} \int_0^{\frac{\pi}{2}} M_{\max}\left(-\frac{g}{2\sin^2\phi}\right) d\phi \\ &\approx \left(\prod_{i=1}^{R} \frac{1}{\sigma_{f_i}^2}\right) \frac{c2^R(R-1)!}{\pi(g\mu\alpha)^R} \sum_{r=1}^{R} \int_0^{\frac{\pi}{2}} \sin^{2R}\phi \left[1 + \alpha\sigma_{f_r}^2 \frac{\log\left(\frac{g\mu(1-\alpha)\sigma_{g_r}^2}{8\sin^2\phi}\right) - \xi(R)}{(1-\alpha)\sigma_{g_r}^2}\right] d\phi. \end{aligned} \tag{B.35}$$

where using (B.21), $\frac{g}{2\sin^2\phi} + B_r$ is accurately approximated with $\frac{g}{2\sin^2\phi}$ for all values of ϕ in high SNR conditions. For deriving the closed-form solution for the integral in (B.35), we decompose it into

$$P_e(R) \approx \Omega(\mu, R)\left[C_1(\mu, R)\int_0^{\frac{\pi}{2}} \sin^{2R}\phi \, d\phi - C_2(R)\int_0^{\frac{\pi}{2}} \sin^{2R}\phi \, \log(\sin\phi)\, d\phi\right], \tag{B.36}$$

where $\Omega(\mu, R)$, $C_1(\mu, R)$ and $C_2(R)$ are defined as

$$\Omega(\mu, R) = \frac{c2^R(R-1)!}{\pi(g\mu\alpha)^R}\prod_{i=1}^{R}\frac{1}{\sigma_{f_i}^2}, \tag{B.37}$$

$$C_1(\mu, R) = \sum_{r=1}^{R}\left[1 + \alpha\sigma_{f_r}^2 \frac{\log\left(\frac{g\mu(1-\alpha)\sigma_{g_r}^2}{8}\right) - \xi(R)}{(1-\alpha)\sigma_{g_r}^2}\right], \tag{B.38}$$

$$C_2(R) = \sum_{r=1}^{R}\frac{\alpha\sigma_{f_r}^2}{(1-\alpha)\sigma_{g_r}^2}. \tag{B.39}$$

Using [28, Eq. (4.387)] for solving the second integral in (B.36), the closed-form SER approximation is obtained as

$$P_e(R) \approx \frac{(2R)!}{\left((2^R R)!\right)^2}\frac{\pi}{2}\Omega(\mu, R)\left\{C_1(\mu, R) - C_2(R)\left(\sum_{k=1}^{R}\frac{(-1)^{k+1}}{k} - \log(2)\right)\right\}. \tag{B.40}$$

In the following theorem, we will study the achievable diversity gains in an opportunistic relaying network containing R relays, based on the SER expression.

Theorem 2 *The AF opportunistic relaying with the scaling factor presented in* (B.3)*, in which relays have no CSI, provides full diversity.*

Proof: *The proof is given in Appendix IV.* □

4.2 SER Expression for AF DSTC

In this subsection, we derive approximate SER expressions for the AF space-time coded cooperation using moment generating function method.

The conditional SER of the protocol described in Section II, with R relays, can be written as [29, Eq. (9.17)]

$$P_e\left(R|\{f_r\}_{r=1}^{R}\{g_r\}_{r=1}^{R}\right) = c\,Q\left(\sqrt{g\sum_{r=1}^{R}\mu_r|f_r g_r|^2}\right), \tag{B.41}$$

where, using (B.2)-(B.6), μ_r can be written as

$$\mu_r = \frac{\frac{P_1 P_{2,r}}{\sigma_{f_r}^2 P_1 + N_1}}{\sum_{k=1}^{R}\frac{P_{2,k}}{\sigma_{f_k}^2 P_1 + N_1}\sigma_{g_k}^2 N_1 + N_2}. \tag{B.42}$$

It is important to note that in (B.42) we approximate the conditional variance of the noise vector $\boldsymbol{w}_T$ in (B.6) as its expected value. The received SNR at the receiver side is denoted

$$\gamma = \sum_{r=1}^{R}\gamma_r, \tag{B.43}$$

where

$$\gamma_r = \mu_r|f_r g_r|^2. \tag{B.44}$$

We can calculate the average SER as

$$P_e(R) = \int_0^\infty P_e\left(R|\{\gamma_r\}_{r=1}^{R}\right)p(\gamma)\,d\gamma = \int_0^\infty c\,Q\left(\sqrt{g\,\gamma}\right)p(\gamma)\,d\gamma. \tag{B.45}$$

Now, we are using the MGF method to calculate the SER expression in (B.45). We also exploit the property that the γ_r's are independent of each other, because of the inherit spatial separation of the relay nodes in the network. Hence, the average SER in (B.45) can be rewritten as

$$\begin{aligned} P_e(R) &= \int_{0;\,R-\text{fold}}^{\infty}\frac{c}{\pi}\int_0^{\frac{\pi}{2}}\prod_{r=1}^{R}e^{-\frac{g\,\gamma_r}{2\sin^2\phi}}\,d\phi\prod_{r=1}^{R}\left(p(\gamma_r)\,d\gamma_r\right) \\ &= \frac{c}{\pi}\int_0^{\frac{\pi}{2}}\int_{0;\,R-\text{fold}}^{\infty}\prod_{r=1}^{R}\left(e^{-\frac{g\,\gamma_r}{2\sin^2\phi}}p(\gamma_r)\,d\gamma_r\right)\,d\phi = \frac{c}{\pi}\int_0^{\frac{\pi}{2}}\prod_{r=1}^{R}M_r(-s)\,d\phi, \end{aligned} \tag{B.46}$$

where $M_r(-s)$ is the MGF of the random variable γ_r, and $s = \frac{g}{2\sin^2\phi}$.

It can be shown that for larger values of average SNR, $\overline{\gamma}$, the behavior of $\gamma/\overline{\gamma}$ becomes increasingly irrelevant because the Q term in (B.45) goes to zero so fast that almost throughout the whole integration range the integrand is almost zero. However, recalling that $Q(0) = 1/2$, regardless of the value of $\overline{\gamma}$, the behavior of $p(\gamma)$ around zero never loses importance. On the other hand, it is shown in [10, Eq. (18)] that the PDF of the random variables γ_r is proportional to the modified bessel function of second kind of zeroth order, i.e,

$$p(\gamma_r) = \frac{2}{\mu_r \sigma_{f_r}^2 \sigma_{g_r}^2} K_0 \left(2 \sqrt{\frac{\gamma_r}{\mu_r \sigma_{f_r}^2 \sigma_{g_r}^2}} \right). \tag{B.47}$$

This PDF has a very large value around zero. Thus, the behavior of the integrand in (B.45) around zero becomes very crucial, and we can approximate $p(\gamma_r)$ in (B.47) with a logarithmic function, which is easier to handling. In Fig. B.2-(a), we have shown that $K_0(x)$ and $\log\left(\frac{1}{x}\right)$ have the same asymptotic behavior when $x \to 0^+$, i.e., $\lim_{x\to 0^+} K_0(x) \longrightarrow -\log(x)$. Hence, we can approximate $M_r(-s)$ as

$$M_r(-s) \approx \int_0^\infty e^{-s\,\gamma_r} \frac{-1}{\mu_r \sigma_{f_r}^2 \sigma_{g_r}^2} \log\left(\frac{4\gamma_r}{\mu_r \sigma_{f_r}^2 \sigma_{g_r}^2} \right) d\gamma_r = \frac{1}{s\mu_r \sigma_{f_r}^2 \sigma_{g_r}^2} \left[\log\left(\frac{s\, \mu_r \sigma_{f_r}^2 \sigma_{g_r}^2}{4} \right) - \kappa \right]. \tag{B.48}$$

Furthermore, for the case of $R = 1$, the closed-form solution for the approximate SER is obtained as

$$\begin{aligned} P_e(R=1) &\approx \frac{c}{\pi} \int_0^{\frac{\pi}{2}} M(-s)\, d\phi = \frac{2c}{\pi g \mu_r \sigma_{f_r}^2 \sigma_{g_r}^2} \int_0^{\frac{\pi}{2}} \sin^2\phi \left[\log\left(\frac{g\, \mu_r \sigma_{f_r}^2 \sigma_{g_r}^2}{8 \sin^2\phi} \right) - \kappa \right] d\phi \\ &= \frac{c}{2\mu_r \sigma_{f_r}^2 \sigma_{g_r}^2} \left[\log\left(\frac{\mu_r \sigma_{f_r}^2 \sigma_{g_r}^2}{2} \right) - (\kappa + 1) \right]. \end{aligned} \tag{B.49}$$

5 Power Control in AF DSTC without Instantaneous CSI at Relays

In this section, we propose two power allocation schemes for the AF distributed space-time codes introduced in [7]. We use the approximate value of the MGF, which was derived in Section III, for the power control among relays. Furthermore, we present another closed-form solution for the

MGF, as a function of the incomplete gamma function, which can be used for a more accurate power control strategy.

The MGF of the random variable γ, $M(-s)$, which is the integrand of the integral in (B.46), is given by the product of MGF of the random variables γ_r. Since $M_r(-s)$ is independent of the other μ_i, $i \neq r$, we can write

$$\frac{\partial M(-s)}{\partial \mu_r} = \frac{\partial M_r(-s)}{\partial \mu_r} \prod_{\substack{i=1 \\ i \neq r}}^{R} M_i(-s), \tag{B.50}$$

which will be used in the next two subsections to find the power control coefficients.

5.1 Power Allocation Based on Exact MGF

The closed-form solution for MGF of random variable γ_r, can be found using [28, Eq. (8.353)] as

$$M_r(-s) = \frac{2}{s\,\mu_r \sigma_{f_r}^2 \sigma_{g_r}^2} \Gamma\left(0, \frac{1}{s\,\mu_r \sigma_{f_r}^2 \sigma_{g_r}^2}\right) e^{\frac{1}{s\,\mu_r \sigma_{f_r}^2 \sigma_{g_r}^2}}, \tag{B.51}$$

where $\Gamma(\alpha, x)$ is the incomplete gamma function of order α [27, Eq. (6.5)]. Moreover, from [28, Eq. (8.356)], we have

$$\frac{-d\,\Gamma(\alpha, x)}{dx} = x^{\alpha-1} e^{-x}. \tag{B.52}$$

Since the MGFs in (B.48) and (B.51) are functions of $x_r \triangleq \mu_r \sigma_{f_r}^2 \sigma_{g_r}^2 s$, we can express (B.50) in terms of x_r. Hence, using (B.52), the partial derivative of $M_r(-s)$ with respect to x_r can be expressed as

$$\frac{\partial M_r(-s)}{\partial x_r} = \frac{\partial}{\partial x_r}\left[\frac{2}{x_r}\Gamma\left(0, \frac{1}{x_r}\right) e^{\frac{1}{x_r}}\right] = \frac{1}{x_r^2}\left[1 - \Gamma\left(0, \frac{1}{x_r}\right)\left(1 + \frac{1}{x_r}\right) e^{\frac{1}{x_r}}\right]. \tag{B.53}$$

Furthermore, the power constraint in the the second phase, i.e., $\sum_{r=1}^{R} P_{2,r} = P_1$, can be expressed as a function of x_r. Thus, using (B.42) and the definition of x_r, under the high SNR assumption, we have the following constraint

$$\sum_{r=1}^{R} \frac{x_r}{\sigma_{g_r}^2 s} \leq \frac{P_1}{N_2}. \tag{B.54}$$

Given the objective function as an integrand of (B.46) and the power constraint in (B.54), the classical Karush-Kuhn-Tucker (KKT) conditions for optimality [30] can be shown as

$$\prod_{\substack{i=1\\ i\neq r}}^{R} \left[\frac{2}{x_i}\Gamma\left(0,\frac{1}{x_i}\right)e^{\frac{1}{x_i}}\right]\frac{1}{x_r^2}\left[1-\Gamma\left(0,\frac{1}{x_r}\right)\left(1+\frac{1}{x_r}\right)e^{\frac{1}{x_r}}\right]+\frac{\lambda}{\sigma_{g_r}^2 s}=0, \quad \text{for } r=1,\ldots,R. \tag{B.55}$$

By solving (B.54) and (B.55), the optimum values of x_r, i.e., x_r^*, $r = 1, \ldots, R$ can be obtained. Now, we can have the following procedure to find the power control coefficients, $P_{2,r}$. First, the x_r^* coefficients can be solved by the above optimization problem. Then, recalling the relationship between x_r and μ_r, i.e., $x_r = \mu_r \sigma_{f_r}^2 \sigma_{g_r}^2 s$, and by taking average μ_r over different values of ϕ, since s is a function of $\sin^2\phi$, the optimum value of μ_r is obtained. However, for computational simplicity in the simulation results, we have assumed $s = 1$, which corresponds to $\phi = \pi/2$. Since the maximum amount of $M_r(-s)$ occurs in $s = 1$, this approximation achieves a good performance as will be confirmed in the simulation results. Finally, using (B.42), we can find the power control coefficients, $P_{2,r}$. If we assume that relays operate in the high SNR region, $P_{2,r}$ would be approximately proportional to μ_r.

5.2 Power Allocation Based on Approximate MGF

The power allocation proposed in Subsection IV-A needs to solve the set of nonlinear equations presented in (B.55), which are function of incomplete gamma functions. Thus, we present an alternative scheme in this subsection. For gaining insight into the power allocation based on minimizing the SER, we are going to minimize the approximate MGF of the random variable γ, obtained in (B.48). Using (B.48) and (B.54), we can formulate the following problem:

$$\min_{\{x_1,x_2,\ldots x_R\}} \prod_{r=1}^{R} \frac{1}{x_r}\left(\log\left(\frac{x_r}{4}\right)-\kappa\right),$$
$$\text{subject to} \sum_{r=1}^{R}\frac{x_r}{\sigma_{g_r}^2 s} \le \frac{P_1}{N_2}, \quad x_r \geqslant 0, \text{ for } r=1,\ldots.R. \tag{B.56}$$

The objective function in (B.56), i.e., $F(x_1,x_2,\ldots,x_R)=\prod_{r=1}^{R}\frac{1}{x_r}\left(\log\left(\frac{x_r}{4}\right)-\kappa\right)$, is *not* a convex function in general. However, it can be shown that for $x_r > 4\,e^{1.5+\kappa}$, the Hessian of $F(x_1,x_2,\ldots,x_R)$, is positive, which corresponds to high SNR conditions, this function is convex. Therefore, the problem stated in (B.56) is a convex problem for high SNR values and has a global optimum point. Now, we are going to derive a solution for a problem expressed in (B.56).

The Lagrangian of the problem stated in (B.56) is

$$L(x_1,x_2,\ldots,x_R)=\prod_{r=1}^{R}\frac{\log(x_r)-\kappa'}{x_r}+\lambda\left(\sum_{r=1}^{R}\frac{x_r}{\sigma_{g_r}^2 s}-\frac{P_1}{N_2}\right), \tag{B.57}$$

where $\lambda > 0$ is the Lagrange multiplier, and $\kappa' = \log(4)+\kappa$. For nodes $r=1,\ldots,R$ with nonzero transmitter powers, the KKT conditions are

$$\left(-\frac{\log(x_r)}{x_r^2}+\frac{1+\kappa'}{x_r^2}\right)\prod_{\substack{i=1\\ i\neq r}}^{R}\frac{\log(x_i)-\kappa'}{x_i}+\frac{\lambda}{\sigma_{g_r}^2 s}=0. \tag{B.58}$$

Using (B.48) and some manipulations, one can rewrite (B.58) as

$$\left(\frac{1}{x_r}-\frac{1}{x_r\left(\log\left(x_r\right)-\kappa'\right)}\right)M(s)=\frac{\lambda}{\sigma_{g_r}^2 s}. \tag{B.59}$$

Since the strong duality condition [30, Eq. (5.48)] holds for convex optimization problems, we have $\lambda\Big(\sum_{r=1}^{R}\frac{x_r}{\sigma_{g_r}^2 s}-\frac{P_1}{N_2}\Big)=0$ for the optimum point. If we assume the Lagrange multiplier has a positive value, we have $\sum_{r=1}^{R}\frac{x_r}{\sigma_{g_r}^2 s}=\frac{P_1}{N_2}$. Therefore, by multiplying the two sides of (B.59) with x_r, and applying the summation over $r = 1, \ldots, R$, we have

$$\left[R - \sum_{i=1}^{R} \frac{1}{\log(x_i) - \kappa'}\right] M(s) = \lambda \frac{P_1}{N_2}. \tag{B.60}$$

Dividing both sides of equalities in (B.59) and (B.60), we have

$$\frac{1}{x_r}\left(1 - \frac{1}{\log(x_r) - \kappa'}\right) = \frac{N_2}{P_1 \sigma_{g_r}^2 s}\left[R - \sum_{i=1}^{R} \frac{1}{\log(x_i) - \kappa'}\right], \tag{B.61}$$

for $r = 1, \ldots, R$. The optimal values of x_r in the problem stated in (B.56) can be easily obtained with initializing some positive values for x_r, $r = 1, \ldots, R$, and using (B.61) in an iterative manner. Then, we apply the same procedure stated in Subsection IV-A to find the power control coefficients, $P_{2,r}$.

6 Simulation Results

In this section, the performance of the AF distributed space-time codes with power allocation are studied through simulations. We utilized distributed version of GABBA codes [10], as practical full-diversity distributed space-time codes, using BPSK modulation. We compare the transmit SNR $\frac{P}{N_1}$ versus BER performance. We use the block fading model, in which channel coefficients changed randomly in time to isolate the benefits of spatial diversity. Assume that the relays and the destination have the same noise power, i.e., $N_1 = N_2$.

In Fig. B.3, the BER performance of the AF DSTC is compared to the proposed AF opportunistic relaying derived in Section III, when the number of available relays are 3 and 4. For AF DSTC, equal power allocation is used among the relays. All links are supposed to have unit-variance Rayleigh flat fading. One can observe from Fig. B.3 that the AF opportunistic scheme gains around 2 and 3 dB in SNR at BER 10^{-3}, when 3 and 4 relays are used, respectively. Furthermore, Fig. B.3 confirms that the analytical results attained in Section IV for finding SER for AF opportunistic relaying coincide with the simulation results. Since the curves corresponding to R relays are parallel to each other in the high SNR region, the AF opportunistic relaying have the same diversity gain as AF DSTC. In low SNR scenarios, due to the noise adding property of AF systems, even opportunistic relaying with $R = 3$ outperforms AF DSTC with $R = 4$.

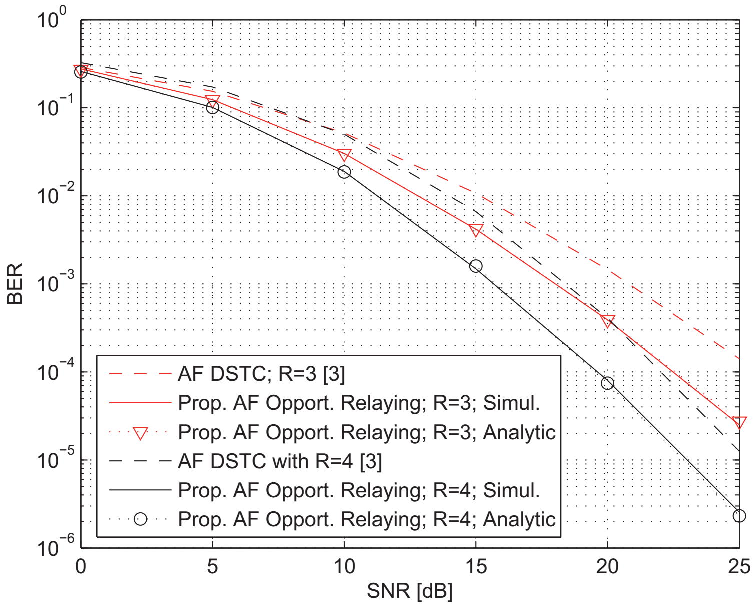

Fig. B.3: The average BER curves of relay networks employing DSTC and opportunistic relaying with partial statistical CSI at relays, BPSK signals and $\sigma^2_{f_i} = \sigma^2_{g_i} = 1$.

Fig. B.4 compares the performance of the two AF schemes introduced in Section III, when the proposed power allocation in two phases is employed. That is, we compare the equal power allocation in two phases [7] with the optimum value of α, which is derived in (B.7). The number of relays is supposed to be $R = 4$. Assuming $d_g = \sqrt{2}d_f = 2$, where d_f and d_g are source-to-relays and relays-to-destination distances, respectively, $\sigma^2_{f_i} = \frac{1}{d_f^4} = 1$ and $\sigma^2_{g_i} = \frac{1}{d_g^4} = \frac{1}{4}$. This is due to the fact that path-loss can be represented by $\frac{1}{d^n}$, where $2 < n < 5$, and we assume $n = 4$. Fig. B.4 demonstrates that by using the optimum value of α in (B.7), around 1 dB gain is achieved for both AF DSTC and AF opportunistic relaying schemes for BER of less than 10^{-3}. Therefore, the amount of performance gain obtainable using the optimal power allocation between two phases is negligible compared to

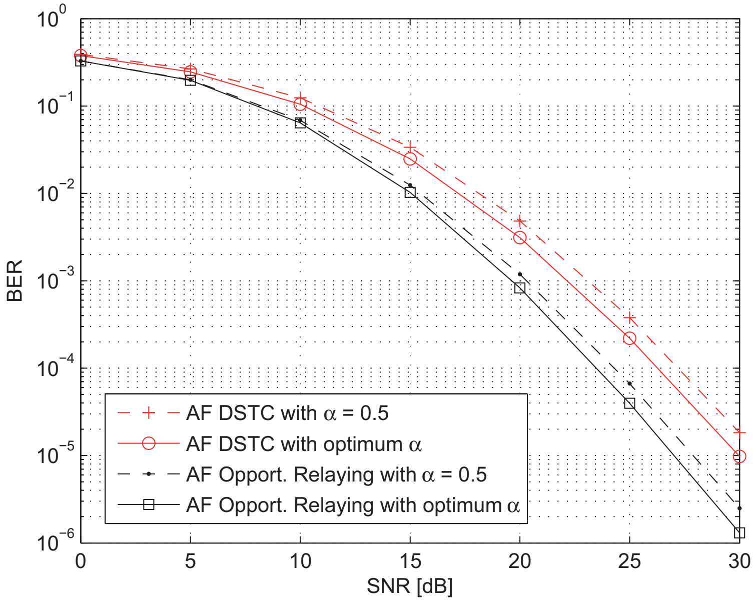

Fig. B.4: The average BER curves of relay networks employing DSTC and opportunistic relaying in AF mode, when equal power between two phases is compared with α in (B.7), and with BPSK signals, $\sigma_{f_i}^2 = 4\sigma_{g_i}^2 = 1$, and $R = 4$.

the equal power allocation, i.e., $\alpha = \frac{1}{2}$.

In Fig. B.5, we compare the approximate BER formula based on MGF given in (B.48) with the full-rate, full-diversity distributed GABBA space-time codes. For GABBA codes, we employed 4×4 GABBA mother codes, i.e., $T = 4$ [10]. Assume all the links have unit-variance Rayleigh flat fading. Fig. B.5 confirms that the analytical results attained in Section III for finding the BER approximate well the performance of the practical full-diversity distributed space-time codes for high SNR values.

Fig. B.6 presents the BER performance of the AF distributed space-time codes using different power allocation schemes. For transmission power among nodes, we employed the two power control schemes introduced in Section IV, and also uniform power transmission among re-

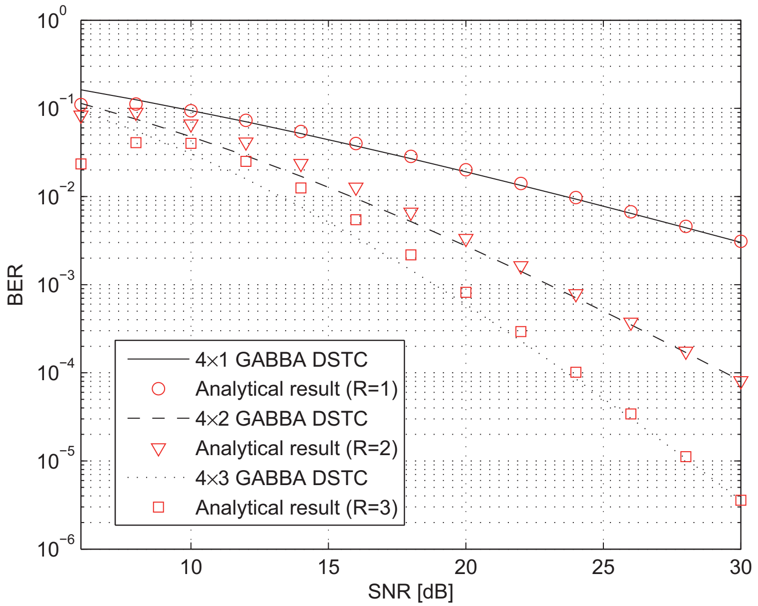

Fig. B.5: The average BER curves versus SNR of relay networks employing distributed space-time codes with BPSK signals.

lays, i.e., $P_1 = \frac{P}{2}$ and $P_{2,r} = \frac{P}{2R}$ [7]. Since the proposed power allocation strategies are designed for high SNR scenarios, we study the system performance in the high SNR regime. Furthermore, since we supposed that the relays are operating in low noise conditions, here, we assume $N_2 = 2N_1$. Slow Rayleigh flat fading channels are considered, with variance of $\sigma^2_{f_r}(r) = \sigma^2_{g_r}(r) = 1/2^{r-1}$, $r = 1, 2, \ldots R$. For the power control scheme expressed in Subsection IV-A (based on the exact MGF), we have used MATLAB optimization toolbox command "fmincon" designed to find the minimum of the given constrained nonlinear multivariable function. Fig. B.6 demonstrates that using the power control schemes of Section V, about 1 and 2 dB gain will be obtained for $R = 2$ and $R = 3$ cases, respectively, comparing to uniform power allocation. The power control strategy given in Subsection V-A (Exact MGF-based power control) has a slightly better performance than the power control strategy presented in Subsection V-B

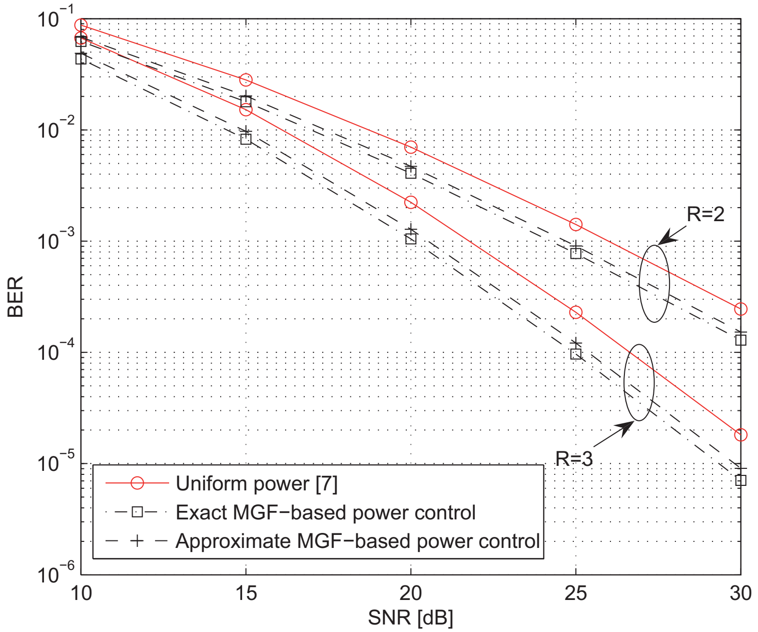

Fig. B.6: Performance comparison of AF DSTC with different power allocation strategies in a network with two and three relays and using BPSK signals.

(Approximate MGF-based power control), at the expense of higher computational complexity.

7 Conclusion

In this paper, we have shown that using maximum instantaneous SNR power allocation at the relays, subject to the fixed transmit power during the second phase, distributed space-time codes under amplify-and-forward led to opportunistic relaying. Therefore, the whole transmission power during the second phase is transmitted by the relay with the best channel conditions. We analyzed the SER performance of the AF opportunistic relaying system with M-PSK and M-QAM signals. Simulations are in accordance with the analytic expressions. We also derived approximate BER formulas of AF DSTC using the moment generating function method, when M-PSK and M-QAM modulations are employed. Simulation results confirmed that the theoretical expressions have a similar performance to the Monte Carlo simulations at high SNR values. Furthermore, we proposed two power allocation methods based on minimizing the BER, which are independent of the knowledge of instantaneous CSI. Simulations showed that up to 2 dB is achieved in the high SNR region compared to an equal power transmission, when using three relays.

Appendix I: Proof of Proposition 2

Suppose $X = |f_r|^2$ and $Y = |g_r|^2$, where X and Y have exponential distribution with mean of $\overline{X} = \sigma^2_{f_r}$ and $\overline{Y} = \sigma^2_{g_r}$, respectively. Therefore, the cumulative density function (CDF) of $Z = XY/(aY + b)$, where $a = N_1$ and $b = \frac{N_2(\sigma^2_{f_r}P_1+N_1)}{P_2}$, can be presented to be

$$\begin{aligned}\Pr\{Z < z\} &= \Pr\{XY/(aY + b) < z\} = \int_0^\infty \Pr\{X < \frac{z(ay + b)}{y}\}p_Y(y)dy \\ &= \frac{1}{\overline{Y}}\int_0^\infty \left(1 - e^{-\frac{z(ay+b)}{\overline{X}y}}\right) e^{-\frac{y}{\overline{Y}}}dy = 1 - \frac{1}{\overline{X}}\int_0^\infty e^{-\frac{az}{\overline{X}}} e^{-\left(\frac{bz}{\overline{X}y}+\frac{y}{\overline{Y}}\right)}dy \\ &= 1 - 2\,e^{-\frac{az}{\overline{X}}}\sqrt{\frac{bz}{\overline{XY}}}K_1\left(2\sqrt{\frac{bz}{\overline{XY}}}\right), \end{aligned} \tag{B.62}$$

where we have used [28, Eq. (3.324)] for the last equality. The PDF of Z can be written as

$$p_Z(z) = \frac{d}{dz}\Pr\{Z < z\} = f_1(z) + f_2(z), \tag{B.63}$$

where $f_1(z)$ and $f_2(z)$ are defined as

$$f_1(z) = \frac{2b}{\overline{XY}}e^{-\frac{az}{\overline{X}}}K_0\left(2\sqrt{\frac{bz}{\overline{XY}}}\right), \tag{B.64}$$

$$f_2(z) = \frac{2a}{\overline{X}}\sqrt{\frac{bz}{\overline{XY}}}e^{-\frac{az}{\overline{X}}}K_1\left(2\sqrt{\frac{bz}{\overline{XY}}}\right), \tag{B.65}$$

where for the derivative of $\frac{d}{dz}\Pr\{Z < z\}$ we have used the following equality [27]

$$x\frac{d}{dx}K_\nu(x) = -xK_{\nu-1}(x) - \nu K_\nu(x).$$

Now, using (B.63)-(B.65), and the fact that the PDF of the random variable $\gamma_r = P_1 Z$ is $\frac{1}{P_1}p_Z(\frac{\gamma_r}{P_1})$, we obtain the result in (B.20).

Appendix II: Proof of Proposition 3

For deriving the PDF of $\gamma_{\max}$ we should first find its CDF, which can be written as

$$\Pr\{\gamma_{\max} < \gamma\} = \Pr\{\gamma_1 \leq \gamma, \gamma_2 \leq \gamma, \ldots, \gamma_R \leq \gamma\} = \prod_{r=1}^{R} \Pr\{\gamma_r \leq \gamma\}. \quad \text{(B.66)}$$

The second equality comes from the fact that we assumed that all channel coefficients are independent of each others. Then the PDF of $\gamma_{\max}$ can be written as

$$p_{\max}(\gamma) = \frac{d}{d\gamma}\Pr\{\gamma_{\max} < \gamma\} = \sum_{r=1}^{R} p_r(\gamma) \prod_{\substack{i=1 \\ i\neq r}}^{R} \Pr\{\gamma_i \leq \gamma\}. \quad \text{(B.67)}$$

Replacing $p_r(\gamma)$ and $\Pr\{\gamma_i \leq \gamma\}$ from (B.20) and (B.62), respectively, in (B.67), the result given in (B.23) is obtained.

Appendix III: Proof of Theorem 1

Considering $p_{\max}(\gamma)$ stated in (B.23), we can express $M_{\max}(-s)$ as

$$\begin{aligned} M_{\max}(-s) &= \int_0^\infty e^{-s\,\gamma} p_{\max}(\gamma)\, d\gamma \approx \sum_{r=1}^{R} \int_0^\infty e^{-s\,\gamma} p_r(\gamma) \prod_{\substack{i=1 \\ i\neq r}}^{R} \left(1 - e^{-B_i \gamma}\right) d\gamma \\ &\approx 2\sum_{r=1}^{R} \int_0^\infty e^{-(s+B_r)\,\gamma} \left[A_r K_0\left(2\sqrt{A_r\gamma}\right) + B_r\sqrt{A_r\gamma}K_1\left(2\sqrt{A_r\gamma}\right)\right] (\prod_{\substack{i=1 \\ i\neq r}}^{R} B_i)\gamma^{R-1} d\gamma, \end{aligned}$$

(B.68)

where in the second equality we have approximated $K_1(x) \approx \frac{1}{x}$ (see, e.g., [27, Eq. (9.6.8)]), and in the third equality $\left(1 - e^{-B_i\gamma}\right)$ is approximated by $B_i\gamma$. These approximations are accurate for all values of B_i, since the fact that e^{-x}, $K_0(x)$, and $K_1(x)$ are decreasing functions of x in the integrand in (B.68), and thus, the value of $B_i\gamma$ around $\gamma = 0$ is critical . Simplifying (B.68), we get

$$M_{\max}(-s) \approx 2\sum_{r=1}^{R} A_r(\prod_{\substack{i=1\\i\neq r}}^{R} B_i)\int_0^\infty e^{-(s+B_r)\gamma} K_0\left(2\sqrt{A_r\gamma}\right)\gamma^{R-1}d\gamma$$
$$+ 2\sum_{r=1}^{R} \sqrt{A_r}(\prod_{r=1}^{R} B_r)\int_0^\infty e^{-(s+B_r)\gamma} K_1\left(2\sqrt{A_r\gamma}\right)\gamma^{R-\frac{1}{2}}d\gamma, \quad \text{(B.69)}$$

The integrals in (B.69) denoted I_1 and I_2, respectively, can be evaluated with the help of [28, Eq. (6.631)], which with some extra manipulations leads to

$$I_1 = \frac{\Gamma^2(R)(s+B_r)^{-R+\frac{1}{2}}}{2\sqrt{A_r}} e^{\frac{A_r}{2(s+B_r)}} W_{-R+\frac{1}{2},0}\left(\frac{A_r}{s+B_r}\right), \quad \text{(B.70)}$$

$$I_2 = \frac{\Gamma(R+1)\Gamma(R)(s+B_r)^{-R}}{2\sqrt{A_r}} e^{\frac{A_r}{2(s+B_r)}} W_{-R,\frac{1}{2}}\left(\frac{A_r}{s+B_r}\right). \quad \text{(B.71)}$$

where $\Gamma(n)$ is the gamma function of order n. Combining (B.69), (B.70), and (B.71), the desired result given in (B.26) is achieved.

Appendix IV: Proof of Theorem 2

From (B.38)-(B.40), and by using a tractable definition of the diversity gain in [31, Eq. (1.19)], we have

$$G_d = -\lim_{\mu\to\infty} \frac{\log\left(P_e(R)\right)}{\log\left(\mu\right)} = -\lim_{\mu\to\infty} \frac{\log\left(\Omega(\mu,R)\right) + \log\left(C_1(\mu,R)\right)}{\log\left(\mu\right)}$$
$$= -\lim_{\mu\to\infty} \frac{\log\left(\mu^{-R}\right)}{\log\left(\mu\right)} - \lim_{\mu\to\infty} \frac{\log\left(\log\left(\mu\right)\right)}{\log\left(\mu\right)} = R \quad \text{(B.72)}$$

where in the second, third, and fourth equations, we have used the l'Hôpital's rule. Hence, it is proven that AF opportunistic relaying scheme derived in Section III, provides full diversity of order R in a network consisting of R

relays.

References

[1] A. Sendonaris, E. Erkip, and B. Aazhang, “User cooperation diversity. Part I. System description,” *IEEE Trans. Commun.*, vol. 51, no. 11, pp. 1927–1938, Nov. 2003.

[2] ——, “User cooperation diversity. Part II. Implementation aspects and performance analysis,” *IEEE Trans. Commun.*, vol. 51, no. 11, pp. 1939–1948, Nov. 2003.

[3] J. N. Laneman and G. Wornell, “Energy-efficient antenna sharing and relaying for wireless networks,” in *Proc. Wireless Communications Networking Conf.*, Chicago, IL, Sep. 2000, pp. 7–12.

[4] ——, “Distributed space-time coded protocols for exploiting cooperative diversity in wireless networks,” in *IEEE GLOBECOM 2002*, vol. 1, no. 11, Taipei, Taiwan, R.O.C., Nov. 2002, pp. 77–81.

[5] R. U. Nabar, H. Bölcskei, and F. W. Kneubuhler, “Fading relay channels: Performance limits and space-time signal design,” *IEEE J. Sel. Areas Commun.*, vol. 22, no. 6, pp. 1099–1109, Aug. 2004.

[6] Y. Hua, Y. Mei, and Y. Chang, “Wireless antennas-making wireless communications perform like wireline communications,” in *IEEE AP-S Topical Conf. on Wireless Comm. Tech.*, Honolulu, Hawaii, Oct. 2003.

[7] Y. Jing and B. Hassibi, “Distributed space-time coding in wireless relay networks,” *IEEE Trans. Wireless Commun.*, vol. 5, no. 12, pp. 3524–3536, Dec. 2006.

[8] ——, “Cooperative diversity in wireless relay networks with multiple-antenna nodes,” in *IEEE Int. Symp. Inform. Theory*, Adelaide, Australia, 2005.

[9] Y. Jing and H. Jafarkhani, "Using orthogonal and quasi-orthogonal designs in wireless relay networks," *IEEE Trans. Info. Theory*, vol. 53, no. 11, pp. 4106–4118, Nov. 2007.

[10] B. Maham, A. Hjørungnes, and G. Abreu, "Distributed GABBA space-time codes in amplify-and-forward relay networks," *IEEE Trans. Wireless Commun.*, vol. 8, no. 4, pp. 2036–2045, Apr. 2009.

[11] G. S. Rajan and B. S. Rajan, "Distributed space-time codes for cooperative networks with partial CSI," in *Proc. IEEE Wireless Communications and Networking Conference (WCNC)*, Hong Kong, China, March 2007, pp. 902–906.

[12] Y.-W. Hong, W.-J. Huang, F.-H. Chiu, and C.-C. J. Kuo, "Cooperative communications in resource-constrained wireless networks," *IEEE Signal Processing Magazine*, vol. 24, pp. 47–57, May 2007.

[13] B. Maham and A. Hjørungnes, "Minimum power allocation in SER constrained amplify-and-forward cooperation," in *Proc. IEEE Vehicular Technology Conference (VTC 2008-Spring)*, Singapore, May 2008, pp. 2431–2435.

[14] M. Chen, S. Serbetli, and A. Yener, "Distributed power allocation strategies for parallel relay networks," *IEEE Trans. Wireless Commun.*, vol. 7, no. 2, pp. 552–561, Feb. 2008.

[15] A. Host-Madsen and J. Zhang, "Capacity bounds and power allocation for wireless relay channels," *IEEE Trans. Inform. Theory*, vol. 51, no. 6, pp. 2020–2040, Jun. 2005.

[16] D. R. Brown, "Energy conserving routing in wireless adhoc networks," in *Proc. Asilomar Conf. Signals, Syst. Computers*, Monterey, CA, USA, Nov. 2004.

[17] A. Reznik, S. R. Kulkarni, and S. Verdú, "Degraded gaussian multirelay channel: Capacity and optimal power allocation," *IEEE Trans. Inform. Theory*, vol. 50, no. 12, pp. 3037–3046, Dec. 2004.

[18] M. O. Hansa and M.-S. Alouini, "Optimal power allocation for relayed transmissions over Rayleigh-fading channels," *IEEE Trans. Wireless Commun.*, vol. 3, no. 6, pp. 1999–2004, Nov. 2004.

[19] M. Dohler, A. Gkelias, and H. Aghvami, "Resource allocation for FDMA-based regenerative multihop links," *IEEE Trans. Wireless Commun.*, vol. 3, no. 6, pp. 1989–1993, Nov. 2004.

[20] J. Luo, R. S. Blum, L. J. Cimini, L. J. Greenstein, and A. M. Haimovich, "Link-failure probabilities for practical cooperative relay networks," in *Proc. IEEE 61st Veh. Technol. Conf., Spring*, May 2005, pp. 1489–1493.

[21] Z. Lin and E. Erkip, "Relay search algorithms for coded cooperative systems," in *Proc. IEEE Global Telecommun. Conf.*, Nov. 2005, pp. 1314–1319.

[22] H. Zheng, Y. Zhu, C. Shen, and X. Wang, "On the effectiveness of cooperative diversity in ad hoc networks: A MAC layer study," in *IEEE Int. Conf. Acoustics, Speech, Signal Processing*, Mar. 2005, pp. 509–512.

[23] A. Bletsas, A. Khisti, D. P. Reed, and A. Lippman, "A simple cooperative method based on network path selection," *IEEE Journal on Selected Areas in Communications*, vol. 24, no. 3, pp. 659–672, Mar. 2006.

[24] A. Bletsas, H. Shin, and M. Win, "Outage optimality of amplify-and-forward opportunistic relaying," *IEEE Comm. Letters*, vol. 11, no. 3, pp. 261–263, Mar. 2007.

[25] Y. Zhao, R. Adve, and T. J. Lim, "Symbol error rate of selection amplify-and-forward relay systems," *IEEE Comm. Letters*, vol. 10, no. 11, pp. 757–759, Nov. 2006.

[26] R. Horn and C. Johnson, *Matrix Analysis*. Cambridge, UK: Cambridge Academic Press, 1985.

[27] M. Abramowitz and I. A. Stegun, *Handbook of Mathematical Functions*. New York, USA: Dover Publications, 1972.

[28] I. S. Gradshteyn and I. M. Ryzhik, *Table of Integrals, Series, and Products*. San Diego, USA: Academic, 1996.

[29] M. K. Simon and M.-S. Alouini, *Digital Communication over Fading Channels: A Unified Approach to Performance Analysis*. New York, USA: Wiley, 2000.

[30] S. Boyd and L. Vandenberghe, *Convex Optimization*. Cambridge, UK: Cambridge Univ. Press, 2004.

[31] H. Jafarkhani, *Space-Time Coding Theory and Practice*. Cambridge, UK: Cambridge Academic Press, 2005.

Paper C

Performance Analysis of Repetition-Based Cooperative Networks with Partial Statistical CSI at Relays

B. Maham and A. Hjørungnes

IEEE Communications Letters, volume 12, issue 11, pages 828-830, November 2008.

Abstract

This letter analyzes the performance of repetition-based cooperative diversity wireless networks using *amplify-and forward* relaying, in which each relay has only statistical knowledge of the source-relay link. The network channels are modeled as independent, non-identical, Rayleigh distributed coefficients. The exact symbol error rate is derived using the moment generating function (MGF). We derive the probability density function and MGF of the total SNR. Then, the MGF is used to determine the symbol error rate (SER). The diversity order of the amplify-and-forward cooperation with partial statistical channel state information is also found via the asymptotic behavior of the average SER, and it is shown that the cooperative network achieves full diversity. Our analytical results are confirmed by simulations.

1 Introduction

Cooperative diversity networks technique is a promising solution for the high data-rate coverage required in future cellular and ad-hoc wireless communications systems. Several cooperation strategies with different relaying techniques, including amplify-and-forward (AF), decode-and-forward (DF), and selective relaying, have been studied in Laneman et al.'s seminal paper [1]. Cooperative transmissions have been categorized into space-time coded cooperation (see, e.g., [2–5]) and repetition-based cooperation (see, e.g., [6–8]).

In [7], the authors derived asymptotic average symbol error rate (SER) for AF cooperative networks, when relays have *instantaneous* channel state information (CSI). An exact average SER analysis for a AF cooperative network (with knowledge of instantaneous CSI at the relays) is presented in [6]. Using scaling factors which depend on partial statistical CSI in AF relays, i.e., each relay has only statistical knowledge of the source-relay channel, were first proposed in [9]. In [3, 10, 11], relays with partial statistical CSI are used in space-time coded cooperation.

In this letter, we apply AF relaying with partial statistical CSI to the case of repetition-based cooperation, in which R amplifying relays retransmit the source's signal in a time-division multiple-access (TDMA) manner. We derive the exact average SER of this system for M-PSK transmissions over Rayleigh-fading channels. We first find closed-form expressions for the cumulative distribution function (CDF), probability density function (PDF) and MGF of the total SNR. Then, the MGF is used to determine the average SER. We also derive the diversity order of the AF cooperation with partial statistical CSI via the asymptotic behavior of the average SER, and show that the cooperative network presented in this paper achieves full diversity order $R + 1$.

2 System Model

Consider a network consisting of a source, R relays, and one destination. We denote the source-to-destination, source-to-*i*th relay, and *i*th relay-to-destination links by f_0, f_i, and g_i, respectively. Suppose each link has Rayleigh fading, independent of the others. Therefore, f_0, f_i, and g_i are complex Gaussian random variables, which are jointly independent, with zero-mean and variances $\sigma^2_{f_0}$, $\sigma^2_{f_i}$, and $\sigma^2_{g_i}$, respectively. Similar to [1], our scheme requires two phase of transmission. During the first phase, the source node transmits a signal $s(n)$, where n is the time index, to *all* relays and the destination. The received signal at the destination and the ith relay from the source in the first phase can be written as

$$y_0(n) = \sqrt{\varepsilon_0} f_0 s(n) + w_0(n), \tag{C.1}$$

$$r_i(n) = \sqrt{\varepsilon_0} f_i s(n) + v_i(n), \tag{C.2}$$

respectively, where ε_0 is the average total transmitted symbol energy of the source, since we assume the information bearing symbols $s(n)$'s are normalized to one (M-PSK), and $w_0(n)$ and $v_i(n)$ are complex zero-mean white Gaussian noises with variances N_0 and N_i, respectively. Under repetition-based amplify-and-forward cooperation, each relay scales its received signal with the scaling factor α_i. Then, the ith relay retransmits the scaled version of the received signal towards the destination in the ith interval of the second phase, i.e.,

$$y_i(n) = g_i \, \alpha_i \, r_i(n) + w_i(n), \tag{C.3}$$

where $w_i(n)$ is a complex zero-mean white Gaussian noise with the variance of N_0. When there is no instantaneous CSI at the relays, but statistical CSI of the source-to-ith relay link is known, a useful constraint is to ensure that a given average transmitted power is maintained. That is,

$$\alpha_i = \sqrt{\frac{\varepsilon_i}{\varepsilon_0 \sigma^2_{f_i} + N_i}}, \tag{C.4}$$

where ε_i is the average transmitted power at relay *i*, such that all relays transmits with the same average power.

Assuming maximum ratio combining (MRC) at the destination, the total received signal-to-noise ratio (SNR) can be written as

$$\gamma_d = \gamma_0 + \sum_{i=1}^{R} \gamma_i, \tag{C.5}$$

where $\gamma_0 = |f_0|^2 \varepsilon_0 / N_0$ is the instantaneous SNR between the source and ith relay, and γ_i can be shown to be

$$\gamma_i = \frac{|f_i|^2|g_i|^2}{A_i|g_i|^2 + B_i}, \tag{C.6}$$

for $i = 1, \ldots, R$, where A_i and B_i are given by

$$A_i = \frac{N_i}{\varepsilon_0}, \ B_i = \frac{N_0(\sigma_{f_i}^2\varepsilon_0 + N_i)}{\varepsilon_0\varepsilon_i}. \tag{C.7}$$

3 Performance Analysis

3.1 Exact Symbol Error Probability Expression

In this subsection, we will derive the SER formula of a repetition-based relay network with noncoherent relays, using the MGF method. First, we will derive the PDF of γ_i in (C.6). This is needed for calculating the average SER.

Using the same procedure for calculating the CDF of product of two exponential random variable which is given in [3, Eq. (19)], and with the help of [12, Eq. (3.324)], the CDF of γ_i in (C.6) can be presented to be

$$\Pr\{\gamma_i < \gamma\} = 1 - 2\, e^{-\frac{A_i\gamma}{\sigma_{g_i}^2}} \sqrt{\frac{B_i\gamma}{\sigma_{f_i}^2\sigma_{g_i}^2}} K_1\left(2\sqrt{\frac{B_i\gamma}{\sigma_{f_i}^2\sigma_{g_i}^2}}\right), \tag{C.8}$$

where $K_j(x)$ is the modified Bessel function of the second kind of order j [13]. Thus, the PDF of γ_i can be found by taking the derivative of (C.8) with respect to γ, and using [14, Eq. (24.55)], yielding

$$\begin{aligned} p(\gamma_i) =& \frac{2B_i}{\sigma_{f_i}^2\sigma_{g_i}^2} e^{-\frac{A_i\gamma_i}{\sigma_{g_i}^2}} K_0\left(2\sqrt{\frac{B_i\gamma_i}{\sigma_{f_i}^2\sigma_{g_i}^2}}\right) \\ &+ \frac{2A_i}{\sigma_{g_i}^2}\sqrt{\frac{B_i\gamma_i}{\sigma_{f_i}^2\sigma_{g_i}^2}} e^{-\frac{A_i\gamma_i}{\sigma_{g_i}^2}} K_1\left(2\sqrt{\frac{B_i\gamma_i}{\sigma_{f_i}^2\sigma_{g_i}^2}}\right). \end{aligned} \tag{C.9}$$

Recalling the independence of f_0, f_i, and g_i, the MGF of γ_d in (C.5), i.e., $M_d(-s) = \mathbb{E}\{e^{-s\gamma_d}\}$, can be written as

$$M_d(-s) = M_0(-s) \prod_{r=1}^{R} M_i(-s), \tag{C.10}$$

where $M_i(-s)$ is the MGF of γ_i in (C.6), while $M_0(-s) = \frac{1}{1+\sigma_{f_0}^2 \varepsilon_0 s/N_0}$ is the MGF of γ_0. Considering (C.9), and with the help of [12, Eq. (6.643)], the MGF of γ_i can be calculated as

$$M_i(-s) = \left[\sqrt{\frac{B_i}{(s+\frac{A_i}{\sigma_{g_i}^2})\,\sigma_{f_i}^2\sigma_{g_i}^2}}\,W_{-\frac{1}{2},0}\left(\frac{B_i}{(s+\frac{A_i}{\sigma_{g_i}^2})\,\sigma_{f_i}^2\sigma_{g_i}^2}\right)\right.$$
$$\left.+\frac{A_i\Gamma(2)}{\sigma_{g_i}^2(s+\frac{A_i}{\sigma_{g_i}^2})}W_{-1,-\frac{1}{2}}\left(\frac{B_i}{(s+\frac{A_i}{\sigma_{g_i}^2})\,\sigma_{f_i}^2\sigma_{g_i}^2}\right)\right] e^{\frac{B_i}{2(s+\frac{A_i}{\sigma_{g_i}^2})\sigma_{f_i}^2\sigma_{g_i}^2}}, \tag{C.11}$$

where $W_{a,b}(x)$ is Whittaker's function of orders a and b (see e.g., [13] and [12, Subsection 9.224]). Note that Whittaker's function can be presented in terms of a generalized hypergeometric function (see, e.g., [12, Eq. (9.220)]).

Using $M_d(-s)$, the the average SER for M-ary phase-shift keying (M-PSK) can be written as [15, p. 271]

$$P_e(R) = \frac{1}{\pi}\int_0^{\frac{(M-1)\pi}{M}} M_d\left(\frac{-\rho}{\sin^2\phi}\right)\,d\phi, \tag{C.12}$$

where $\rho = \sin^2\left(\frac{\pi}{M}\right)$. The result of (C.12) can also be used to find average SER for nonconstant modulus transmissions like M-ary amplitude modulation (M-AM and M-QAM as indicated in [15, Eqs. (9.19) and (9.21)].

3.2 Diversity Analysis

In this subsection, we will study the achievable diversity gain in a AF repetition-based network containing R relays with partial statistical CSI at the relays.

A tractable definition of the diversity, or diversity gain, is $G_d = -\lim_{\mu\to\infty}\frac{\log(P_e(R))}{\log(\mu)}$, where μ is the SNR [16, Eq. (1.19)]. Furthermore, (C.12) can be upper-bounded by $P_e(R) \le \left(1-\frac{1}{M}\right) M_d(-\rho) < M_d(-\rho)$ [15, p. 271]. Hence, we have

$$G_d \ge -\lim_{\mu\to\infty}\frac{\log(M_d(-\rho))}{\log(\mu)}. \tag{C.13}$$

Therefore, using (C.10), we can find the diversity order of repetition-based AF system in which relays have partial statistical CSI as follows:

$$\begin{aligned} G_d &\geq -\lim_{\mu\to\infty}\frac{\log\left(M_d\left(-\rho\right)\right)}{\log\left(\mu\right)} = -\lim_{\mu\to\infty}\frac{\sum_{k=0}^{R}\log\left(M_k\left(-\rho\right)\right)}{\log\left(\mu\right)} \\ &= -\sum_{k=0}^{R}\lim_{\mu\to\infty}\frac{\log\left(M_k\left(-\rho\right)\right)}{\log\left(\mu\right)}. \end{aligned} \tag{C.14}$$

For the simplicity in deriving the expressions and without lose of generality, similar to [11], we assume equal power allocation among the two transmission phases and among the relays, i.e., $\varepsilon_0 = R\,\varepsilon_i$, for $i = 1, \ldots, R$, and $N_i = N_0$. Then, by defining $\mu = \frac{N_0}{\varepsilon_0}$, we have

$$\lim_{\mu\to\infty}\frac{-\log\left(M_0\left(-\rho\right)\right)}{\log\left(\mu\right)} = \lim_{\mu\to\infty}\frac{\log\left(1+\sigma_{f_0}^2\mu\rho\right)}{\log\left(\mu\right)} = 1. \tag{C.15}$$

Now, for calculating (C.14) we need to solve $\lim_{\mu\to\infty}\frac{\log(M_i(-\rho))}{\log(\mu)}$, for $i = 1, \ldots, R$.

With the help of the integral in [12, Eq. (9.22)], it can be shown that $W_{\beta,\frac{1}{2}+\beta}(x) = x^{-\beta}e^{x/2}\Gamma(2\beta+1, x)$, where $\Gamma(\cdot,\cdot)$ is the incomplete gamma function [12, Eq. (8.350)]. On the other hand, the incomplete gamma function can be represented as exponential integrals $E_n(x) = x^{n-1}\Gamma(1-n, x)$, where n is an integer [13, Eq. (5.1.45)]. Thus, we can represent $W_{-\frac{1}{2},0}(\cdot)$ and $W_{-1,-\frac{1}{2}}(\cdot)$ in terms of exponential integrals, $E_n(\cdot)$:

$$W_{-\frac{1}{2},0}(x) = x^{\frac{1}{2}}e^{\frac{x}{2}}E_1(x),\ W_{-1,-\frac{1}{2}}(x) = e^{\frac{x}{2}}E_2(-x). \tag{C.16}$$

Therefore, $M_i\left(-\rho\right)$ in (C.11) can be rewritten as

$$\begin{aligned} M_i(-\rho) = e^{\frac{B_i}{(\rho+\frac{A_i}{\sigma_{g_i}^2})\sigma_{f_i}^2\sigma_{g_i}^2}}\Bigg[&\frac{B_i}{(\rho+\frac{A_i}{\sigma_{g_i}^2})\sigma_{f_i}^2\sigma_{g_i}^2}E_1\left(\frac{B_i}{(\rho+\frac{A_i}{\sigma_{g_i}^2})\sigma_{f_i}^2\sigma_{g_i}^2}\right) \\ &+\frac{A_i\Gamma(2)}{\sigma_{g_i}^2(\rho+\frac{A_i}{\sigma_{g_i}^2})}E_2\left(\frac{B_i}{(\rho+\frac{A_i}{\sigma_{g_i}^2})\,\sigma_{f_i}^2\sigma_{g_i}^2}\right)\Bigg]. \end{aligned} \tag{C.17}$$

Furthermore, using [13, Eq. (5.1.11)], the series representation of $E_i(x)$, for $x > 0$, can be expressed as

$$E_1(x) = -\kappa - \log(x) - \sum_{k=1}^{\infty} \frac{-x^k}{k\,k!}, \tag{C.18}$$

$$E_2(x) = e^{-x} + \kappa\,x + x\log(x) + \sum_{k=1}^{\infty} \frac{(-x)^{k+1}}{k\,k!}. \tag{C.19}$$

where κ is Euler's constant, i.e., $\kappa \approx 0.5772156$ [12]. Then, using (C.18) and (C.19), and by defining $C_i = \frac{R}{\mu\rho\,\sigma^2_{g_i}}$, we have

$$\begin{aligned}
&\lim_{\mu\to\infty} \frac{-\log\left(M_i\left(-\rho\right)\right)}{\log\left(\mu\right)} \\
&= \lim_{\mu\to\infty} \frac{-\log\left(e^{C_i}\left[C_i E_1(C_i) + \frac{2A_i\Gamma(2)}{\sigma^2_{g_i}g} E_2(C_i)\right]\right)}{\log\left(\mu\right)} \\
&= \lim_{\mu\to\infty} \frac{-\log\left(e^{C_i} C_i E_1(C_i)\right)}{\log\left(\mu\right)} \\
&= \lim_{\mu\to\infty} -\frac{C_i + \log\left(C_i\right) + \log\left(-\log\left(C_i\right)\right)}{\log\left(\mu\right)} = 1.
\end{aligned} \tag{C.20}$$

In the last equation, we have used the l'Hôpital's rule. As a result, by substituting (C.15) and (C.20) in (C.14), we find that the system provides full diversity, i.e., $G_d = R + 1$.

4 Simulation Results

In this section, we show numerical results of the analytical SER for binary phase shift keying (BPSK) modulation. We plot the performance curves in terms of average SER versus SNR of the transmitted signal (ε_T/N_0), where ε_T is the total transmitted power during two phases, i.e., $\varepsilon_T = \varepsilon_0 + \sum_{i=1}^{R} \varepsilon_i$. We use the block fading model and it is assumed that the relays and the destination have the same value of noise power ($N_i = N_0$). We assume all the source-relays and relays-destination links have unit-variance Rayleigh flat fading, i.e., $\sigma^2_{f_i} = \sigma^2_{g_i} = 1$, and the direct source-destination has doubled distance as source-relays link, which by assuming path loth exponent 2, $\sigma^2_{f_0} = 1/4$. Furthermore, we assume equal power allocation scheme, i.e., $\varepsilon_0 = R\,\varepsilon_i$, for $i = 1, \ldots, R$, which is a reasonable choice [7, 10].

Fig. C.1 confirms that the analytical SER expressions in Subsection

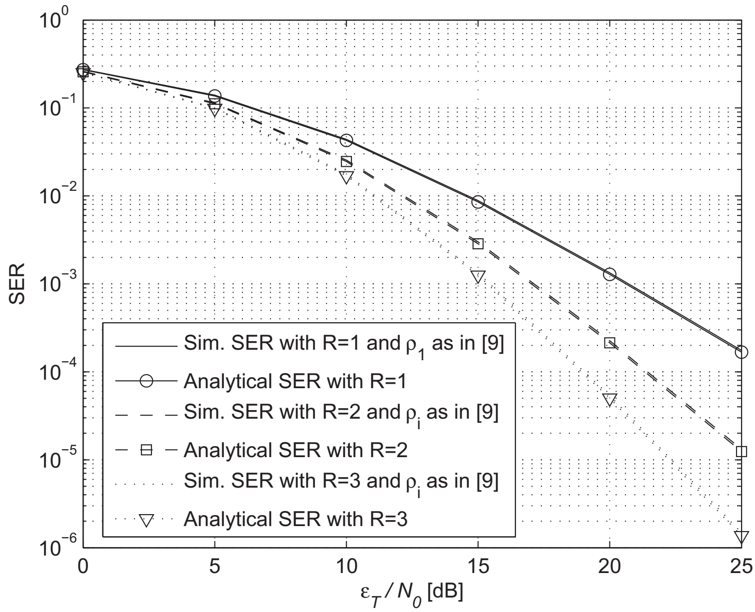

Fig. C.1: The average SER curves of relay networks employing repetition-based transmission with scaling factor in (C.4) and BPSK signals.

III-A for finding the average SER have similar performance as simulation result. We consider a network with $R = 1, 2, 3$ and we have averaged the error rate over 200 000 fading realization. The analytical results are based on (C.12).

5 Conclusion

Performance analyzes for AF cooperative networks with noncoherent relays over independent, non-identical, Rayleigh fading channels has been investigated. The closed-form expressions for the CDF, pdf, and MGF of the total received SNR at the destination have been derived. Then, we have computed the exact SER of a repetition-based cooperative network with R parallel relays and M-PSK signaling using the gain in (C.4). Using the asymptotic analysis of the SER expression, we have shown that this cooperative network achieves full diversity order $R+1$. Simulations are in accordance with analytic results.

References

[1] J. N. Laneman, D. Tse, and G. Wornell, "Cooperative diversity in wireless networks: Efficient protocols and outage behavior," *IEEE Trans. Inform. Theory*, vol. 50, no. 12, pp. 3062–3080, Dec. 2004.

[2] R. U. Nabar, H. Bölcskei, and F. W. Kneubuhler, "Fading relay channels: Performance limits and space-time signal design," *IEEE J. Sel. Areas Commun.*, vol. 22, no. 6, pp. 1099–1109, Aug. 2004.

[3] B. Maham and A. Hjørungnes, "Distributed GABBA space-time codes in amplify-and-forward cooperation," in *Proc. IEEE Information Theory Workshop (ITW'07)*, Bergen, Norway, Jul. 2007, pp. 189–193.

[4] K. Seddik, A. Sadek, A. Ibrahim, and K. Liu, "Design criteria and performance analysis for distributed space-time coding," *IEEE Trans. on Vehicular Technology*, vol. 57, no. 4, pp. 2280–2292, Jul. 2008.

[5] T. Wang, Y. Yao, and G. B. Giannakis, "Non-coherent distributed space-time processing for multiuser cooperative transmissions," *IEEE Trans. Wireless Commun.*, vol. 5, no. 12, pp. 3339–3343, Dec. 2006.

[6] P. A. Anghel and M. Kaveh, "Exact symbol error rate probability of a cooperative network in a Rayleigh-fading environment," *IEEE Trans. Wireless Commun.*, vol. 3, no. 5, pp. 1416–1421, Sep. 2004.

[7] A. Ribeiro, A. Cai, and G. B. Giannakis, "Symbol error probablity for general cooperative links," *IEEE Trans. Wireless Commun.*, vol. 4, no. 3, pp. 1264–1273, May 2005.

[8] T. Wang, A. Cano, G. B. Giannakis, and J. N. Laneman, "High-performance cooperative demodulation with decode-and-forward relays," *IEEE Trans. Commun.*, vol. 55, no. 6, pp. 830–841, Apr. 2007.

[9] D. Chen and J. N. Laneman, "Cooperative diversity for wireless fading channels without channel state information," in *Proc. Asilomar Conf. Signals, Systems, and Computers*, Monterey, CA, Nov. 2004.

[10] Y. Jing and B. Hassibi, "Distributed space-time coding in wireless relay networks," *IEEE Trans. Wireless Commun.*, vol. 5, no. 12, pp. 3524–3536, Dec. 2006.

[11] Y. Jing and H. Jafarkhani, "Using orthogonal and quasi-orthogonal designs in wireless relay networks," *IEEE Trans. Info. Theory*, vol. 53, no. 11, pp. 4106–4118, Nov. 2007.

[12] I. S. Gradshteyn and I. M. Ryzhik, *Table of Integrals, Series, and Products*. San Diego, USA: Academic, 1996.

[13] M. Abramowitz and I. A. Stegun, *Handbook of Mathematical Functions*. New York, USA: Dover Publications, 1972.

[14] M. R. Spiegel and J. Liu, *Schaum's Mathematical Handbook of Formulas and Tables*. United States: McGraw-Hill, 1998.

[15] M. K. Simon and M.-S. Alouini, *Digital Communication over Fading Channels: A Unified Approach to Performance Analysis*. New York, USA: Wiley, 2000.

[16] H. Jafarkhani, *Space-Time Coding Theory and Practice*. Cambridge, UK: Cambridge Academic Press, 2005.

Paper D

Asymptotic Performance Analysis of Amplify-and-Forward Cooperative Networks in a Nakagami-m Fading Environment

B. Maham and A. Hjørungnes

IEEE Communications Letters, volume 13, issue 5, pages 300-302, May 2009.

Abstract

This letter analyzes the performance of repetition-based cooperative wireless networks using *amplify-and forward* relaying. The network consists of a source, R parallel relays, and a destination, and the channel coefficients are distributed as independent, non-identical, Nakagami-m. The approximated average symbol error rate (SER) is investigated. For sufficiently large SNR, this letter derives a close-form average SER when m is an integer. The simplicity of the asymptotic results provides valuable insights into the performance of cooperative networks and suggests means of optimizing them. We also use simulation to verify the analytical results. Results show that the derived error rates are tight approximations particularly at medium and high SNR.

1 Introduction

Cooperative diversity networks technique is a promising solution for the high data-rate coverage required in future cellular and ad-hoc wireless communications systems. Cooperative transmissions have been categorized into space-time coded cooperation (see, e.g., [1, 2]) and repetition-based cooperation, in which relays retransmit the source's signal in a time-division multiple-access (TDMA) manner (see, e.g., [3–5]).

In [4], the authors derived asymptotic average symbol error rate (SER) for amplify-and-forward (AF) cooperative networks. An exact average SER analysis for a AF cooperative network is presented in [3]. An asymptotic analysis of the SER of a selection AF network over Rayleigh fading channels is studied in [6]. In [7], semianalytical lower-bounds of the outage probability of single-branch AF multihop wireless systems over Nakagami-m fading channels is evaluated. Authors in [8] derived the closed-form lower-bounds on the outage probability and SER of single-branch AF multihop wireless systems over Nakagami-m fading channels.

In this letter, we derive tight approximations for the average SER of repetition-based cooperative networks over independent non-identical Nakagami-m fading channels in AF mode. We first find the approximated expression for the average SER. For sufficiently high SNR, we derive a simple closed-form average SER expression for a network with multiple cooperating branches. We verify the obtained analytical results using simulations. Results show that the derived error rates are tight bounds particularly at medium and high SNR.

2 System Model

Consider a network consisting of a source, R relays, and one destination. We denote the source-to-destination, source-to-ith relay, and ith relay-to-destination links by h, f_i, and g_i, respectively (see [2, Fig. 1] for an illustration of the system model). Suppose each link has Nakagami-m fading, independent of the others. Similar to [9], our scheme requires two phases of transmission. During the first phase, the source node transmits a signal $s(n)$, where n is the time index, to *all* relays and the destination. The received signal at the destination and the ith relay from the source in the first phase can be written as

$$y_0(n) = \sqrt{\varepsilon_0}\, h\, s(n) + w_0(n), \tag{D.1a}$$
$$r_i(n) = \sqrt{\varepsilon_0} f_i s(n) + v_i(n), \tag{D.1b}$$

respectively, where ε_0 is the average total transmitted symbol energy of the source, since we assume $E\{\boldsymbol{s}^H \boldsymbol{s}\} = 1$, and $w_0(n)$ and $v_i(n)$ are complex zero-mean white Gaussian noises with variances N_0 and N_i, respectively. Under repetition-based amplify-and-forward cooperation, each relay scales its received signal with the scaling factor α_i. Then, the ith relay retransmits the scaled version of the received signal towards the destination in the ith interval of the second phase, i.e.,

$$y_i(n) = g_i\, \alpha_i\, r_i(n) + w_i(n), \tag{D.2}$$

where $w_i(n)$ is a complex zero-mean white Gaussian noise with variance N_0. To constrain transmit power at the relay, the scaling factor can be chosen as $\alpha_i = \sqrt{\frac{\varepsilon_i}{\varepsilon_0 |f_i|^2 + N_i}}$, where ε_i is the transmit power at relay *i*, such that all relays transmits with the same power.

Assuming maximum ratio combining (MRC) at the destination, the total received signal-to-noise ratio (SNR) can be written as

$$\gamma_d = \gamma_h + \sum_{i=1}^{R} \frac{\gamma_{f_i}\gamma_{g_i}}{\gamma_{f_i} + \gamma_{g_i} + 1}, \tag{D.3}$$

where $\gamma_h = |h|^2 \varepsilon_0 / N_0$, $\gamma_{f_i} = |f_i|^2 \varepsilon_0 / N_i$, and $\gamma_{g_i} = |g_i|^2 \varepsilon_i / N_i$.

3 Performance Analysis

3.1 Approximate SER Expression

In this subsection, we will derive a closed-form SER formula of AF repetition-based cooperative networks over Nakagami-m fading channels in the high SNR regime. This simple expression can also be used for a power allocation strategy among the cooperative nodes, or to get an insight on the diversity-multiplexing tradeoff of the system.

The total SNR in (D.3) can be upper-bounded as $\gamma_u = \gamma_h + \sum_{i=1}^{R} \gamma_i$, where $\gamma_i = \min\{\gamma_{f_i}, \gamma_{g_i}\}$ [3, 5].

The PDF of γ_h is as follows [10, Eq. (5.14)]

$$p_h(\gamma) = \frac{m_0^{m_0}\gamma^{m_0-1}}{\overline{\gamma}_h^{m_0}\Gamma(m_0)} e^{-\frac{m_0\gamma}{\overline{\gamma}_h}}, \tag{D.4}$$

where m_0 is the Nakagami-m fading parameter of h, $\Gamma(\cdot)$ is the gamma function, and $\overline{\gamma}_h = \mathbb{E}[\gamma_h]$.

In [11, Eq. (6)], the PDF of γ_i is derived as

$$p_i(\gamma) = \Bigg[\left(\frac{m_{f_i}}{\overline{\gamma}_{f_i}}\right)^{m_{f_i}} \gamma^{m_{f_i}-1} e^{-\frac{m_{f_i}\gamma}{\overline{\gamma}_{f_i}}} \Gamma\left(m_{g_i}, \frac{m_{g_i}}{\overline{\gamma}_{g_i}}\gamma\right) + \left(\frac{m_{g_i}}{\overline{\gamma}_{g_i}}\right)^{m_{g_i}} \gamma^{m_{g_i}-1} e^{-\frac{m_{g_i}\gamma}{\overline{\gamma}_{g_i}}} \Gamma\left(m_{f_i}, \frac{m_{f_i}}{\overline{\gamma}_{f_i}}\gamma\right)\Bigg] / [\Gamma(m_{f_i})\Gamma(m_{g_i})], \tag{D.5}$$

where $\Gamma(\alpha, x)$ is the incomplete gamma function of order α [12, Eq. (8.350)], $\overline{\gamma}_{f_i} = \mathbb{E}[\gamma_{f_i}]$, $\overline{\gamma}_{g_i} = \mathbb{E}[\gamma_{g_i}]$, m_{f_i} and m_{g_i} are the Nakagami-m fading parameters of f_i and g_i, respectively.

Now, we are deriving the SER expression for the repetition-based cooperative scheme with M-PSK signals. Averaging over conditional SER $P_e\left(R|h, \{\gamma_i\}_{i=1}^R\right) = Q\left(\sqrt{\rho\,\gamma_u}\right)$, where $\rho = 2\sin^2\left(\frac{\pi}{M}\right)$ and $Q(x) = 1/\sqrt{2\pi}\int_x^\infty e^{-u^2/2}\,du$, the average SER can be written as a $(R+1)$-folded integral given by [10, Eq. (9.9)]

$$P_e(R) = \int_{0;(R+1)-\text{fold}}^{\infty} P_e\left(R|h, \{\gamma_i\}_{i=1}^R\right) p_h(\gamma_h)\,d\gamma_h \prod_{i=1}^{R} (p_i(\gamma_i)\,d\gamma_i)\,. \tag{D.6}$$

The result of (D.6) can also be used to find the average SER for nonconstant modulus transmissions like M-ary amplitude modulation (M-AM) and M-QAM as indicated in [10, Eqs. (9.19) and (9.21)].

3.2 Asymptotic SER Expression

Now, we are going to derive a closed-form SER formula at the destination, which is valid in the high SNR regime. Before deriving the asymptotic expression, we present two lemmas.

Lemma 1 *Let the Nakagami-m fading parameters of channels be integer numbers, and $m_i \triangleq \min\{m_{f_i}, m_{g_i}\}$. The $(m_i - 1)$th order derivative of $p_i(\gamma)$*

with respect to γ at zero is computed as

$$\frac{\partial^{m_i-1}p_i}{\partial\gamma^{m_i-1}}(0)=\frac{m_i^{m_i}(m_i-1)!}{\Gamma(m_i)}\Lambda(m_i,\overline{\gamma}_{f_i},\overline{\gamma}_{g_i}). \tag{D.7}$$

where $\Lambda(m_i,\overline{\gamma}_{f_i},\overline{\gamma}_{g_i})$ is defined as

$$\Lambda(m_i,\overline{\gamma}_{f_i},\overline{\gamma}_{g_i})=\begin{cases}\overline{\gamma}_{f_i}^{-m_i}, & \text{if } m_{f_i}<m_{g_i}\\ \overline{\gamma}_{f_i}^{-m_i}+\overline{\gamma}_{g_i}^{-m_i}, & \text{if } m_{f_i}=m_{g_i}\\ \overline{\gamma}_{g_i}^{-m_i}, & \text{if } m_{f_i}>m_{g_i}\end{cases} \tag{D.8}$$

Furthermore, the nth ($n<m_i-1$) order derivatives of $p_i(\gamma)$ with respect to γ at zero are null.

Proof: *Using the definition of incomplete gamma function, we have $\Gamma(m_i,0)=\Gamma(m_i)$. Moreover, from [12, Eq. (8.356)], we have $\frac{-d\,\Gamma(\alpha,x)}{dx}=x^{\alpha-1}e^{-x}$. Thus, applying the chain rule for differentiating composite functions, the desired result in (D.7) is obtained. The second part of the lemma can straightforwardly be calculated using the same procedure given above.* □

Lemma 2 *Consider a finite set of nonnegative random variables $\mathcal{X}=\{X_0,X_1,\ldots,X_R\}$ whose (m_j-1)th order derivative PDFs p_j, $j=0,1,\ldots,R$, have nonzero values at zero. If the random variable Y is the sum of the components of the set $\mathcal{X}$, i.e. $Y=\sum_{j=0}^{R}X_i$, then all the derivatives of p_Y evaluated at zero up to order $\nu-1$, $\nu=\sum_{i=1}^{R}m_i+m_0-1$, are zero, while the ν-th order derivative is given by*

$$\frac{\partial^{\nu}p_{\gamma}}{\partial\gamma^{\nu}}(0)=\prod_{j=0}^{R}\frac{\partial^{m_j-1}p_j}{\partial\gamma^{m_j-1}}(0), \tag{D.9}$$

Proof: *As we are interested in the value at zero, we can use the initial value theorem of Laplace transforms [13] to arrive at (D.9). Since Y is the sum of $R+1$ independent random variables, we have $M_{\gamma}(s)=\prod_{j=0}^{R}M_j(s)$, where $M_{\gamma}(s)$ and $M_j(s)$, $j=0,1,\ldots,R$, are the Laplace transforms of $p_{\gamma}(\gamma)$ and $p_j(\gamma)$, $j=0,1,\ldots,R$, respectively.*

The Laplace transform of the νth order derivative of $p_{\gamma}(\gamma)$, where $\nu=\sum_{i=1}^{R}m_i+m_0-1$, can be computed as $s^{\nu}M_{\gamma}(s)-s^{\nu-1}p_{\gamma}(0)-\cdots-s\frac{\partial^{\nu-2}p_{\gamma}}{\partial\gamma^{\nu-2}}(0)-\frac{\partial^{\nu-1}p_{\gamma}}{\partial\gamma^{\nu-1}}(0)$ [13, Eq. (7.29)]. Using the initial value theorem, we have

$$\frac{\partial^{\nu}p_{\gamma}}{\partial\gamma^{\nu}}(0)=\lim_{s\to\infty}s^{\nu+1}M_{\gamma}(s), \tag{D.10}$$

where we have used that $p_\gamma(0) = \cdots = \frac{\partial^{\nu-2} p_\gamma}{\partial \gamma^{\nu-2}}(0) = \frac{\partial^{\nu-1} p_\gamma}{\partial \gamma^{\nu-1}}(0) = 0$*. Substituting* $M_\gamma(s)$ *as its equivalent representation based on* $M_j(s)$*, we can rewrite* (D.10) *as*

$$\frac{\partial^\nu p_\gamma}{\partial \gamma^\nu}(0) = \lim_{s\to\infty} \prod_{j=0}^{R} s^{m_j} M_j(s) = \prod_{j=0}^{R} \lim_{s\to\infty} s\, s^{m_j-1} M_j(s). \tag{D.11}$$

However, each of the limits in (D.11) *is precisely corresponding the* $(m_j - 1)$*th order PDF of* $p_j(\gamma)$*, evaluated at zero, from where we obtain* (D.9).

The fact that this limit is not infinite validates the assumption of considering $p_\gamma(0) = \cdots = \frac{\partial^{\nu-2} p_\gamma}{\partial \gamma^{\nu-2}}(0) = \frac{\partial^{\nu-1} p_\gamma}{\partial \gamma^{\nu-1}}(0) = 0$ *(using the initial value theorem,* $\frac{\partial^{k-1} p_\gamma}{\partial \gamma^{k-1}}(0) = \lim_{s\to\infty} s^k M_\gamma(s)$*,* $k \le \nu = \sum_{i=1}^{R} m_i + m_0 - 1$*, but if the limit with* $s^{\nu+1}$ *is finite, the limit with* s^k *should be* 0*) which completes the proof.* □

Asymptotic expression for the SER of the system under Nakagami-*m* fading is presented in the following theorem.

Theorem 1 *Suppose the relay network consisting of* R *relays with Nakagami-*m *fading channels, where* m *parameters are integer number. The SER of this system at high SNRs can be calculated as*

$$P_e \approx \frac{\Delta(R)}{\overline{\gamma}_h^m} \prod_{i=1}^{R} \Lambda(m_i, \overline{\gamma}_{f_i}, \overline{\gamma}_{g_i}), \tag{D.12}$$

where $\Lambda(m_i, \overline{\gamma}_{f_i}, \overline{\gamma}_{g_i})$ *is defined in* (D.8) *and*

$$\Delta(R) = \frac{c}{2\rho^{\nu+1}(\nu+1)!} \prod_{j=0}^{R} \frac{(m_j - 1)!\, m_j^{m_j}}{\Gamma(m_j)} \prod_{i=1}^{\nu+1} (2i-1) \tag{D.13}$$

where $\nu = \sum_{i=1}^{R} m_i + m_0 - 1$.

Proof: *To deduce the asymptotic behavior of the average SER (as* $\gamma \to \infty$*), we are using the approximate expression given in [14]. When the derivatives of* $p_\gamma(\gamma)$ *up to* ν*-th order are null at* $\gamma = 0$*, then the SER at high SNRs can be given by*

$$P_e \approx \frac{\prod_{i=1}^{\nu+1}(2i-1)}{2(\nu+1)\rho^{\nu+1}} \frac{c}{\nu!} \frac{\partial^\nu p_\gamma}{\partial \gamma^\nu}(0). \tag{D.14}$$

Applying Lemmas 1 and 2, (D.14) *can be rewritten as*

$$P_e \approx \frac{\prod_{i=1}^{\nu+1}(2i-1)}{2(\nu+1)\rho^{\nu+1}} \frac{c}{\nu!} \frac{\partial^{m_0-1} p_h}{\partial \gamma^{m_0-1}}(0) \prod_{i=1}^{R} \frac{\partial^{m_i-1} p_i}{\partial \gamma^{m_i-1}}(0). \tag{D.15}$$

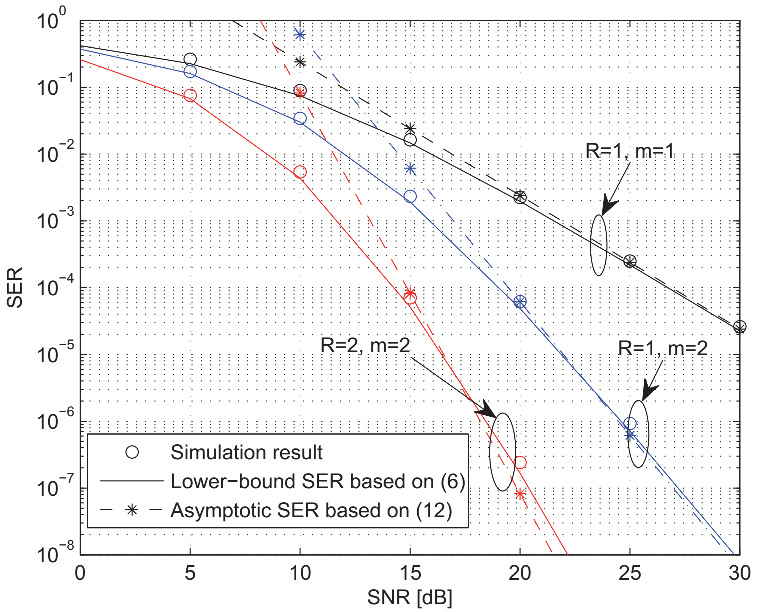

Fig. D.1: The average SER curves of relay networks employing repetition-based transmission with different relay number R and Nakagami-m, and using QPSK signals.

Furthermore, using (D.4), *it can be shown that*

$$\frac{\partial^{m_0-1} p_h(\gamma)}{\partial \gamma^{m_0-1}}(0) = \frac{m_0^{m_0}(m_0-1)!}{\Gamma(m_0)} \frac{1}{\overline{\gamma}_h^{m_0}}. \quad \text{(D.16)}$$

Combining (D.15)-(D.16) *and using Lemma 1,* (D.12) *is obtained.* □

4 Simulation Results

In this section, we show numerical results of the analytical SER for QPSK modulation. We plot the performance curves in terms of average SER versus the transmit SNR (ε_0/N_0). It is assumed that the relays and the destination have the same value of noise power ($N_i = N_0$) and all channels have the same value of m, i.e., $m_h{=}m_{f_i}{=}m_{g_i}$. We assume the network channels have Nakagami-m flat fading with parameter $m = 1, 2$. The source-relays and relays-destination links assumed to be equal, i.e., $\mathbb{E}[|f_i|^2] = \mathbb{E}[|g_i|^2] = 1$, and the direct source-destination has doubled distance of source-relays links, which by assuming path-loss exponent 3, $\mathbb{E}[|h|^2] = 1/8$. Furthermore, we assume equal power allocation scheme, i.e., $\varepsilon_0 = R\varepsilon_i$, for $i = 1, \ldots, R$, which is a reasonable choice [2, 4].

Fig. D.1 confirms that the analytical SER expressions in Section III for finding the average SER have similar performance as simulation result. We consider a network with $R = 1, 2$. One observe that the analytical result based on (6) approximates the simulated result with a good precision. Furthermore, we have sketched the asymptotic average SER derived in Theorem 1. It can be seen that the asymptotic expression well approximate the simulations in high SNR conditions.

5 Conclusion

Performance analysis for AF repetition-based cooperative networks over independent non-identical Nakagami-m fading channels have been investigated. The approximated average SER is obtained, when M-PSK modulation is employed. Moreover, we have derived a simple closed-form expression for the average SER in the high SNR regime when m is an integer, which is valid for any number of relays. Our numerical results show that derived SER expressions are tight bounds at medium and high SNR values.

References

[1] R. U. Nabar, H. Bölcskei, and F. W. Kneubuhler, "Fading relay channels: Performance limits and space-time signal design," *IEEE J. Sel. Areas Commun.*, vol. 22, no. 6, pp. 1099–1109, Aug. 2004.

[2] B. Maham, A. Hjørungnes, and G. Abreu, "Distributed GABBA space-time codes in amplify-and-forward relay networks," *IEEE Trans. Wireless Commun.*, vol. 8, no. 4, pp. 2036–2045, Apr. 2009.

[3] P. A. Anghel and M. Kaveh, "Exact symbol error rate probability of a cooperative network in a Rayleigh-fading environment," *IEEE Trans. Wireless Commun.*, vol. 3, no. 5, pp. 1416–1421, Sep. 2004.

[4] A. Ribeiro, A. Cai, and G. B. Giannakis, "Symbol error probablity for general cooperative links," *IEEE Trans. Wireless Commun.*, vol. 4, no. 3, pp. 1264–1273, May 2005.

[5] T. Wang, A. Cano, G. B. Giannakis, and J. N. Laneman, "High-performance cooperative demodulation with decode-and-forward relays," *IEEE Trans. Commun.*, vol. 55, no. 6, pp. 830–841, Apr. 2007.

[6] Y. Zhao, R. Adve, and T. J. Lim, "Symbol error rate of selection amplify-and-forward relay systems," *IEEE Comm. Letters*, vol. 10, no. 11, pp. 757–759, Nov. 2006.

[7] M. O. Hansa and M. S. Alouini, "Outage probability of multihop transmissions over Nakagami fading channels," *IEEE Commun. Letters*, vol. 7, no. 1, pp. 216–218, May 2003.

[8] G. K. Karagiannidis, "Performance bounds of multihop wireless communications with blind relays over generalized fading channels," *IEEE Trans. Wireless Commun.*, vol. 5, no. 3, pp. 498–503, Mar. 2006.

[9] J. N. Laneman, D. Tse, and G. Wornell, "Cooperative diversity in wireless networks: Efficient protocols and outage behavior," *IEEE Trans. Inform. Theory*, vol. 50, no. 12, pp. 3062–3080, Dec. 2004.

[10] M. K. Simon and M.-S. Alouini, *Digital Communication over Fading Channels: A Unified Approach to Performance Analysis*. New York, USA: Wiley, 2000.

[11] S. Ikki and M. H. Ahmed, "Performance analysis of cooperative diversity wireless networks over Nakagami-*m* fading channel," *IEEE Comm. Letters*, vol. 11, no. 4, pp. 334–336, Apr. 2007.

[12] I. S. Gradshteyn and I. M. Ryzhik, *Table of Integrals, Series, and Products*. San Diego, USA: Academic, 1996.

[13] C. L. Phillips and J. M. Parr, *Signals, System, and Transforms*. New Jersey, USA: Prentice Hall, Inc., 1999.

[14] Z. Wang and G. Giannakis, "A simple and general parameterization quantifying performance in fading channels," *IEEE Trans. Commun.*, vol. 51, no. 8, pp. 1389–1398, Aug. 2003.

Paper E

Performance Analysis of Amplify-and-Forward Opportunistic Relaying in Rician Fading

B. Maham and A. Hjørungnes

IEEE Signal Processing Letters, volume 16, issue 8, pages 643-646, August 2009.

Abstract

This letter analyzes the performance of single relay selection cooperative wireless networks using *amplify-and forward* relaying. The network channels are modeled as independent, non-identical, Rician distributed coefficients. We derive approximate formulas for the symbol error rate (SER) of the opportunistic relaying cooperative network. We first derive the PDF of the approximate value of the total SNR. Then, assuming M-PSK or M-QAM modulations, the PDF is used to determine the SER. For sufficiently large SNR, this letter derives the close-form average SER. The simplicity of the asymptotic results provides valuable insights into the performance of cooperative networks and suggests means of optimizing them. We also use simulation to verify the analytical results. Results show that the derived error rates are tight bounds particularly at medium and high SNR.

1 Introduction

Cooperative diversity networks technique is a promising solution for the high data-rate coverage required in future cellular and ad-hoc wireless communications systems. Several cooperation strategies with different relaying techniques, including amplify-and-forward (AF), decode-and-forward (DF), and selective relaying, have been studied in Laneman et al.'s seminal paper [1]. In [2], the authors derived asymptotic average symbol error rate (SER) for AF repetition-based cooperative networks. An exact average SER analysis for a AF cooperative network is presented in [3]. The performance analysis of AF-based space-time cooperation under Rayleigh fading is studied in [4].

In [5], an opportunistic relaying scheme is introduced. According to opportunistic relaying, a single relay among a set of R relay nodes is selected, depending on which relay provides for the *best* end-to-end path between source and destination. Performance and outage analysis of this relay selection scheme is studied in [6] and [7]. Also in [8], we analyzed the performance of AF opportunistic relaying networks over Rayleigh fading, when the relays have statistical CSI of the local source-relay channels.

In practice, the desired user often has a line-of-sight (LOS) to the receiver, therefore, this channel can be modeled as Rician fading. The presence of LOS has been confirmed through physical measurement for a number of applications, such as micro-cellular mobile and indoor radio. In contrast to the Rayleigh distribution, there are few performance results for wireless relay networks in these practical Rician fading conditions. Similar to [9], we have modeled the source-to-destination, source-to-relay, and relay-to-destination links as fixed LOS component and a randomly varying non-LOS component, which is often the case in cellular fixed relaying and wireless mesh networks.

In this letter, we derive tight approximations for the average SER of opportunistic relaying networks over independent non-identical Rician fading channels in AF mode. We first find the closed-form expressions for the cumulative distribution function (CDF) and the probability density function (PDF) of the total SNR. Then, the PDF is used to determine the lower and upper bounds. For sufficiently high SNR, we derive a simple closed-form average SER expression, for AF opportunistic relaying links with multiple cooperating branches. Based on the proposed approximated SER expression, it is shown that using AF opportunistic relaying over Rician fading channels, full-diversity can be obtained. We verify the obtained analytical results using simulations. Results show that the derived error rates are tight bounds particularly at medium and high SNR.

2 System Model

Consider a network consisting of a source, R relays, and one destination. We denote the source-to-destination, source-to-i-th relay, and i-th relay-to-destination links by h, f_i, and g_i, respectively. Suppose each link has Rician flat fading, independent of the others. Similar to [1], our scheme requires two phase of transmission. During the first phase, the source node transmits a signal $s(n)$, where n is the time index, to *all* relays and the destination. The received signal at the destination and the i-th relay from the source in the first phase can be written as

$$y_1(n) = \sqrt{\varepsilon_s} h\, s(n) + w_1(n), \tag{E.1a}$$

$$r_i(n) = \sqrt{\varepsilon_s} f_i s(n) + v_i(n), \tag{E.1b}$$

respectively, where ε_s is the average total transmitted symbol energy of the source, since we assume the information bearing symbols $s(n)$'s are normalized to one, and $w_1(n)$ and $v_i(n)$ are complex zero-mean white Gaussian noise vectors with variances N_0 and N_i, respectively.

In the second phase of transmission, we use an opportunistic relaying scheme. That is, the relay with the highest value of $\gamma_i = \min\{\gamma_{f_i}, \gamma_{g_i}\}$ is selected for retransmitting of the source's signal, where $\gamma_{f_i} = |f_i|^2\varepsilon_s/N_i$ is the instantaneous SNR between the source and i-th relay, and $\gamma_{g_i} = |g_i|^2\varepsilon_s/N_0$ is the instantaneous SNR between the i-th relay and destination.

The received signal at the destination in the second phase becomes

$$y_2(n) = g_{\max}\, \alpha\, r_{\max}(n) + w_2(n), \tag{E.2}$$

where the index $\max$ is indicating the selected relay and $w_2(n)$ is a complex zero-mean white Gaussian noise vector with the variance of N_0. The parameter $\alpha = \sqrt{\frac{\varepsilon_s}{\varepsilon_s|f_{\max}|^2+N_{\max}}}$ is the amplifying factor at the selected relay.

Assuming maximum ratio combining (MRC) between the received signals $y_1(n)$ and $y_2(n)$, the total SNR at the destination can be written as [2], [10]

$$\gamma_d = \gamma_h + \frac{\gamma_{f_{\max}}\gamma_{g_{\max}}}{\gamma_{f_{\max}} + \gamma_{g_{\max}} + 1}, \tag{E.3}$$

where $\gamma_h = |h|^2\varepsilon_s/N_0$.

3 Performance Analysis

3.1 Approximate SER Expression

In this subsection, we will derive the SER formula of the best relay selection strategy in AF mode over Rician fading channels.

The total SNR in (E.3) can be approximated by its upper bound (γ_b) as follows

$$\gamma_d \leq \gamma_b = \gamma_h + \gamma_{\max}, \tag{E.4}$$

where $\gamma_{\max} \triangleq \max\{\gamma_1, \gamma_2, \ldots, \gamma_R\}$ and $\gamma_i = \min\{\gamma_{f_i}, \gamma_{g_i}\}$. The approximate SNR value γ_b is analytically more tractable than the exact value in (E.3). This approximation is adopted in many recent papers (e.g., [5], [11], [12]) and it is shown to be accurate enough at medium and high SNR values.

The PDF of γ_h is as follows [13, Eq. (5.10)]

$$p_h(\gamma) = \frac{(K_0+1)}{\overline{\gamma}_h} e^{-\left[K_0+(K_0+1)\frac{\gamma}{\overline{\gamma}_h}\right]} I_0\left(2\sqrt{\frac{K_0(K_0+1)\gamma}{\overline{\gamma}_h}}\right), \tag{E.5}$$

where K_0 is the Rician factor of the source-destination link, which is defined as the ratio of the power in the LOS component to the power in the other (non-LOS) multipath components [13]. In (E.5), $I_0(\cdot)$ is the modified Bessel function of first kind and order zero, and $\overline{\gamma}_h = \mathbb{E}[\gamma_h]$ where $\mathbb{E}[\cdot]$ is the expectation operation.

In the following, we will derive the PDF of γ_i, which is required for calculating the average SER. Using the definition of the first-order Marcum Q-Function $Q_1(\cdot,\cdot)$ in [13, Eq. (4.10)], we find the CDF of γ_i as

$$\begin{aligned}\Pr(\gamma_i < \gamma) &= 1 - \Pr(\gamma_{f_i} > \gamma)\Pr(\gamma_{g_i} > \gamma)\\ &= 1 - Q_1\left(\sqrt{2K_{f_i}}, \sqrt{\frac{2(K_{f_i}+1)\gamma}{\overline{\gamma}_{f_i}}}\right) Q_1\left(\sqrt{2K_{g_i}}, \sqrt{\frac{2(K_{g_i}+1)\gamma}{\overline{\gamma}_{g_i}}}\right),\end{aligned} \tag{E.6}$$

where $\overline{\gamma}_{f_i} = \mathbb{E}[\gamma_{f_i}]$, $\overline{\gamma}_{g_i} = \mathbb{E}[\gamma_{g_i}]$, and K_{f_i} and K_{g_i} are the Rician factors of f_i and g_i, respectively. Thus, the PDF can be found by taking the derivative of (E.6) with respect to γ, yielding

$$p_i(\gamma) = \frac{d}{d\gamma}P(\gamma_i < \gamma) = Q_1\left(\sqrt{2K_{g_i}}, \sqrt{\frac{2(K_{g_i}+1)\gamma}{\overline{\gamma}_{g_i}}}\right) p_{f_i}(\gamma) + Q_1\left(\sqrt{2K_{f_i}}, \sqrt{\frac{2(K_{f_i}+1)\gamma}{\overline{\gamma}_{f_i}}}\right) p_{g_i}(\gamma), \quad \text{(E.7)}$$

where $p_{f_i}(\gamma)$ and $p_{g_i}(\gamma)$ are similar to $p_h(\gamma)$ in (E.5), with substituting $\overline{\gamma}_h$ for $\overline{\gamma}_{f_i}$ and $\overline{\gamma}_{g_i}$, respectively.

The conditional SER of the best relay selection system under AF mode with *R* relays can be written as $P_e\left(R \,|\, h, \{\gamma_i\}_{i=1}^{R}\right) = c\,Q\left(\sqrt{g\,\gamma_b}\right)$, where $Q(x) = 1/\sqrt{2\pi}\int_x^{\infty} e^{-u^2/2}\,du$ and the parameters c and g are represented as

$$c_{\text{QAM}} = 4\frac{\sqrt{M}-1}{\sqrt{M}}, c_{\text{PSK}} = 2, g_{\text{QAM}} = \frac{3}{M-1}, g_{\text{PSK}} = 2\sin^2\!\left(\frac{\pi}{M}\right).$$

For calculating the average SER, we need to find the PDF of $\gamma_{\max}$. Using the result from order statistics, and by assuming that all channel coefficients are independent of each other, the PDF of $\gamma_{\max}$ can be written as

$$p_{\max}(\gamma) = \sum_{i=1}^{R} p_i(\gamma) \prod_{\substack{j=1 \\ j\neq i}}^{R} \Pr\{\gamma_j \leq \gamma\}. \quad \text{(E.8)}$$

where $\Pr\{\gamma_j < \gamma\}$ and $p_i(\gamma)$ are derived in (E.6) and (E.7), respectively.

Now, we are deriving the SER expression for the selection relaying scheme discussed in Section II. Averaging over conditional SER, and by assuming that γ_h and $\gamma_{\max}$ are independent, the average SER would be

$$P_e(R) = \int_0^{\infty}\!\!\int_0^{\infty} P_e\!\left(R|h, \{\gamma_i\}_{i=1}^{R}\right) p_h(\gamma_h) p_{\max}(\gamma_{\max}) d\gamma_h d\gamma_{\max} = \int_0^{\infty}\!\!\int_0^{\infty} c\,Q\left(\sqrt{g\,\gamma_b}\right) p_h(\gamma_h) p_{\max}(\gamma_{\max})\, d\gamma_h\, d\gamma_{\max}. \quad \text{(E.9)}$$

Note that it is possible to obtain an upper-bound expression for the average SER, when we define $\hat{\gamma}_i = \frac{1}{2}\gamma_i = \frac{1}{2}\min\{\gamma_{f_i}, \gamma_{g_i}\}$. In this case, using

(E.8), the PDF of $\hat{\gamma}_{\max} \triangleq \max\{\hat{\gamma}_1, \hat{\gamma}_2, \ldots, \hat{\gamma}_R\}$ can be calculated as

$$\hat{p}_{\max}(\gamma) = 2\sum_{i=1}^{R} p_i(2\gamma)\prod_{\substack{j=1\\ j\neq i}}^{R}\Pr\{\gamma_j < 2\gamma\}. \tag{E.10}$$

Using (E.9) and (E.10), an upper-bound expression for SER is

$$P_e(R) \leq \int_0^{\infty}\int_0^{\infty} c\, Q\left(\sqrt{g\gamma_b}\right) p_h(\gamma_h)\hat{p}_{\max}(\hat{\gamma}_{\max}) d\gamma_h d\hat{\gamma}_{\max}. \tag{E.11}$$

3.2 Asymptotic SER Expression

Now, we are going to derive a closed-form SER formula at the destination, which is valid in high SNR regime. This simple expression can be used for a power allocation strategy among the cooperative nodes, or to get an insight on the diversity-multiplexing tradeoff of the system.

Using the series representation of $I_0(\cdot)$ in [14, Eq. (24.32)] and $Q_1(x, 0) = 1$, it can be shown that $\frac{d^n p_i}{d\gamma^n}(0)$, $n \in \mathbb{N}$, has a limited nonzero value. Therefore, using the chain rule, (E.8), and the fact that $\Pr\{\gamma_j < 0\} = 0$, it can be shown that

$$\frac{d^{R-1}p_{\max}}{d\gamma^{R-1}}(0) = R\prod_{j=1}^{R} p_j(0), \tag{E.12}$$

and $\frac{d^v p_{\max}}{d\gamma^v}(0) = 0$, for $v < R - 1$.

Before deriving the SER expression for high SNR values, the following lemma is needed.

Lemma 1 *All the derivatives of the PDF of γ_b, i.e., p_γ, evaluated at zero up to order $(R-1)$ are zero, while the R-th order derivative is given by*

$$\frac{\partial^R p_\gamma}{\partial\gamma^R}(0) = p_h(0)\,\frac{d^{R-1}p_{\max}}{d\gamma^{R-1}}(0). \tag{E.13}$$

Proof: *As we are interested in the value at zero, we can use the initial value theorem of Laplace transforms [15] to arrive at* (E.13). *Since γ_b is the sum of two independent random variables, we have $M_\gamma(s) = M_h(s)\, M_{\max}(s)$, where $M_h(s) = \mathbb{E}\{e^{s\gamma_h}\}$ and $M_{\max}(s) = \mathbb{E}\{e^{s\gamma_{\max}}\}$ are the Laplace transforms of $p_h(\gamma)$ and $p_{\max}(\gamma)$, respectively.*

The Laplace transform of R-th order derivative of $p_\gamma(\gamma)$ can be computed as $s^R M_\gamma(s) - s^{R-1} p_\gamma(0) - \cdots - s \frac{\partial^{R-2} p_\gamma}{\partial \gamma^{R-2}}(0) - \frac{\partial^{R-1} p_\gamma}{\partial \gamma^{R-1}}(0)$ [15, Eq. (7.29)]. Using the initial value theorem, we have

$$\frac{\partial^R p_\gamma}{\partial \gamma^R}(0) = \lim_{s\to\infty} s\left(s^R M_\gamma(s)\right), \tag{E.14}$$

where we have used that $p_\gamma(0) = \cdots = \frac{\partial^{R-2} p_\gamma}{\partial \gamma^{R-2}}(0) = \frac{\partial^{R-1} p_\gamma}{\partial \gamma^{R-1}}(0) = 0$. Substituting $M_\gamma(s)$ as its equivalent representation based on $M_h(s)$ and $M_{\max}(s)$, we can rewrite (E.14) *as*

$$\frac{\partial^R p_\gamma}{\partial \gamma^R}(0) = \lim_{s\to\infty} s^{R+1} M_h(s)\, M_{\max}(s) \tag{E.15}$$

However, $\lim_{s\to\infty} s M_h(s) = p_h(0)$ and $\lim_{s\to\infty} s^R M_{\max}(s) = \dfrac{\partial^{R-1} p_{\max}}{\partial \gamma^{R-1}}(0)$, from where we obtain (E.13).
The fact that this limit is not infinite validates the assumption of considering $p_\gamma(0) = \cdots = \frac{\partial^{R-2} p_\gamma}{\partial \gamma^{R-2}}(0) = \frac{\partial^{R-1} p_\gamma}{\partial \gamma^{R-1}}(0) = 0$ (using the initial value theorem, $\frac{\partial^{v-1} p_\gamma}{\partial \gamma^{v-1}}(0) = \lim_{s\to\infty} s^v M_\gamma(s)$, $v \le R$, but if the limit with s^{R+1} is finite, the limit with s^v should be 0) which completes the proof. □

Asymptotic expression for the average SER of the selection relaying system under Rician fading is presented in the following theorem.

Theorem 1 *Suppose the relay network consisting of R relays with Rician fading channels with the parameter K. The average SER of the system described in Section II at high SNRs can be approximated by*

$$P_e \approx \Omega(R) \frac{(K_0+1)}{\overline{\gamma}_h e^{K_0}} \prod_{r=1}^{R} \left(\frac{K_{f_r}+1}{\overline{\gamma}_{f_r} e^{K_{f_r}}} + \frac{K_{g_r}+1}{\overline{\gamma}_{g_r} e^{K_{g_r}}} \right), \tag{E.16}$$

where

$$\Omega(R) = \frac{R}{2g^{R+1}(R+1)!} \prod_{r=1}^{R+1} (2r-1). \tag{E.17}$$

Proof: *To deduce the asymptotic behavior of the average SER (as $\gamma \to \infty$), we are using the approximate expression given in [16]. When the derivatives of $p_\gamma(\gamma)$ up to the kth order are null at $\gamma = 0$, where k is an integer number, then the SER at high SNRs can be approximated using the McLaurin series* *of* $p_\gamma(\gamma)$ *as follows*

$$P_e \approx \frac{\prod_{i=1}^{k+1}(2i-1)}{2(k+1)g^{k+1}}\frac{1}{k!}\frac{\partial^k p_\gamma}{\partial \gamma^k}(0), \tag{E.18}$$

where $\frac{\partial^k p_\gamma}{\partial \gamma^k}(0)$ *is the* k*th order derivative of the PDF of the equivalent channel, and the derivatives of* $p_\gamma(\gamma)$ *up to order* $(k-1)$ *are supposed to be zero. Applying Lemma 1 and* (E.12)*, we have*

$$P_e \approx \frac{\prod_{i=1}^{R+1}(2i-1)}{2(R+1)g^{R+1}}\frac{1}{(R-1)!}p_h(0)\prod_{r=1}^{R}p_i(0). \tag{E.19}$$

Furthermore, from (E.5) *and* (E.7) *we have* $p_h(0) = \frac{(K_0+1)}{\overline{\gamma}_h}e^{-K_0}$ *and* $p_i(0) = e^{-K_{f_i}}\frac{(K_{f_i}+1)}{\overline{\gamma}_{f_i}} + e^{-K_{g_i}}\frac{(K_{g_i}+1)}{\overline{\gamma}_{g_i}}$*. By replacing* $p_h(0)$ *and* $p_i(0)$ *in* (E.19)*, the result given in* (E.16) *is obtained.* □

A tractable definition of the diversity gain is [17, Eq. (1.19)] $G_d = -\lim_{\mu\to\infty}\frac{\log(P_e(R))}{\log(\mu)}$, where μ denotes the transmit SNR. Now, we replace the asymptotic average SER obtained in (E.16), and by the fact that $\overline{\gamma}_{f_i} = \mu\,\mathbb{E}[|f_i|^2]$ and $\overline{\gamma}_{g_i} = \mu\,\mathbb{E}[|g_i|^2]$, it is easy to show that the diversity order G_d becomes $R+1$.

By defining the coding gain as the reduction in the required SNR to achieve a specified BER (see [17, page 49]), we have the following corollary:

Corollary 2 *Opportunistic relaying provides the same diversity gain as repetition-based cooperation and the coding gain in high SNR of* R *times less, while providing multiplexing gain of* $(R+1)/2$ *over repetition-based cooperation.*

Proof: *In [2, Proposition 2], it is shown that for a finite set of nonnegative random variables* $\{\gamma_1, \gamma_2, \ldots, \gamma_m\}$ *whose PDFs* $p_1, p_2, \ldots, p_m$ *have nonzero values at zero, and* $\gamma = \sum_{i=1}^{m}\gamma_i$*, all the derivatives of* $p_\gamma(\gamma)$ *evaluated at zero up to order* $(m-2)$ *are zero, while the* $(m-1)$*th order derivative is given by*

$$\frac{\partial^{m-1}p_\gamma}{\partial\gamma^{m-1}}(0) = \prod_{i=1}^{m}p_i(0). \tag{E.20}$$

Using [2, Proposition 2] and (E.18)*, we get an asymptotic expression for the average SER of repetition-based cooperation under Rician channels as*

$$P_e \approx \frac{\Omega(R)}{R}\frac{(K_0+1)}{\overline{\gamma}_h e^{K_0}}\prod_{r=1}^{R}\left(\frac{K_{f_r}+1}{\overline{\gamma}_{f_r}e^{K_{f_r}}} + \frac{K_{g_r}+1}{\overline{\gamma}_{g_r}e^{K_{g_r}}}\right). \tag{E.21}$$

By comparing (E.21) *with* (E.16) *and* (E.17), *we find that selection relaying provides the same diversity gain as the repetition-based cooperation and the coding gain of R times less.*

On the other hand, the opportunistic relaying described in Section II has two phases of transmission with equal time slots, while the repetition-based cooperation, in which each relay retransmit the source data in a TDMA manner, requires $R+1$ phases of transmission. This means that the spectral efficiency of the opportunistic relaying system is $(R+1)/2$ times higher than a repetition-based cooperation network. □

4 Simulation Results

In this section, we show numerical results of the analytical SER for QPSK modulation. We plot the performance curves in terms of average SER versus the transmit SNR (ε_s/N_0). We use the block fading model and it is assumed that the relays and the destination have the same value of noise power ($N_i = N_0$). We assume all the network channels have Rician flat fading with parameter $K_0 = K_{f_i} = K_{g_i} = 1$. The source-relays and relays-destination links assumed to be equal, i.e., $\mathbb{E}[|f_i|^2] = \mathbb{E}[|g_i|^2] = 1$, and the direct source-destination has doubled distance of source-relays links, which by assuming path loth exponent 3, $\mathbb{E}[|h|^2] = 1/8$. Furthermore, we assume equal power allocation in two phases, which is a reasonable choice [2, 18].

Fig. E.1 confirms that the analytical SER expressions in Subsection III-A for finding the average SER have similar performance as simulation results. We consider a network with $R = 1, 2, 3, 4$. One observe that the analytical result based on (E.9) approximates the simulated results with a good precision. The difference between the analytical result and the simulated results comes from the upper-bound expression in (E.4) for the received SNR. Furthermore, we have sketched the asymptotic average SER derived in Theorem 1. It can be seen that the asymptotic expression well approximates the simulations in high SNR conditions. The quality of the approximation decreases when the number of cooperating terminals increases, a reasonable result due to the accumulation of approximations. In addition, Fig. E.1 shows an upper-bound for the average SER, which is obtained by substituting $\hat{p}_{\max}(\gamma)$ in (E.10) into (E.9). Moreover, in Fig. E.1, we compare the asymptotic SER of repetition-based cooperation derived in (E.21) with the AF opportunistic relaying. As stated in Corollary 1, repetition-based cooperation obtain $\log(R)$ dB coding gain in high SNR

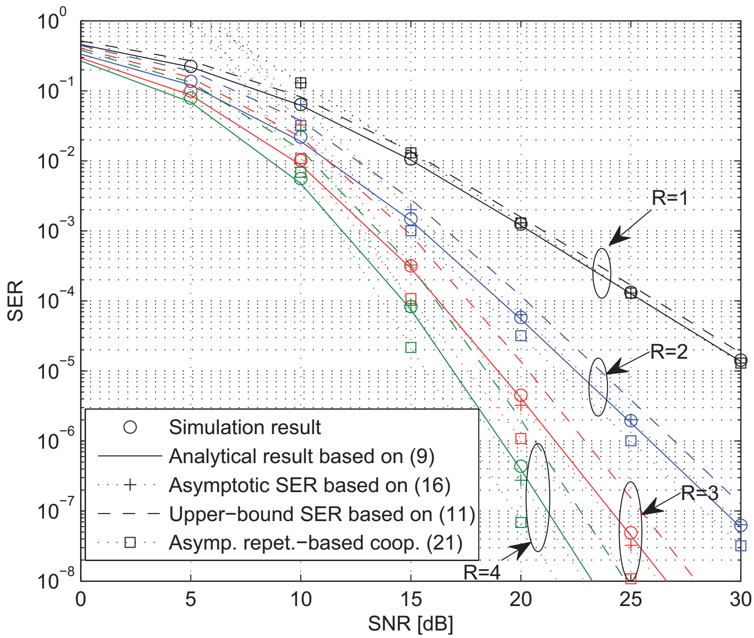

Fig. E.1: Performance comparison of AF opportunistic relaying with different relay number R in Rician fading with the parameter $K_0 = K_{f_i} = K_{g_i} = 1$ and using QPSK signals.

compared to opportunistic relaying in expense of $(R+1)/2$ less multiplexing gain.

5 Conclusion

Performance analysis for opportunistic relaying networks over independent non-identical Rician fading channels have been investigated. The total SNR is approximated by its lower and upper bounds. Then, closed-form expressions for the CDF and PDF of the approximate total SNR have been derived. The PDF is used to determine the approximate average SER, when M-PSK or M-QAM modulations are employed. Moreover, we have derived the simple closed-form solution for the average SNR in high SNR scenarios, which is valid for any number of relays. Our numerical results show that derived SER expressions are tight bounds particularly at medium and high SNR values.

References

[1] J. N. Laneman, D. Tse, and G. Wornell, “Cooperative diversity in wireless networks: Efficient protocols and outage behavior,” *IEEE Trans. Inform. Theory*, vol. 50, no. 12, pp. 3062–3080, Dec. 2004.

[2] A. Ribeiro, A. Cai, and G. B. Giannakis, “Symbol error probablity for general cooperative links,” *IEEE Trans. Wireless Commun.*, vol. 4, no. 3, pp. 1264–1273, May 2005.

[3] P. A. Anghel and M. Kaveh, “Exact symbol error rate probability of a cooperative network in a Rayleigh-fading environment,” *IEEE Trans. Wireless Commun.*, vol. 3, no. 5, pp. 1416–1421, Sep. 2004.

[4] B. Maham and A. Hjørungnes, “Distributed GABBA space-time codes in amplify-and-forward cooperation,” in *Proc. IEEE Information Theory Workshop (ITW’07)*, Bergen, Norway, Jul. 2007, pp. 189–193.

[5] A. Bletsas, A. Khisti, D. P. Reed, and A. Lippman, “A simple cooperative method based on network path selection,” *IEEE Journal on Selected Areas in Communications*, vol. 24, no. 3, pp. 659–672, Mar. 2006.

[6] A. Bletsas, H. Shin, and M. Win, “Outage optimality of amplify-and-forward opportunistic relaying,” *IEEE Comm. Letters*, vol. 11, no. 3, pp. 261–263, Mar. 2007.

[7] Y. Zhao, R. Adve, and T. J. Lim, “Symbol error rate of selection amplify-and-forward relay systems,” *IEEE Comm. Letters*, vol. 10, no. 11, pp. 757–759, Nov. 2006.

[8] B. Maham and A. Hjørungnes, “Opportunistic relaying through amplify-and-forward distributed space-time codes with partial statistical CSI at relays,” in *the Allerton Conference on Communication,*

Control, and Computing (Allerton'08), Monticello, IL, USA, Sep. 23-27, 2008.

[9] O. Oyman, J. N. Laneman, and S. Sandhu, "Multihop relaying for broadband wireless mesh networks: From theory to practice," *IEEE Communications Magazine*, vol. 45, no. 11, pp. 116–122, Nov. 2007.

[10] M. O. Hansa and M.-S. Alouini, "Optimal power allocation for relayed transmissions over Rayleigh-fading channels," *IEEE Trans. Wireless Commun.*, vol. 3, no. 6, pp. 1999–2004, Nov. 2004.

[11] T. Wang, A. Cano, G. B. Giannakis, and J. N. Laneman, "High-performance cooperative demodulation with decode-and-forward relays," *IEEE Trans. Commun.*, vol. 55, no. 6, pp. 830–841, Apr. 2007.

[12] S. Ikki and M. H. Ahmed, "Performance analysis of cooperative diversity wireless networks over Nakagami-*m* fading channel," *IEEE Comm. Letters*, vol. 11, no. 4, pp. 334–336, Apr. 2007.

[13] M. K. Simon and M.-S. Alouini, *Digital Communication over Fading Channels: A Unified Approach to Performance Analysis*. New York, USA: Wiley, 2000.

[14] M. R. Spiegel and J. Liu, *Schaum's Mathematical Handbook of Formulas and Tables*. United States: McGraw-Hill, 1998.

[15] C. L. Phillips and J. M. Parr, *Signals, System, and Transforms*. New Jersey, USA: Prentice Hall, Inc., 1999.

[16] Z. Wang and G. Giannakis, "A simple and general parameterization quantifying performance in fading channels," *IEEE Trans. Commun.*, vol. 51, no. 8, pp. 1389–1398, Aug. 2003.

[17] H. Jafarkhani, *Space-Time Coding Theory and Practice*. Cambridge, UK: Cambridge Academic Press, 2005.

[18] Y. Jing and B. Hassibi, "Distributed space-time coding in wireless relay networks," *IEEE Trans. Wireless Commun.*, vol. 5, no. 12, pp. 3524–3536, Dec. 2006.

Paper F

Power Allocations in Minimum-Energy SER Constrained Cooperative Networks

B. Maham, A. Hjørungnes, and M. Debbah

Special issue on Cognitive Radio, *Annals of Telecommunications - Annales des Télécommunications*, vol. 64, no. 7, pp. 545-555, Aug. 2009 (ISI impact factor: 0.206; Published by Institut Telecom and Springer; Indexed in ISI and Scopus databases).

Abstract

In this paper, we propose minimum power allocation strategies for repetition-based amplify-and-forward (AF) relaying, given a required symbol error rate (SER) at the destination. We consider the scenario where one source and multiple relays cooperate to transmit messages to the destination. We derive the optimal power allocation strategy for two-hop AF cooperative network that minimizes the total relay power subject to the SER requirement at the destination. Two outstanding features of the proposed schemes are that the power coefficients have a simple solution and are independent of knowledge of instantaneous channel state information (CSI). We further extend the SER constraint minimum power allocation to the case of multi-branch, multihop network, and derive the closed-form solution for the power control coefficients. For the case of power-limited relays, we propose two iterative algorithms to find the power coefficients for the SER constraint minimum-energy cooperative networks. However, these power minimization strategy does not necessarily maximize the lifetime of battery-limited systems. Thus, we propose two other AF cooperative schemes which consider the residual battery energy, as well as the statistical CSI, for the purpose of lifetime maximization. Simulations show that the proposed minimum power allocation strategies could considerably save the total transmitted power compared to the equal transmit power scheme.

This article is removed.

Paper G

Energy-Efficient Space-Time Coded Cooperative Routing in Multihop Wireless Networks

B. Maham, R. Narasimhan, and A. Hjørungnes

Proc. of IEEE Global Telecommunications Conference (GLOBECOM 2009), Honolulu, Hawaii, USA, November - December 2009.

Abstract

Due to the limited energy supplies of nodes in many applications like wireless sensor networks, energy efficiency is crucial for extending the lifetime of these networks. This paper addresses the routing problem for outage-restricted multihop wireless ad hoc networks based on cooperative transmission. The source node wants to transmit messages to a single destination. Other nodes in the network may operate as relay nodes. In this paper, a new cooperative routing protocol is introduced using the Alamouti space-time code for the purpose of energy savings, given a required outage probability at the destination. Two efficient power allocation schemes are derived, which depend only on the statistics of the channels. In the first scheme, each node needs to know only the local channel statistics, and can be implemented in a distributed manner. In the second scheme, a centralized power control strategy is proposed, which has a higher energy efficiency, at the expense of more complexity and signalling overhead. Compared to non-cooperative multihop routing, an energy saving of 80% is achievable in line networks with 3 relays and an outage probability constraint of 10^{-3} at the destination.

1 Introduction

Energy consumption in multihop wireless networks is a crucial issue that needs to be addressed at all the layers of a communication system, from the hardware up to the application. The focus of this paper is on energy efficiency when messages may be transmitted via multiple radio hops. After substantial research efforts in the last several years, routing for multihop wireless networks is broadly investigated problem [1, 2]. Nevertheless, with the emergence of new multiple-antennas technologies, existing routing solutions in the traditional radio transmission model are no longer efficient. For instance, it is feasible to *coordinate* the simultaneous transmissions from multiple transmitters to one receiver simultaneously. As a result, simultaneous transmitter signals from several different nodes to the same receiver are not considered a collision, but instead could be combined at the receiver to obtain stronger signal. In [3], the concept of multihop diversity is introduced where the benefits of spatial diversity are achieved from the concurrent reception of signals that have been transmitted by multiple previous terminals along the single primary route. This scheme exploits the broadcast nature of wireless networks where the communications channel is shared among multiple terminals. On the other hand, the routing problem in the cooperative radio transmission model over static channels is studied in [4], where it is allowed that multiple nodes along a path coordinate together to transmit a message to the next hop as long as the combined signal at the receiver satisfies a given SNR threshold value. In [4], it is assumed that transmitting nodes adjust their phases in such a way that the coherent reception of signals at the receiving node is possible. However, the knowledge of the instantaneous channels at the transmitting nodes is difficult to realize.

In this paper, a cooperative multihop routing scheme is proposed for Rayleigh fading channels. The investigated system can achieve considerable energy savings compared to non-cooperative multihop transmission, when there is an outage probability quality-of-service (QoS) requirement at the destination node. Two power control schemes, i.e., *distributed* and *centralized* power allocations are derived to minimize the total transmission power given the outage probability constraint. Using some tight approximations, simple closed-form power allocations are presented without requiring the knowledge of instantaneous channel state information (CSI);

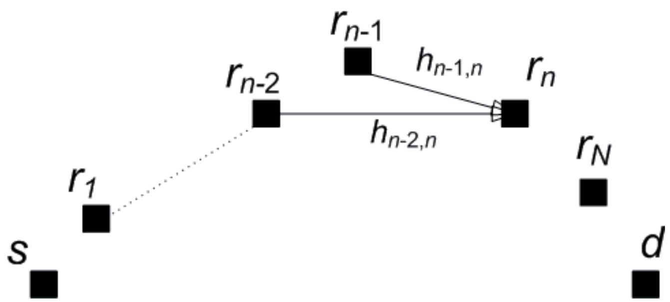

Fig. G.1: Wireless multihop network with space-time coded cooperative routing.

hence, the proposed schemes can be implemented in real wireless systems. Numerical results show that the proposed power allocation strategies provide considerable gains compared to non-cooperative multihop transmission.

The remainder of this paper is organized as follows. In Section II, the system model is given. The formulation of link costs based on a per-hop outage probability constraint for distributed power control is presented in Section III. In Section IV, the end-to-end outage probability is used to formulate the minimum energy link costs for centralized power control. In Section V, the overall performance of the system is presented for classical line networks. Finally, the conclusion is presented in Section VI.

2 System Model and Protocol Description

Consider a wireless communication scenario where the source node s transmits information to the destination node d with the assistance of

N intermediate relays (see Fig. G.1). Due to the broadcast nature of the wireless channel, some relays can overhear the transmitted information, and thus, can cooperate with the source to send its data. The wireless link between any two nodes in the network is modeled as a Rayleigh fading narrowband channel. For medium access, the relays are assumed to transmit over orthogonal channels, thus, no inter-relay interference is considered in the signal model. As in [4], each transmission is either a broadcast transmission where a single node transmits the information that is received by multiple nodes, or a cooperative transmission where multiple nodes simultaneously send the information to a single receiver.

The cooperation protocol has $N+1$ phases, where each phase consists of two time slots. The signals transmitted by the source terminal during the first and second time slots of Phase 1 are denoted as $s_1(t)$ and $s_2(t)$, respectively. In the following, symbol-by-symbol transmission is considered such that the time index t can be dropped; hence, s_1 and s_2 are the symbols transmitted in the first and second time slots, respectively, where $\mathbb{E}\{s_i\} = 0$ and $\mathbb{E}\{|s_i|^2\} = 1$ for $i = 1, 2$. The data symbols may be chosen from a complex- valued finite constellation such as quadrature amplitude modulation (QAM) or from a Gaussian codebook. In Phase 1, the source transmits the information, and the signal received at the first selected node in the first two time slots is given by

$$y_{1,i} = \sqrt{P_{0,1}}\, h_{0,1} s_i + v_{1,i}, \text{ for } i = 1, 2, \tag{G.1}$$

where $P_{0,1}$ is the average transmitted symbol energy of the source during the first phase (since the information symbols s_i's have zero mean and unit variance) and $v_{1,i}$ denotes complex zero-mean white Gaussian noise with variance $\mathcal{N}_0$. The channel coefficients from Node j to Node k $h_{j,k}$, $j = 0, 1, \ldots, N$, $k = 1, 2 \ldots, N+1$, are complex Gaussian random variables with zero-mean and variances $\sigma^2_{j,k}$, where Node $(N+1)$ node is the destination node d. We assume coherence times of the channels are such that channel coefficients $h_{j,k}$ are not varying during two consecutive time slots.

In contrast to [4] where transmitters are able to adjust their phases, in this paper, the *instantaneous CSI* is not known at the transmitter nodes. This assumption is realistic for most wireless systems. Therefore, space-times codes are the appropriate choice to achieve the spatial diversity gain. The Alamouti space-time code is used for this purpose. In Phase 2, relay nodes are sorted based on their received SNR, such that Relay 1 has the highest received SNR. Then, in Phase n, $2 \le n \le N+1$, the previous two nodes transmit their signals toward the next node using the Alamouti code structure [5], with a simple power allocation. Thus, the received signal at the nth receiving node in Phase n is $\boldsymbol{y}_n = [y_{n,1}, y_{n,2}]^T$, which is given by

$$\boldsymbol{y}_n = \boldsymbol{S}_n \boldsymbol{\Lambda}_n \boldsymbol{h}_n + \boldsymbol{v}_n, \tag{G.2}$$

for $n = 2, \ldots, N, N+1$, where $\boldsymbol{h}_n = [h_{n-2,n}, h_{n-1,n}]^T$, $\boldsymbol{\Lambda}_n = \begin{bmatrix} P_{n-2,n} & 0 \\ 0 & P_{n-1,n} \end{bmatrix}$, and $P_{n-i,n}$, $i = 1, 2$, is the average transmit power of node $n - i$ during the ith time slot of Phase n. In (G.2), $\boldsymbol{S}_n$ is given by

$$\boldsymbol{S}_n = \begin{bmatrix} \hat{s}_{n-2,1} & \hat{s}_{n-1,2} \\ -\hat{s}^*_{n-2,2} & \hat{s}^*_{n-1,1} \end{bmatrix}, \tag{G.3}$$

in which $\hat{s}_{n,i}$ is the re-encoded symbol of s_i at the nth relay. Note that in the first stage of Alamouti transmission, we have $\hat{s}_{0,i} = s_i$.

It is assumed that all hops use the total bandwidth W. The objective of the system is the reliable delivery of symbols generated at the source node s at a bandwidth-normalized rate (henceforth just called the rate of R bits per second per Hertz, i.e., RW bits per second) to the destination node by consuming the least total transmit power. To achieve the end-to-end rate R, it is obvious that all hops should guarantee the rate R.

The rate r_1 achieved at the first hop is

$$r_1 = \frac{1}{N+1} \log\left(1 + \frac{P_{0,1}|h_{0,1}|^2}{\mathcal{N}_0 W}\right), \tag{G.4}$$

and from (G.2) the rate r_n achieved at hop $n = 2, \ldots, N+1$ is

$$r_n = \frac{1}{N+1} \log\left(1 + \sum_{i=1}^{2} \frac{P_{n-i,n}|h_{n-i,n}|^2}{\mathcal{N}_0 W}\right), \tag{G.5}$$

where it is assumed that $\hat{s}_{n-2,1} = \hat{s}_{n-1,1} = s_1$ and $\hat{s}_{n-2,2} = \hat{s}_{n-1,2} = s_2$. In the sequel, the outage probability $\rho_{n-1,n} \triangleq \Pr\{r_n < R\}$ of the nth receiving node in hop n is investigated, which describes the probability that the transmit rate R is greater than the supported rate r_n. This probability expressed as a cumulative distribution function (CDF) and depends on the fixed transmission parameters and the channel condition within the hops. By defining $\gamma_{\text{th}} \triangleq (2^{R(N+1)} - 1)\mathcal{N}_0 W$, the outage probability can be represented as

$$\rho_{n-1,n} = \Pr\left\{\sum_{i=1}^{2} P_{n-i,n}|h_{n-i,n}|^2 < \gamma_{\text{th}}\right\}, \tag{G.6}$$

for $n = 1, 2 \ldots, N+1$, where $P_{-1,1} = 0$.

3 Distributed Per-Hop Outage Constrained Link Cost Formulation

In this section, we derive the required power for the direct (non-cooperative) and cooperative transmission modes in order to achieve a certain rate R. Two distinct cases described as follows are considered to derive explicit expressions for the link costs.

3.1 Non-Cooperative Multihop Link Cost

First, consider the non-cooperative case where only one node is transmitting within a time slot to a single receiving node. The transmitter node should decide the value of its transmit power $P_{n-1,n}$ to satisfy the target rate R with a target outage probability of ρ_0 at each hop. The per-hop outage probability constraint is used for distributed power allocation. The receiver can correctly decode the source data whenever $P_{n-i,n}|h_{n-i,n}|^2 \geq \gamma_{\text{th}}$. Hence, the probability of correct detection for each hop is

$$1 - \rho_0 = \Pr\left\{|h_{n-1,n}|^2 \geq \frac{\gamma_{\text{th}}}{P_{n-1,n}}\right\} = e^{\frac{-\gamma_{\text{th}}}{P_{n-1,n}\,\sigma^2_{n-1,n}}}. \tag{G.7}$$

Therefore, the required transmit power can be calculated as

$$P_{n-1,n} = \frac{-\gamma_{\text{th}}}{\sigma^2_{n-1,n}\ln(1-\rho_0)}. \tag{G.8}$$

Now, assume a connection from the source node to the destination via N intermediate nodes. For decoding the message reliably, the outage probability must be less than the desired end-to-end outage probability $\rho_{\max}$. The probability of correct end-to-end reception is

$$P_c(N) = \prod_{n=1}^{N+1} \Pr\left\{|h_{n-1,n}|^2 \geq \frac{\gamma_{\text{th}}}{P_{n-1,n}}\right\} = \prod_{n=1}^{N+1} e^{\frac{-\gamma_{\text{th}}}{P_{n-1,n}\sigma^2_{n-1,n}}}. \tag{G.9}$$

Thus, in the multihop case, a target outage probability $\rho_0 = 1 - \sqrt[N+1]{1-\rho_{\max}}$ is required at each hop. Since $\ln(1-\rho_{\max}) = (N+1)\ln(1-\rho_0)$, the total power for transmitting two symbols, and hence, the non-cooperative multihop link cost is given by

$$P_T(\text{non-coop}) = \sum_{n=1}^{N+1} 2\,\mathcal{C}(n-1,n) = \sum_{n=1}^{N+1} \frac{-2\,\gamma_{\text{th}}\,(N+1)}{\sigma^2_{n-1,n}\ln(1-\rho_{\max})}, \tag{G.10}$$

where $\mathcal{C}(n-1,n)$ is the point-to-point link cost when the $(n-1)$th node transmits to the nth node, which is given in (G.8).

3.2 Cooperative Multihop Link Cost

In this case, from (G.8) the source node transmits with the power $P_{0,1} = \frac{-\gamma_{\text{th}}}{\sigma^2_{0,1}\ln(1-\rho_0)}$ during the first phase. In Phase n, $n = 2, \ldots, N+1$, a set of *two* nodes $\text{Tx}_n = \{\text{tx}_{n,1}, \text{tx}_{n,2}\}$ cooperate to transmit the source's information to a *single* receiver node rx_n, using the Alamouti space-time code, as stated in (G.2). For coherent detection at the receiving node, the signals simply add up at the receiver, and acceptable decoding is possible when $\gamma_n^{\text{rec}} = \sum_{i=1}^{2} P_{n-i,n}|h_{n-i,n}|^2 \geq \gamma_{\text{th}}$. The total transmitted power from Node k is denoted by $P_k = P_{k,k+1} + P_{k,k+2}$. Our objective is to find the minimum value of the total transmission power in Phase n, i.e., the cost function $\mathcal{C}(\text{Tx}_n, n) = P_{n-1,n} + P_{n-2,n}$, such that the outage probability at the receiving node rx_n becomes less than the target value ρ_0. In this case, the probability of outage can be calculated as in (G.6).

Now, a tractable outage probability formula is derived for the sum of independent-not-identical exponentially distributed random variables at the receiving node rx_n. The moment generating function (MGF) of the random variable γ_n^{rec} is derived to calculate $\Pr\{\gamma_n^{\text{rec}} < \gamma_{\text{th}}\}$. Since the γ_i's are independent exponential random variables, the MGF of γ_n^{rec}, i.e., $M_n(-s) = \mathbb{E}\{e^{-s\gamma_n^{\text{rec}}}\}$, can be written as $M_n(-s) = \prod_{i=1}^{2} \frac{1}{1+P_{n-i,n}\sigma^2_{n-i,n}s}$. Using partial fraction expansion, and by assuming that the products $P_{n-i,n}\sigma^2_{n-i,n}$ are distinct for all links, the MGF can be decomposed into

$$M_n(-s) = \sum_{i=1}^{2} \frac{\alpha_{n,i}}{1 + P_{n-i,n}\sigma^2_{n-i,n}s}, \tag{G.11}$$

where

$$\alpha_{n,1} = \frac{1}{1 - \frac{P_{n-2,n}\sigma^2_{n-2,n}}{P_{n-1,n}\sigma^2_{n-1,n}}}, \ \alpha_{n,2} = \frac{1}{1 - \frac{P_{n-1,n}\sigma^2_{n-1,n}}{P_{n-2,n}\sigma^2_{n-2,n}}}. \tag{G.12}$$

Since each term in the summation in (G.11) corresponds to the MGF of an exponential distribution, $\Pr\{\gamma_n^{\text{rec}} < \gamma_{\text{th}}\}$ can be written as

$$\begin{aligned}\rho_{n,n-1} = \Pr\{\gamma_n^{\text{rec}} < \gamma_{\text{th}}\} &= \sum_{i=1}^{2} \alpha_{n,i}\left(1 - e^{\frac{-\gamma_{\text{th}}}{P_{n-i,n}\,\sigma^2_{n-i,n}}}\right) \\ &= 1 - \alpha_{n,1} e^{\frac{-\gamma_{\text{th}}}{P_{n-1,n}\,\sigma^2_{n-1,n}}} - \alpha_{n,2} e^{\frac{-\gamma_{\text{th}}}{P_{n-2,n}\,\sigma^2_{n-2,n}}}\end{aligned} \tag{G.13}$$

Now, we formulate the problem of power allocation in the cooperative multihop networks. The link cost or total transmitted power for the multipoint-to-point case is $\mathcal{C}(\text{Tx}_n, n) = \sum_{i=1}^{2} P_{n-i,n}$. Therefore, the power allocation problem, which has a required outage probability constraint on the receiving node, can be formulated as

$$\begin{aligned}&\min \sum_{i=1}^{2} P_{n-i,n}, \\ &\text{s.t.} \ \sum_{i=1}^{2} \alpha_{n,i}\left(1 - e^{\frac{-\gamma_{\text{th}}}{P_{n-i,n}\,\sigma^2_{n-i,n}}}\right) \le \rho_0. \\ &\quad P_{n-i,n} \ge 0, \ \text{for } i = 1, 2.\end{aligned} \tag{G.14}$$

The constraint function in (G.14) is not convex. For tractability, the outage probability in (G.13) is rewritten in terms of its series representation as

$$\rho_{n-1,n} = \sum_{i=1}^{2} \alpha_{n,i} \sum_{k=1}^{\infty} \frac{1}{k!}\left(\frac{-\gamma_{\text{th}}}{P_{n-i,n}\,\sigma^2_{n-i,n}}\right)^k, \tag{G.15}$$

and by replacing $\alpha_{n,i}$ from (G.12) into (G.15), we have

$$\rho_{n-1,n} = \frac{1}{\beta_n} \sum_{k=1}^{\infty} \frac{(-\gamma_{\text{th}})^k}{k!} \frac{P^{k-1}_{n-1,n}\sigma^{2k-2}_{n-1,n} - P^{k-1}_{n-2,n}\,\sigma^{2k-2}_{n-2,n}}{\sigma^{2k-2}_{n-1,n}\sigma^{2k-2}_{n-2,n}P^{k-1}_{n-1,n}P^{k-1}_{n-2,n}}, \tag{G.16}$$

where $\beta_n = P_{n-1,n}\,\sigma^2_{n-1,n} - P_{n-2,n}\,\sigma^2_{n-2,n}$. Furthermore, from (G.16), ρ_{out} can be well approximated in high SNR as

$$\rho_{n-1,n} \approx \frac{\gamma_{\text{th}}^2}{2\,\sigma_{n-1,n}^2\sigma_{n-2,n}^2 P_{n-1,n}P_{n-2,n}} \triangleq \tilde{\rho}_{n-1,n}, \tag{G.17}$$

which is a tight upper-bound on the outage probability, and thus, it can be reliably used in the optimization problem (G.14). Consequently, each power allocation strategy satisfying the constraint on $\tilde{\rho}_{n-1,n}$ fulfills the original constraint on $\rho_{n-1,n}$ automatically; hence, the original optimization problem (G.14) can be simplified to

$$\begin{aligned} &\min \sum_{i=1}^{2} P_{n-i,n}, \\ &\text{s.t. } \frac{\gamma_{\text{th}}^2}{2\,\sigma_{n-1,n}^2\sigma_{n-2,n}^2 P_{n-1,n}P_{n-2,n}} \leq \rho_0, \\ &\quad P_{n-i,n} \geq 0, \text{ for } i = 1, 2. \end{aligned} \tag{G.18}$$

The objective function and the second set of constraints in (G.18) are linear functions of the power allocation coefficients, and thus, they are convex functions. The first constraint in (G.18) can be written as $f(P_{n-1,n}, P_{n-2,n}) \leq 0$, where

$$f(P_{n-1,n}, P_{n-2,n}) = \frac{\gamma_{\text{th}}^2}{2\sigma_{n-1,n}^2\sigma_{n-2,n}^2 P_{n-1,n}P_{n-2,n}} - \rho_0, \tag{G.19}$$

with $D_f = \{P_{n-i,n} \in (0,\infty), i \in \{1,2\} \,|\, f(P_{n-1,n}, P_{n-2,n}) \leq 0\}$, $f : D_f \longrightarrow \mathbb{R}$. $f(P_{n-1,n}, P_{n-2,n})$ is a *geometric* function [6], which is a convex function. Hence, since the objective function and the constraints are convex, the optimum power allocation coefficients $P_{n-1,n}$ and $P_{n-2,n}$ in the optimization problem stated in (G.18) are unique.

The optimal power allocation strategy for high SNRs is found in the following. Since the approximate outage probability expression derived in (G.17) is an upper-bound on the outage probability, this result can be used reliably for all SNR scenarios.

Theorem 1 *The optimum power allocation $P_{n-1,n}^*$ and $P_{n-2,n}^*$ in the optimization problem stated in* (G.18) *are equal and is expressed as*

$$P_{n-i,n}^* = \frac{\gamma_{th}}{\sigma_{n-1,n}\sigma_{n-2,n}\sqrt{2\rho_0}}, \; i = 1, 2. \tag{G.20}$$

Proof: *The Lagrangian of the problem stated in* (G.18) *is*

$$L(P_{n-1,n}, P_{n-2,n}) = \sum_{i=1}^{2} P_{n-i,n} + \lambda f(P_{n-1,n}, P_{n-2,n}). \tag{G.21}$$

For node $n-1$, $n = 2, \ldots, N+1$, with a nonzero transmitter power in Phase n, the Kuhn-Tucker condition is

$$\frac{\partial}{\partial P_{n-1,n}} L(P_{n-1,n}, P_{n-2,n}) = 1 + \lambda \frac{\partial}{\partial P_{n-1,n}} f(P_{n-1,n}, P_{n-2,n}) = 0, \tag{G.22}$$

where

$$\frac{\partial}{\partial P_{n-1,n}} f(P_{n-1,n}, P_{n-2,n}) = \frac{-\gamma_{th}^2}{2\sigma_{n-1,n}^2 \sigma_{n-2,n}^2 P_{n-1,n}^2 P_{n-2,n}}. \tag{G.23}$$

Since the strong duality condition [6, Eq. (5.48)] holds for convex optimization problems, we have $\lambda f(P_{n-1,n}, P_{n-2,n}) = 0$ for the optimum point. If we assume Lagrange multiplier has a positive value, we have $f(P_{n-1,n}, P_{n-2,n}) = 0$, which is equivalent to the equality in the constraint in (G.18)*, i.e.,*

$$\rho_0 = \frac{\gamma_{th}^2}{2\,\sigma_{n-1,n}^2 \sigma_{n-2,n}^2 P_{n-1,n} P_{n-2,n}}. \tag{G.24}$$

Combining (G.22)-(G.24)*, we can find the optimum value of the power coefficient $P_{n-1,n}$, yielding* (G.20)*. The same procedure can be followed for $P_{n-2,n}$ to yield* (G.20). □

An outstanding property of Theorem 1 is that each power coefficient is only depending on the channel statistics of local nodes, and thus, can be implemented in a distributed manner. One possible distributed scheme is that Node n broadcasts the product of $\sigma_{n-1,n}^2 \sigma_{n-2,n}^2$ to nodes $n-2$ and $n-1$. It is assumed that the end-to-end communication is in outage if any of the receiving nodes cannot correctly decode the information [7]. For decoding the message reliably, the outage probability at the destination must be less than the desired end-to-end outage probability $\rho_{\max}$. We denote the required outage probability at the nth phase be ρ_0. The outage probability ρ_n at the nth node is affected by all previous $n-1$ hops and can be iteratively calculated according to the recursion

$$\rho_n = 1 - (1 - \rho_{n-1,n}) \prod_{i=n-2}^{n-1} (1 - \rho_i), \tag{G.25}$$

for $n = 3, \ldots, N+1$, where $\rho_1 = \rho_{0,1}$, $\rho_2 = 1 - (1 - \rho_{1,2})(1 - \rho_{0,1})$, and $\rho_{n-1,n}$ is the outage probability of the nth transmission phase given by (G.13) or (G.17). If the power allocation strategy derived in Theorem 1 is used, (G.25) can be rewritten as $\rho_n = 1 - (1 - \rho_0) \prod_{i=n-2}^{n-1} (1 - \rho_i)$. The end-to-end outage probability is computed using $n = N + 1$ in (G.25), and is given by

$$\rho_{\text{out}} = \rho_{N+1} = 1 - \prod_{\nu=0}^{N} (1 - \rho_{N-\nu,N-\nu+1})^{\Omega(\nu)}, \tag{G.26}$$

where $\Omega(\nu) = \Omega(\nu - 1) + \Omega(\nu - 2)$, $\Omega(-1) = 0$, $\Omega(0) = 1$. Note that $\{\Omega(\nu)\}$ is a Fibonacci sequence. To get an insight into the relationship between the end-to-end outage probability $\rho_{\max} = \rho_{N+1}$ and ρ_0, we have

$$\rho_{\max} = 1 - \prod_{\nu=0}^{N} (1 - \rho_0)^{\Omega(\nu)} = 1 - (1 - \rho_0)^{\sum_{\nu=0}^{N} \Omega(\nu)}. \tag{G.27}$$

Thus, the target outage probability at each hop ρ_0 can be represented in terms of the end-to-end desired outage probability $\rho_{\max}$. It is important to note that based on (G.25), outage at the destination occurs even if one intermediate node experience an outage. This guarantees that by using the power allocation strategies given in Theorem 1, the outage probability QoS at the destination is satisfied.

3.3 Energy Savings via Cooperative Routing

The problem of finding the optimal cooperative route from the source node to the destination node can be mapped to a Dynamic Programming (DP) problem [4]. As the network nodes are allowed only to either fully cooperate or broadcast, finding the best cooperative path from the source node to the destination has a special layered structure. In [4], it is shown that in a network with $N + 1$ nodes, which has 2^N nodes in the cooperation graph, standard shortest path algorithms have a complexity of $O(2^N)$. Hence, finding the optimal cooperative route in an arbitrary network becomes computationally intractable for larger networks. For this reason, we restrict the cooperation to nodes along the optimal noncooperative route. That is, at each transmission slot, all nodes that have received the information cooperate to send the information to the next node along the minimum energy noncooperative route [4]. Therefore, with the help of the link cost expressed in Subsection III-A, the minimum-energy non-cooperative

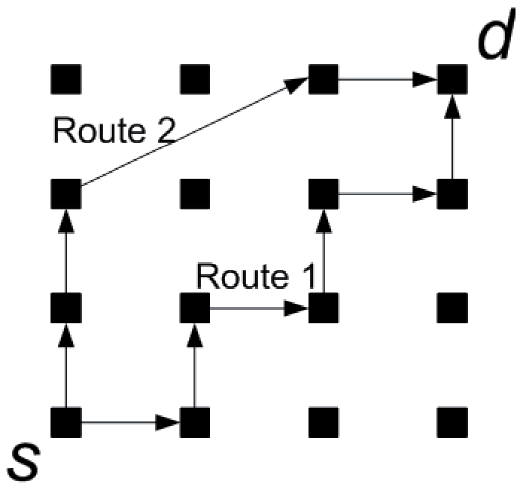

Fig. G.2: A regular 4×4 grid topology with the source *s* and destination *d* where two possible routing paths are demonstrated.

route is first selected, which has N intermediate relays. Fig. G.2 demonstrate an example of a selected route in a regular 4×4 grid topology with the source *s* and destination *d* located at the opposite corners. An $n \times n$ grid can be decomposed into many 2×2 grids. Fig. G.2 shows two possible routes for an 4×4 grid. Without lose of generality, we assume that a transmission to a neighbor in vertical or horizontal direction has a cost of 1 unit. Under this assumption, the diagonal transmission in Route 2 has a cost of 5 units. Thus, Route 1 has cost of 6, and Route 2 has cost of 8. Therefore, in this example, it can be checked that stair-like noncooperative path (Route 1) is the minimum energy cost route. Then, nodes along the optimal non-cooperative route cooperate to transmit the source information toward the destination. That is, at each transmission slot, the two nodes that have most recently received the information cooperate to send the information to the next node along the minimum energy non-cooperative route. The transmit power can be estimated using (G.20).

Therefore, assuming a connection from the source node to the destination via the cooperative routing around the best non-cooperative path with N intermediate nodes, the total transmission power for the cooperative multihop system is

$$P_T(\text{coop}) = \sum_{n=1}^{N+1} \mathcal{C}(\text{Tx}_n, n) = \sum_{n=1}^{N+1} 2P_{n-1,n}. \tag{G.28}$$

Note that the nth node denotes the nth relay when $n \leq N$, and the destination node when $n = N + 1$.

The energy savings for a cooperative routing strategy relative to the optimal non-cooperative strategy is defined as

$$\text{Energy Savings} = \frac{P_T(\text{non-coop}) - P_T(\text{coop})}{P_T(\text{non-coop})}, \tag{G.29}$$

where $P_T(\text{non-coop})$ and $P_T(\text{coop})$ are computed in (G.10) and (G.28), respectively.

4 Centralized End-to-End Outage Constrained Link Cost Formulation

The power allocation proposed in Theorem 1 can be implemented distributively. However, it is not optimal in terms of minimizing the total transmit power given an end-to-end outage probability constraint $\rho_{\max}$. If the intermediate relays do not intend to use the source's data, and act only as passive nodes to relay source's messages, the outage probability constraint ρ_0 for each hop is not required. Therefore, in this section, we propose a centralized power allocation schemes to achieve the rate R with an end-to-end outage probability constraint $\rho_{\max}$ at the destination.

4.1 Non-Cooperative Multihop Link Cost

Now, we investigate non-cooperative transmit powers $P_{n-1,n}$ to satisfy the target rate R with a target outage probability of $\rho_{\max}$ at the destination. We consider that the receiver can correctly decode the source data whenever $P_{n-i,n}|h_{n-i,n}|^2 \geq \gamma_{\text{th}}$. Hence, in $1 - \rho_{\max}$ of the total transmissions, we have a reliable detection of symbols. That is

$$\rho_{\text{out}} = 1 - \prod_{n=1}^{N+1} e^{\frac{-\gamma_{\text{th}}}{P_{n-1,n}\sigma^2_{n-1,n}}} = 1 - e^{\sum_{n=1}^{N+1} \frac{-\gamma_{\text{th}}}{P_{n-1,n}\sigma^2_{n-1,n}}}. \tag{G.30}$$

Now, we formulate the problem of power allocation in the non-cooperative multihop networks with the acceptable outage probability of $\rho_{\max}$ at the destination. The link cost or total transmitted power for all $(N+1)$ phases becomes $\mathcal{C} = \sum_{n=1}^{N+1} P_{n-1,n}$. Therefore, the power allocation problem, which has a required outage probability constraint on the destination node, can be formulated as

$$\begin{aligned} \min \; & \sum_{n=1}^{N+1} P_{n-1,n}, \\ \text{s.t.} \; & \sum_{n=1}^{N+1} \frac{\gamma_{\text{th}}}{P_{n-1,n}\sigma^2_{n-1,n}} \leq -\ln(1-\rho_{\max}), \\ & P_{n-1,n} \geq 0, \; \text{for} \; n = 1, \ldots, N+1. \end{aligned} \tag{G.31}$$

Therefore, the required transmit power can be calculated in the following theorem:

Theorem 2 *The optimum power allocation values $P^*_{n-1,n}$ and $P^*_{n-2,n}$ in the optimization problem* (G.31) *are expressed as*

$$P^*_{n-1,n} = \frac{-\gamma_{th}}{\sigma_{n-1,n}\ln(1-\rho_{\max})} \sum_{k=1}^{N+1} \frac{1}{\sigma_{k-1,k}}. \tag{G.32}$$

Proof: *The Lagrangian of the problem stated in* (G.31) *is*

$$L(P_{0,1}, \ldots, P_{N,N+1}) = \sum_{n=1}^{N+1} P_{n-1,n} + \lambda f(P_{0,1}, \ldots, P_{N,N+1}). \tag{G.33}$$

By solving Kuhn-Tucker condition as in (G.22)*, the inverse of Lagrange multiplier can be computed as*

$$\lambda^{-1} = \frac{\gamma_{th}}{P^2_{n-1,n}\sigma^2_{n-1,n}}. \tag{G.34}$$

Assuming that the equality in the first constraint in (G.31) *is satisfied, we have*

$$\sum_{n=1}^{N+1} \frac{\gamma_{th}}{P_{n-1,n}\sigma_{n-1,n}^2} = -\ln(1-\rho_{\max}). \quad \text{(G.35)}$$

Next, we substitute $P_{n-1,n}$ *from* (G.34) *into* (G.35), *and we get*

$$\sqrt{\lambda} = \sum_{n=1}^{N+1} \frac{-\sqrt{\gamma_{th}}}{\sigma_{n-1,n}\ln(1-\rho_{\max})}. \quad \text{(G.36)}$$

Using (G.34) *and* (G.36), *the optimum value of the power coefficient* $P_{n-1,n}$, *is found in* (G.32). □

Hence, the non-cooperative multihop link cost is given by

$$P_T(\text{non-coop}) = \sum_{n=1}^{N+1} \frac{-\gamma_{\text{th}}}{\sigma_{n-1,n}\ln(1-\rho_{\max})} \sum_{k=1}^{N+1} \frac{1}{\sigma_{k-1,k}}. \quad \text{(G.37)}$$

4.2 Cooperative Multihop Link Cost

In this subsection, our objective is to find the minimum power allocation required for the cooperative transmission in order to achieve certain rate R with the successful reception of source's data at the destination. For decoding the message reliably, the outage probability at the destination must be less than the desired end-to-end outage probability $\rho_{\max}$.

As stated in Section II, the source node transmits two symbols s_1 and s_2 with the power $P_{0,1}$ during the first phase. In Phase n, $n = 2, \ldots, N+1$, a set of *two* nodes $\text{Tx}_n = \{\text{tx}_{n,1}, \text{tx}_{n,2}\}$ cooperate to transmit information of the source to a *single* receiver node rx_n, using the Alamouti space-time code, as stated in (G.2). Therefore, the total transmission power in all phases becomes $\mathcal{C} = 2P_{0,1} + \sum_{n=2}^{N+1}(P_{n-1,n} + P_{n-2,n})$, such that the outage probability at the destination becomes less than the target value $\rho_{\max}$.

From (G.13) and (G.26), the probability of outage can be calculated

$$\rho_{\text{out}} = 1 - \prod_{n=1}^{N+1} \left(\sum_{i=1}^{2} \alpha_{n,i}\, e^{\frac{-\gamma_{\text{th}}}{P_{n-i,n}\sigma_{n-i,n}^2}} \right)^{\Omega(N-n+1)}, \quad \text{(G.38)}$$

where $\alpha_{1,2} = 0$, $\alpha_{1,1} = 1$, and $\alpha_{n,i} = 1$, $n = 2, \ldots, N+1$, is calculated in (G.12).

Now, ρ_{out} in (G.26) can be approximated as follows:

$$\rho_{\text{out}} \approx \sum_{\nu=0}^{N} \Omega(\nu)\, \rho_{N-\nu,N-\nu+1} \triangleq \hat{\rho}_{\text{out}}. \tag{G.39}$$

With a derivation similar to [8], it is straightforward to show that the approximated form (G.39) serves as an upper bound for the exact outage probability (G.26), i.e., $\rho_{\text{out}} \leq \hat{\rho}_{\text{out}}$. Thus, if $\hat{\rho}_{\text{out}}$ is considered for distributing the power within the multi-hop system, the applied end-to-end probability constraint is more stringent. Using (G.13), (G.38) and (G.39), we have

$$\rho_{\text{out}} \approx \sum_{n=1}^{N+1} \Omega(N-n+1) \sum_{i=1}^{2} \alpha_{n,i} \left(1 - e^{\frac{-\gamma_{\text{th}}}{P_{n-i,n}\sigma^2_{n-i,n}}}\right). \tag{G.40}$$

From $1 - e^{-x} \leq x$, (G.17), and (G.40), an upper-bound for ρ_{out} can be obtained as

$$\rho_{\text{out}} \approx \frac{\gamma_{\text{th}}\, \Omega(N)}{\sigma^2_{0,1} P_{0,1}} + \sum_{n=2}^{N+1} \frac{\gamma^2_{\text{th}}\, \Omega(N-n+1)}{2\, \sigma^2_{n-1,n}\sigma^2_{n-2,n} P_{n-1,n} P_{n-2,n}}. \tag{G.41}$$

Then, we formulate the outage restricted minimum power allocation problem as

$$\begin{aligned}
&\min \; 2P_{0,1} + \sum_{n=2}^{N+1} \left(P_{n-1,n} + P_{n-2,n}\right), \\
&\text{s.t.} \; \frac{\gamma_{\text{th}}\, \Omega(N)}{\sigma^2_{0,1} P_{0,1}} + \sum_{n=2}^{N+1} \frac{\gamma^2_{\text{th}}\, \Omega(N-n+1)}{2\sigma^2_{n-1,n}\sigma^2_{n-2,n} P_{n-1,n} P_{n-2,n}} \leq \rho_{\max}, \\
&\quad P_{n-i,n} \geq 0, \; \text{for } i = 1, 2.
\end{aligned} \tag{G.42}$$

Due to the symmetry between $P_{n-1,n}$ and $P_{n-2,n}$ in the objective and constraint function in (G.42), it follows that $P_{n-1,n} = P_{n-2,n}$. Therefore, the optimization problem in (G.42) is equivalent to

$$\begin{aligned}
&\min \; \sum_{n=1}^{N+1} 2\, P_{n-1,n} \\
&\text{s.t.} \; \frac{\gamma_{\text{th}}\, \Omega(N)}{\sigma^2_{0,1} P_{0,1}} + \sum_{n=2}^{N+1} \frac{\gamma^2_{\text{th}}\, \Omega(N-n+1)}{2\, \sigma^2_{n-1,n}\sigma^2_{n-2,n} P^2_{n-1,n}} \leq \rho_{\max}, \\
&\quad P_{n-1,n} \geq 0.
\end{aligned} \tag{G.43}$$

The outage constraint in (G.43) is a *posynomial* function [6], which is a convex function. Hence, since the objective function and the constraints are convex, the optimum power allocation values $P_{n-1,n}$ and $P_{n-2,n}$ in the optimization problem (G.43) are unique.

From the Lagrangian (G.33) and the Kuhn-Tucker condition, the following set of equations can be found as

$$P_{0,1}=\sqrt{\lambda\frac{\gamma_{\text{th}}\Omega(N)}{\sigma_{0,1}^2}},\ P_{n-1,n}=\sqrt[3]{\lambda\frac{\gamma_{\text{th}}^2\Omega(N-n+1)}{2\sigma_{n-1,n}^2\sigma_{n-2,n}^2}}, \tag{G.44}$$

for $n=2,\ldots,N+1$. Since the strong duality condition [6, Eq. (5.48)] holds for convex optimization problems, the constraint in (G.43) is satisfied with equality:

$$\frac{\gamma_{\text{th}}\,\Omega(N)}{\sigma_{0,1}^2 P_{0,1}}+\sum_{n=2}^{N+1}\frac{\gamma_{\text{th}}^2\,\Omega(N-n+1)}{2\,\sigma_{n-1,n}^2\sigma_{n-2,n}^2 P_{n-1,n}^2}=\rho_{\max}. \tag{G.45}$$

Combining (G.44) and (G.45), we can find the optimum value of power coefficients $P_{n-1,n}$, $n=1,\ldots,N{+}1$. By defining $a=\frac{\sqrt{\gamma_{\text{th}}\,\Omega(N)}}{\sigma_{0,1}}$, $b=\sum_{n=2}^{N+1}\sqrt[3]{\frac{\gamma_{\text{th}}^2\Omega(N-n+1)}{2\,\sigma_{n-1,n}^2\sigma_{n-2,n}^2}}$, and $x=\lambda^{-1/6}$, we can find the optimum value of λ by solving $a\,x^3+b\,x^4=\rho_{\max}$. It can be shown that this equation has two real roots, and the single positive root corresponds to the desired value of λ.

5 Numerical Analysis

In this section, numerical results are provided to quantify the energy savings using the proposed cooperative routing scheme. A regular line topology is considered where nodes are located at *unit* distance from each other on a straight line. The optimal non-cooperative routing in this network is to always send the information to the next nearest node in the direction of the destination. Assume that the noise power $\mathcal{N}_0$, rate R, and bandwidth W are normalized to 1.

In Fig. G.3, we compare the achieved energy savings of the proposed outage-restricted cooperative routings with respect to the non-cooperative multihop scenario. We compare the distributed power allocations derived in Section III and the centralized power allocation given in Section IV. Here, $\sigma_{i,j}^2$ is proportional to the inverse of the squared distance, and the end-to-end outage probability of $\rho_{\max}=10^{-3}$ at the destination, Fig. G.3 demon-

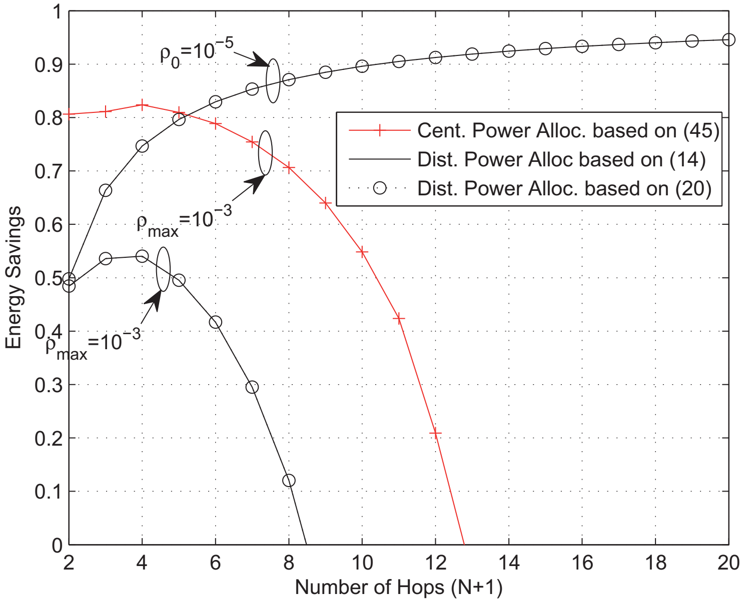

Fig. G.3: The average energy savings curves versus the number of hops, using the distributed and centralized power allocations for space-time coded cooperative routing in outage-restricted wireless multihop network.

strates the energy savings curves obtained from (G.29) versus the number of transmitting nodes $N + 1$. It can be observed that using the centralized power control based on optimization problem in (G.43), more than 80% saving in energy is achieved when 3 relays are employed. We have used power allocation derived in (G.32) for the case of non-cooperative multihop transmission. It is shown that cooperative routing is beneficial for networks with small number of relays. Notice that the depicted curves are obtained by the pessimistic model for the end-to-end outage probability (G.25). Thus, these curves are lower-bounds on the actual energy savings obtainable by the proposed cooperative routing. Fig. G.3 confirms that the closed-form distributed power allocation derived in (G.20) has the same performance as the original optimization problem stated in (G.14). In this numerical example, we have also depicted the energy savings via cooperative routing when the outage probability $\rho_0 = 10^{-5}$ is required at each step.

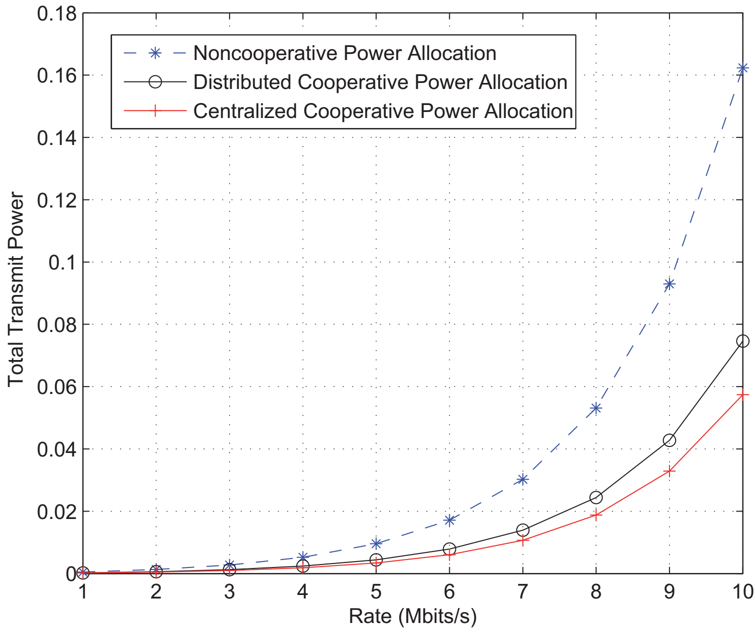

Fig. G.4: The total transmit power curves versus the achievable rate in a wireless multihop network with $N = 3$ and $\rho_{\max} = 10^{-3}$.

In this case, it can be seen that using the distributed cooperative routing, a substantial gain can be achieved comparing to the non-cooperative transmission. For example, for the network with 19 relays, up to 95% savings in energy is achievable. Moreover, the ene-to-end outage probability can be represented in terms of ρ_0 from (G.27).

Next, the energy-efficiency versus rate efficiency of the multi-hop network with $(N + 1) = 4$ hops is studied when the nodes are located at a distance of 1 km from each other on a straight line. It is assumed that the communication over a bandwidth of $W = 5$ MHz should meet an end-to-end outage probability constraint $\rho_{\max} = 10^{-3}$ for noise power $\mathcal{N}_0 = -174$ dBm/Hz according to the UMTS standard. In Fig. G.4, the total transmit power of the different power allocation schemes is plotted versus the achievable end-to-end data rate RW (Mbits/s). For the non-cooperative multihop transmission, the power allocation given in Theorem

2 is used. For the cooperative routing protocols with distributed and centralized power allocation, (G.20) and (G.43) are used, respectively. For example, one can observe that given a total power of $P_T = 0.06$ watt, the rate is increased by 1.5 and 2 Mbits/sec using the distributed and centralized power allocated cooperative routing protocols, respectively, compared to non-cooperative routing.

6 Conclusion

In this paper, we formulated the problems of finding the minimum energy cooperative route for a wireless network under Rayleigh fading. We proposed a space-time coded cooperative multihop routing for the purpose of energy savings, constrained on a required outage probability at the destination. The calculated distributed and centralized power allocations are independent of instantaneous channel variation, and thus, can be used in practical wireless systems. It is shown that energy savings of up to 80% is achievable in line networks with 3 relays for an outage probability constraint of $\rho_{\max} = 10^{-3}$ at the destination.

References

[1] N. Vaidya, "Open problems in mobile ad-hoc networks," in *Keynote talk at the Workshop on Local Area Networks*, Tampa, Florida, Nov. 2001.

[2] F. Li, K. Wu, and A. Lippman, "Energy-efficient cooperative routing in multi-hop wireless ad hoc networks," in *IEEE International Performance, Computing, and Communications Conference*, Apr. 2006, pp. 215–222.

[3] J. Boyer, D. D. Falconer, and H. Yanikomeroglu, "Multihop diversity in wireless relaying channels," *IEEE Trans. Commun.*, vol. 52, no. 10, pp. 1820–1830, Oct. 2004.

[4] A. E. Khandani, J. Abounadi, E. Modiano, and L. Zheng, "Cooperative routing in static wireless networks," *IEEE Trans. Commun.*, vol. 55, no. 11, pp. 2185–2192, Nov. 2007.

[5] S. M. Alamouti, "A simple transmitter diversity scheme for wireless communications," *IEEE Journal on Selected Areas in Communications*, vol. 16, no. 8, pp. 1451–1458, Oct. 1998.

[6] S. Boyd and L. Vandenberghe, *Convex Optimization*. Cambridge, UK: Cambridge Univ. Press, 2004.

[7] M. Dohler, "Virtual antenna arrays," Ph.D. dissertation, King's College, University of London, London, UK, 2003.

[8] D. Wubben and Y. Lang, "Near-optimum power allocation for outage restricted distributed MIMO multi-hop networks," in *IEEE GLOBECOM 2008*, New Orlean, USA, Nov. 2008.